Bureau of Safety and Environmental Enforcement Oil Spill Preparedness Division

Oil Spill Boom Computational Fluid Dynamics and Physical Modeling

Final Report

August 2024

Gregory Johnson, Brent Paul, Michele Fitzpatrick, Daniel Granda, Gino Ferraj, Teresa Mendez, and Ken Dykstra

US Department of the Interior Bureau of Safety and Environmental Enforcement Oil Spill Preparedness Division



Oil Spill Boom Computational Fluid Dynamics and Physical Modeling

Final Report

OSRR # 1137

August 2024

Authors: Gregory Johnson Serco, Inc.

Brent Paul Serco, Inc.

Michele Fitzpatrick Consultant

This study was funded by the Bureau of Safety and Environmental Enforcement (BSEE), U.S. Department of the Interior, Washington, D.C., under Contract 140E0121C0011

By Serco, Inc. New London, CT, USA

US Department of the Interior Bureau of Safety and Environmental Enforcement Oil Spill Preparedness Division



DISCLAIMER

Study concept, oversight, and funding were provided by the US Department of the Interior (DOI), Bureau of Safety and Environmental Enforcement (BSEE), Oil Spill Preparedness Division (OSPD), Sterling, VA, under Contract Number 140E0121C0011. This report has been technically reviewed by BSEE, and it has been approved for publication. The views and conclusions contained in this document are those of the authors and should not be interpreted as representing the opinions or policies of the US Government, nor does mention of trade names or commercial products constitute endorsement or recommendation for use.

REPORT AVAILABILITY

The PDF file for this report is available through the following sources. Click on the URL and enter the appropriate search term to locate the PDF:

Document Source	Search Term	URL
Bureau of Safety and Environmental Enforcement (BSEE)	Project Number – 1137	https://www.bsee.gov/oil-spill-containment-boom- computational-fluid-dynamics-and-physical-modeling- study
U.S. Department of the Interio Library	rOil Spill Boom Computational Fluid Dynamics and Physical Modeling	https://library.doi.gov
National Technical Reports Library	Oil Spill Boom Computational Fluid Dynamics and Physical Modeling	https://ntrl.ntis.gov/NTRL/

Sources: a) BSEE (2019), b) DOI [2021], c) National Technical Information Service (2021)

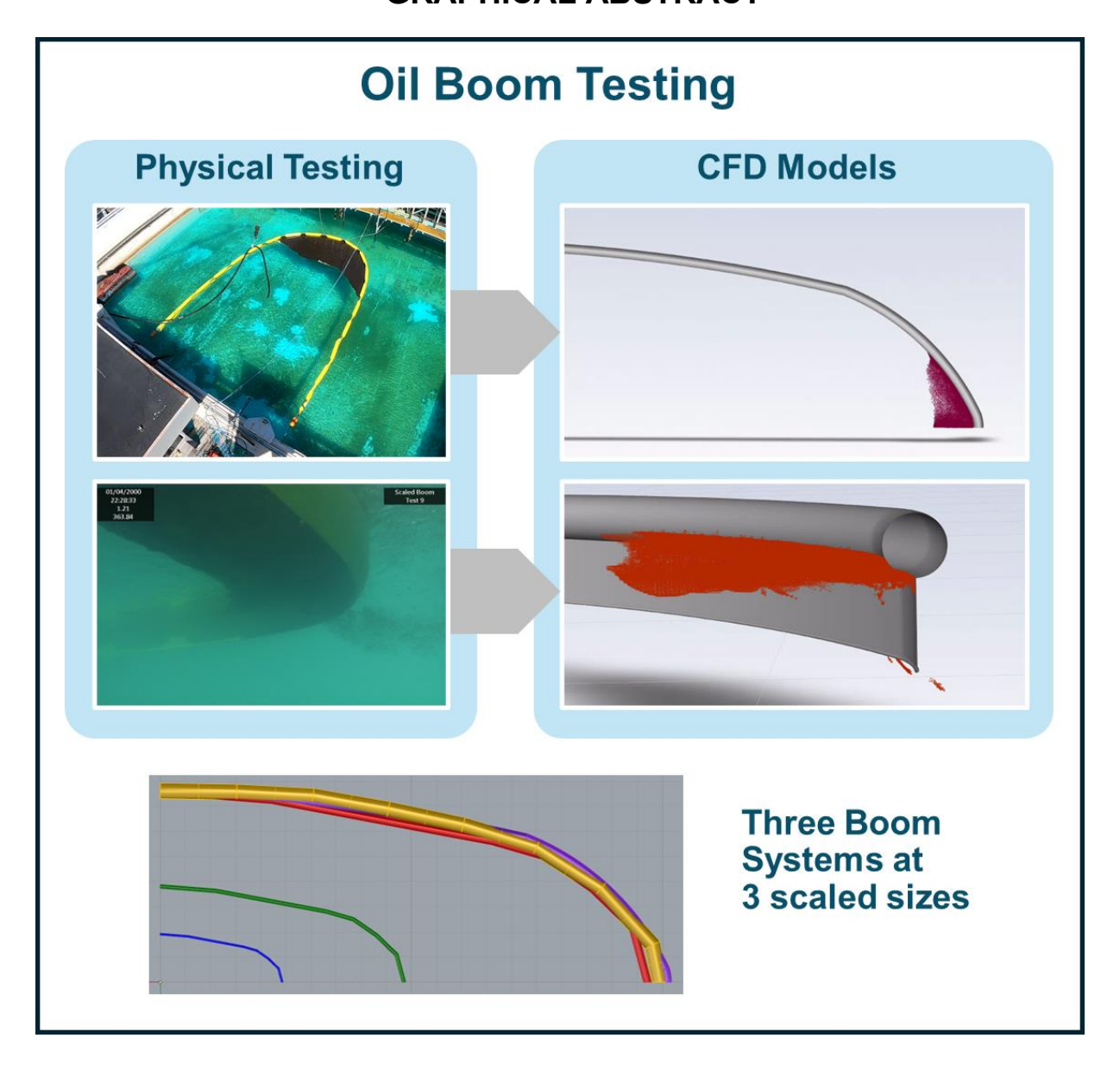
CITATION

Johnson G, Fitzpatrick M, Paul B. 2024. Oil Spill Boom Computational Fluid Dynamics and Physical Modeling. U.S. Department of the Interior, Bureau of Safety and Environmental Enforcement. Report No.: 1137 Contract No.: 140E0121C0011. https://doi.org/10.70149/328390

ACKNOWLEDGEMENTS

This study was funded by the Bureau of Safety and Environmental Enforcement (BSEE), U.S. Department of the Interior, Washington, D.C., under Contract 140E0121C0011.

GRAPHICAL ABSTRACT



EXECUTIVE SUMMARY

Testing of towed booms to assess their oil containment abilities is important, especially with ongoing work to develop high-speed oil containment systems. However, field testing using oils is not possible within U.S. waters due to permitting issues surrounding intentional release of hydrocarbons. There are alternatives, including testing a full-scale boom section in a tow tank, such as the Bureau of Safety and Environmental Enforcement's (BSEE) National Oil Spill Response and Renewable Energy Test Facility (Ohmsett) (https://ohmsett.bsee.gov/). However, in spite of Ohmsett's large tank size, testing of booms at higher speeds for long durations is not possible due to the limitation of the tank's length. A boom's swath width and draft are also limited due to bottom and sidewall effects imposed by the tank. Literature states that the tank depth should be a minimum of four times the boom's draft to minimize bottom effects (Amini et al., 2008) This limits effective boom testing at Ohmsett to booms with drafts of less than 0.6 meter (m) (2 feet (ft)). Although flume test tanks can produce constant current for long-length tests, they impose greater restrictions on maximum boom size due to their smaller widths and water depths.

BSEE project 1089 (Baker et al., 2019) conducted an extensive literature review on the existing knowledge in oil spill boom science and technology. The literature described how computational fluid dynamics (CFD) modeling and scaled boom model testing could be used to predict the performance of a full-scale towed containment boom. One of the project's conclusions was that assumptions regarding scaling factors used for scaled model tests may not be fully understood, and that it was possible that performance observed through the physical modeling experiments may not translate to results that might be expected from full-scale boom equipment.

This work is a follow-on study to investigate towed oil containment boom systems to assess how physical scaled model testing results may predict full-scale boom performance and whether CFD modeling results predict physical boom performance at various scales. This report describes the results from physical testing conducted at Ohmsett in August and December of 2022 and the results from a series of CFD models that were developed and then compared to results from the physical testing.

Results of the physical testing indicate that physical scale modeling can provide an indication of full-scale performance with some error. The computational results for the full-scale booms were similar to the experimental results, showing great promise for predicting the performance of boom systems. However, the results for the Elastec Foam boom at 50% and 25% scale were noticeably different showing oil loss over the top of the boom prior to entrainment. This is most likely due to sensitivity of the model to the step-function speed increases and could be alleviated by using more gradual speed increases at the expense of longer computational time. This may not be a significant issue since the need for conducting numerical analyses at smaller scales is questionable.

Some recommended changes to the American Society for Testing and Materials (ASTM) F2084 test standard are proposed based on the physical test and modeling experiences. These include:

- When possible, within the constraints of the test facility, increase the time spent at each speed increment.
- Consider eliminating the preload testing.

Additional work is proposed to assess the performance of a modified boom system with reduced drag (and improved tow speed) and also to assess how much complexity can be removed from the CFD models and still achieve acceptable performance.

Contents

1	Introd	uction	1
2	Physic	cal Scale Model Testing	2
	2.1.	Boom Systems	2
	2.2.	Test Configuration	5
	2.3.	Test Procedure	7
	2.4.	Physical Testing Results	9
	2.4.1.	ASTM Preload Tests	9
	2.4.2.	Entrainment Results	14
	2.4.3.	Weather	17
3	Comp	utational Fluid Dynamics Modeling	18
	3.1.	CFD Plan	18
	3.1.1.	Background	18
	3.1.2.	Approach	19
	3.1.3.	Initial Conditions	21
	3.2.	CFD Simulation and Results	21
	3.2.1.	Model Development	21
	3.2.2.	Grid Development	24
	3.2.3.	Boundary Conditions	28
	3.2.4.	Initial Conditions	29
	3.2.5.	CFD Results	31
4	Concl	usions	48
	4.1.	Physical Testing Conclusions	48
	4.2.	CFD Modeling Conclusions	49
5	Recor	mmendations	50
6	Refere	ences	51
Αp	pendix	A: Technical Summary	53
Αp	pendix l	B: Abbreviations and Acronyms	54
Αp	pendix	C: All Boom Systems	55
Αp	pendix	D: Underwater Pictures of Boom Systems	64
Αp	pendix	E. Viscosity Data	73
Αp	pendix	F. Entrainment Pictures	74
An	nendix (G. Weather	83

List of Figures

Fig. 1 Example of one boom segment	3
Fig. 2 Elastec Foam full-size boom.	3
Fig. 3 Elastec Airmax half-size boom.	4
Fig. 4 Abasco quarter and half-size inflatable booms	4
Fig. 5 Booms tied at South end of tank after testing	5
Fig. 6 Boom test setup at Ohmsett	6
Fig. 7 Boom preload determination test, first loss speed vs. preload volume (ASTM F2084)	9
Fig. 8 First loss results for all full-scale booms	10
Fig. 9 First loss results for all 50% - 60% scale booms.	10
Fig. 10 First loss results for all 25% - 33% scale booms.	11
Fig. 11 Full-size boom, 500 gallons of oil at start of test.	12
Fig. 12. Calculated catenary shape, oil area (red) and thickness, 500 gallons of oil	12
Fig. 13 The 500 gallons of oil compressed into the apex during the entrainment run	13
Fig. 14 The calculated oil thickness for the 500 gallons of oil compressed into the apex	13
Fig. 15 First loss speeds plotted by boom type and scale	15
Fig. 16 First loss speed vs. boom scale.	16
Fig. 17 First loss speed vs. boom scale.	17
Fig. 18 Entrainment failure mode	19
Fig. 19 Drainage failure mode	19
Fig. 20 CAD boom models	22
Fig. 21 CAD geometry of all booms, view from above.	23
Fig. 22 Elastec Foam boom at three scales.	23
Fig. 23 Geometric models used for CFD analyses; symmetry plane portion removed	24
Fig. 24 Surface grid for full-scale Elastec Foam boom	25
Fig. 25 Computational domain for Elastec Foam with water surface	26
Fig. 26 Selections for cuts in the X direction.	26
Fig. 27 Two X-cuts for the Elastec Foam grid.	27
Fig. 28 Two X-cuts for the Elastec Foam grid.	27

Fig. 29 Y= -5.0 cut for Elastec Foam grid	28
Fig. 30 Z = -0.25 cut (middle of skirt) as viewed from below.	28
Fig. 31 Boundary conditions.	29
Fig. 32 Viscosity curves for Hydrocal 300 and Calsol 8240.	30
Fig. 33 Initial condition for oil (Baker et al., 2019).	31
Fig. 34 Iso-surfaces for results.	32
Fig. 35 Elastec Foam, 100%. Initial condition of oil at Z = 0.035, as viewed from above	33
Fig. 36 Elastec Foam, 100%. Oil in the domain after 44.015 s at a speed of 0.5 knots.	34
Fig. 37 Elastec Foam, 100%	35
Fig. 38 Elastec Foam, 100%	35
Fig. 39 Elastec Foam, 100%. Cells with oil at 74.195 s at 0.5 kts.	36
Fig. 40 Elastec Foam, 100%. Cells with oil at 176.185 s and 0.8 kts.	36
Fig. 41 The 500 gal of oil compressed into the apex during the entrainment run.	37
Fig. 42 Elastec Foam, 100%. Cells with oil at 201.27 s and 0.9 kts.	37
Fig. 43 Elastec Foam, 100%.	38
Fig. 44 Elastec Foam, 100%.	38
Fig. 45 Elastec Foam, 100%. Cells with oil at 236.07 s and 1.0 kts.	38
Fig. 46 Elastec Foam, 50%. Cells with oil at 82.66 s and 0.65 kts.	39
Fig. 47 Elastec Foam, 50%. Cells with oil at 91.19 s and 0.725 kts.	40
Fig. 48 Elastec Foam, 50%. Cells with oil at 93.09 s and 0.725 kts.	40
Fig. 49 Elastec Foam, 25%. Cells with oil at 53.37 s and 0.50 kts.	41
Fig. 50 Elastec Foam, 25%. Water surface colored by height at 53.37 s and 0.5 kts	42
Fig. 51 Elastec Foam, 25%. Cells with oil at 60.865 s and 0.55 kts.	42
Fig. 52 Elastec Foam, 25%. Water surface colored by height at 60.865 s and 0.55 kts	43
Fig. 53 Abasco, 100%. Velocity on (a) y = -2.5 and (b) z = 0.03 planes at 1.1 kts.	43
Fig. 54 Abasco, 100%. Phase on (a) y = -2.5 and (b) z = 0.03 planes at 1.1 kts.	44
Fig. 55 Abasco, 100%. Cells with oil at 120.92 s and 1.1 kts.	44
Fig. 56 Elastec Airmax, 100%. Velocity on (a) y = -2.5, (b) y = -1.0, and (c) z = 0.03 planes at 1.2 kts	45
Fig. 57 Elastec Airmax, 100%. Phase on (a) y = -2.5 and (b) y = -1.0 planes at 1.1 kts	45

Fig. 58 Elastec Airmax, 100%. Water surface color by height at 1.1 kts.	45
Fig. 59 Elastec Airmax, 100%. Cells with oil at 172.98 s and 1.2 kts.	46
Fig. 60 Elastec Airmax, 100%. Cells with oil at 196.90 s and 1.2 kts.	46
Fig. 61 Elastec Airmax, 100%. Water surface at 196.90 s and 1.2 kts.	47
Figure 62 Elastec Foam 100% scale – first loss entrainment	74
Figure 62 Elastec Foam 100% scale – gross loss entrainment	74
Figure 63 Elastec Foam 50% scale – first loss entrainment	75
Figure 63 Elastec Foam 50% scale – gross loss entrainment	75
Figure 64 Elastec Foam 25% scale – first loss entrainment	76
Figure 64 Elastec Foam 25% scale – gross loss entrainment	76
Figure 62 Abasco 100% scale – first loss entrainment	77
Figure 62 Abasco 100% scale – gross loss entrainment	77
Figure 62 Abasco 50% scale – first loss entrainment	78
Figure 62 Abasco 50% scale – gross loss entrainment	78
Figure 64 Abasco 25% scale – first loss entrainment	79
Figure 64 Abasco 25% scale – gross loss entrainment	79
Figure 62 Elastec Airmax 100% scale – first loss entrainment	80
Figure 62 Elastec Airmax 100% scale – gross loss entrainment	80
Figure 62 Elastec Airmax 66% scale – first loss entrainment	81
Figure 62 Elastec Airmax 66% scale – gross loss entrainment	81
Figure 62 Elastec Airmax 33% scale – first loss entrainment	82
Figure 62 Elastec Airmax 33% scale – gross loss entrainment	82
List of Tables	
Table 1. Specifications for the Boom Systems Tested	
Table 2. Measured test oil properties	6
Table 3. Boom lengths and gaps	6
Table 4. Condensed list of tests	8

Table 5. Speed ranges for each scale (all speeds in knots)	8
Table 6 First and gross loss results for all booms (average of 3 trials each)	14
Table 7. Tabulated data and error estimates for extrapolated first loss speeds using square root of scale factor	16
Table 8 Tabulated data and error estimates for extrapolated first loss speeds using cube root of scale factor	17
Table 9. Grid cell counts and spacing for different booms	25
Table 10 Initial velocity and speed increments for each scale boom	29
Table 11 Different simulations as well as the estimated top speed	31
Table 12 Physical and CFD entrainment comparison	47

1 Introduction

The use of mechanical systems to collect, contain, and recover oil is considered to be a primary technique in responding to offshore oil spills. This method has the advantage of immediate removal of oil from the environment. A typical recovery operation involves a boom towed in a catenary configuration by one or two vessels, which collects surface oil in the boom apex. Once sufficient thickness of oil is collected, a skimmer system recovers the collected oil. This oil is stored in temporary storage devices prior to being taken to shore and offloaded.

During an offshore response operation there are multiple factors that can limit the response. One potentially limiting factor is the rate at which oil is collected and contained within the boom. This rate can be influenced by the length of the boom which translates to swath width, and the speed at which the boom is towed by the vessels. Typical booms can be towed at speeds of 0.36-0.51 meters per second (m/s) (0.7-1.0 knots (kts)). Beyond this speed, oil is typically lost from underneath the boom by entrainment or drainage.

Testing of towed booms to assess their oil containment abilities is important, especially with ongoing work to develop high-speed oil containment systems. However, field testing using oils is not possible within U.S. waters due to permitting issues surrounding intentional release of hydrocarbons. Some full-scale boom sections can be tested in a tow tank such as the National Oil Spill Response and Renewable Energy Test Facility (Ohmsett) (https://ohmsett.bsee.gov/). However, the testing is limited by the tank dimensions. For example, the duration of a test run is limited by the tank length which becomes problematic at higher test speeds, and the width and depth of the tank impose limits on the boom's swath width and draft. Literature states that the tank depth should be a minimum of four times the boom's draft to minimize bottom effects (Amini et al., 2008). Since the water depth at Ohmsett is about 2.4 meters (m) (8 feet (ft)), this limits effective boom testing at Ohmsett to booms with drafts of a maximum of 0.6m (2 ft).

Bureau of Safety and Environmental Enforcement (BSEE) project 1089 (Baker et al., 2019) conducted an extensive literature review on the existing knowledge in oil spill boom science and technology. The literature described how computational fluid dynamics (CFD) modeling and scaled boom model testing could be used to predict the performance of a full-scale towed containment boom. Both CFD and physical modeling were then used to test several boom systems at high speeds. The modeling was all conducted at 1/8 scale. Since no testing was done at full-scale, one of the project's conclusions was that assumptions regarding scaling factors used for scaled model tests may not be fully understood, and that it was possible that performance observed through the smaller scale physical modeling experiments may not translate to results that might be expected from full-scale boom equipment.

BSEE project 1137 was started in 2021 to address these questions. The purpose of the project is to investigate towed oil containment boom systems to assess how physical scaled model testing and CFD modeling results may predict full-scale boom performance. The primary goals of this project are to assess 1) if scaled physical models replicate the results of full-scale systems to sufficient accuracy, and 2) if CFD models produce results that match physical testing to sufficient accuracy. To accomplish this, we conducted CFD modeling and physical testing of three boom systems at multiple scales. This report describes results of the testing as well as recommendations for potential changes to the American Society for Testing and Materials

(ASTM) Standard and recommendations as to the viability of physical scale modeling for boom systems. It also includes results of the CFD modeling and recommendations as to the efficacy of CFD modelling for testing boom systems.

2 Physical Scale Model Testing

A total of three different booms systems (one foam and two inflatable), at three scales each, were tested following ASTM Standard F2084 (*Standard Guide for Collecting Containment Boom Performance Data in Controlled Environments*, 2018). The boom systems were tested using two different oils: Hydrocal 300 and Calsol 8240.

2.1. Boom Systems

Three sets of curtain booms were selected for testing: two inflatable booms and one internal foam flotation boom. These were selected after discussion with BSEE as being representative of typical oil spill response booms in inventory with Oil Spill Response Organizations (OSROs). Each boom was procured in three scaled sizes; the goal was to have a full size, half size, and quarter size for each boom. With the scaled sizes we attempted to keep the construction of the boom as close to that scaling as possible (freeboard scaled, skirt scaled, and length scaled) while also trying to use stock booms. All of the booms were constructed in single continuous pieces so that there were no slide connectors along the length. Each boom is segmented though since the air pockets and foam floats are not single compartments for the entire length of the boom. We attempted to keep the number of segments the same, scaling the length of the segments, but this was not always possible due to vender manufacturing constraints. Table 1 shows the measurements of the booms tested; these are the as-built measurements. Skirt length and draft are given in centimeters (cm) while total boom length is given in meters. Fig. 1 shows a representative sketch of a single boom segment. Fig. 2 through Fig. 5 show the three different boom systems tested. Additional pictures are in Appendix C and D.

Table 1. Specifications for the Boom Systems Tested

Boom	Planned Scale	Skirt (cm)	Draft ¹ (cm)	Draft Scale as Tested	# Segments	Length (m)
Elastec Foam	100%	60.96	63.5	100%	25	45.72
Elastec Foam	50%	30.48	31.75	50%	19	22.68
Elastec Foam	25%	13.97	13.97	24%	21	11.20
Abasco Inflatable	100%	60.96	62.23	100%	5	45.72
Abasco Inflatable	50%	27.94	30.48	49%	5	22.86
Abasco Inflatable	25%	15.24	16.51	27%	5	11.43
Elastec Airmax	100%	58.42	60.96	100%	15	45.72
Elastec Airmax	60%	33.02	35.56	58%	15	26.86
Elastec Airmax	33%	17.78	20.32	33%	14	14.40

¹draft is the distance from waterline to bottom of skirt as measured in the water at Ohmsett - typically about 2.5cm larger than skirt length

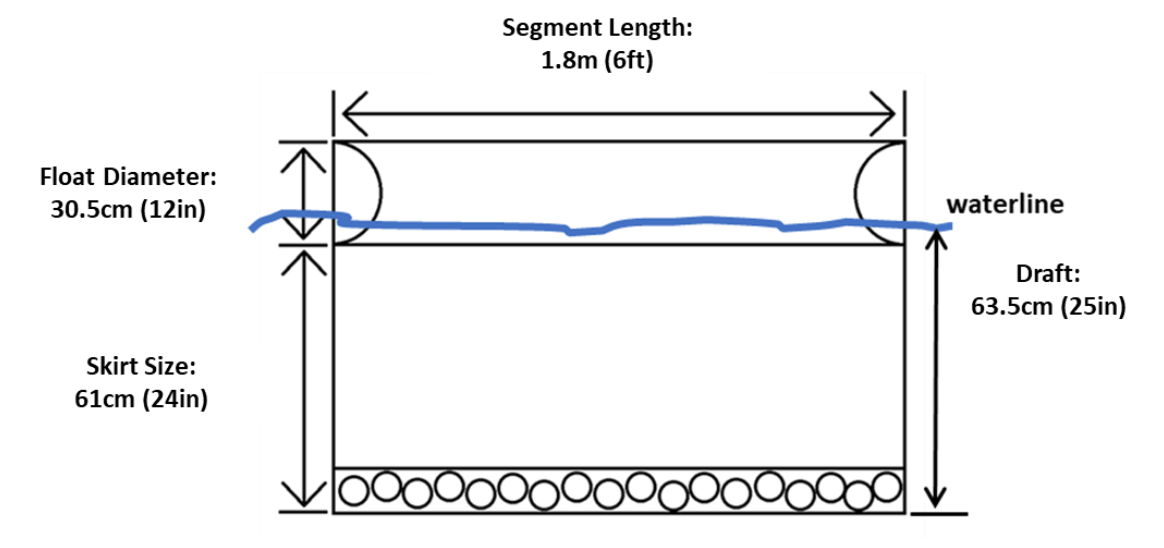


Fig. 1 Example of one boom segment.The chain pocket at bottom is included in skirt size and draft.



Fig. 2 Elastec Foam full-size boom.



Fig. 3 Elastec Airmax half-size boom.

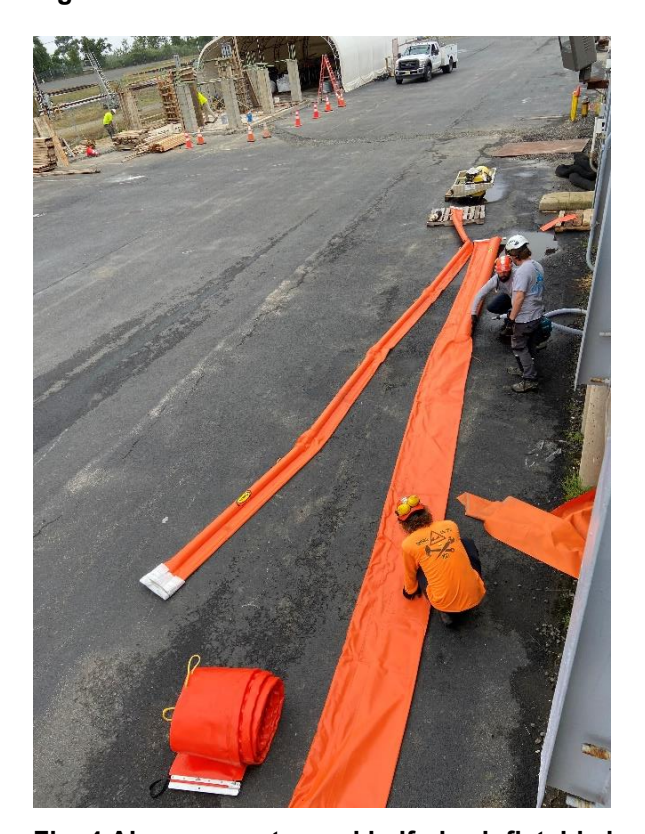


Fig. 4 Abasco quarter and half-size inflatable booms.

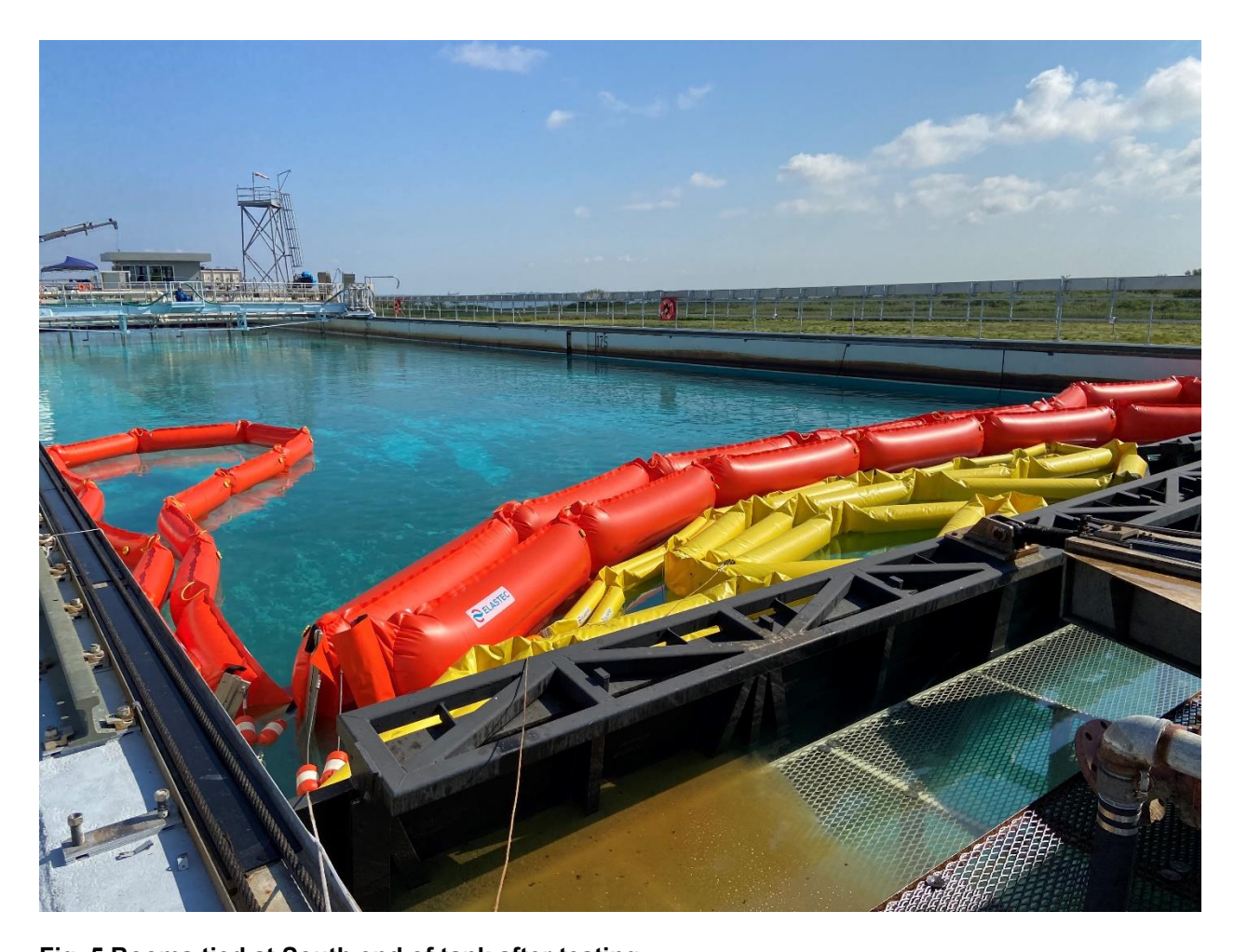


Fig. 5 Booms tied at South end of tank after testing.
Includes Elastec Airmax full and half-size booms (orange) and Elastec Foam full and half-size booms (yellow).

2.2. Test Configuration

The boom systems were tested at the Ohmsett facility in Leonardo, NJ in August and December of 2022. Testing was conducted to measure the tow speed at which the boom first loses oil (first loss) and the speed at which the boom reaches a gross oil loss condition. The testing was conducted in calm water in accordance with the ASTM F2084 Standard, modified as described in Section 4.1.

Hydrocal 300 and Calsol 8240 were selected for testing to represent a category I and category II oil as specified in ASTM F2084. These are refined oils commonly used at Ohmsett for testing due to their stable properties. Table 2 provides their properties as measured from samples collected during the tests. Daily viscosity data is provided in Appendix E. Hydrocal 300 was used with each boom system during the August tests, and Calsol 8240 was used with two of the systems during the December tests. The units for density are grams per cubic centimeter (g/cm³) and the units for viscosity are centipoise (cP).

Table 2. Measured test oil properties

Test Oil	Measured Density (g/cm³)	Viscosity (cP)
Hydrocal 300	0.8986 - 0.9022 @20°C	194.7 – 206.6 @20°C
Calsol 8240	0.9434 − 0.9411 @10°C	14,400 – 18,600 @20°C

Each boom was rigged in a catenary configuration (see Fig. 6) with the gap equal to 33 percent of the length. The full-size booms (Elastec Airmax, Elastec Foam, and Abasco Inflatable) were 45.7m (150-ft) long and were rigged with a 15.2m (50-ft) gap. The smaller scales were adjusted accordingly as shown in Table 3. The booms were attached to tow points located on the main bridge using tow bridles. An oil delivery hose was rigged to the main bridge crane for dispensing oil into the middle of the boom catenary from the tank located on the main bridge.

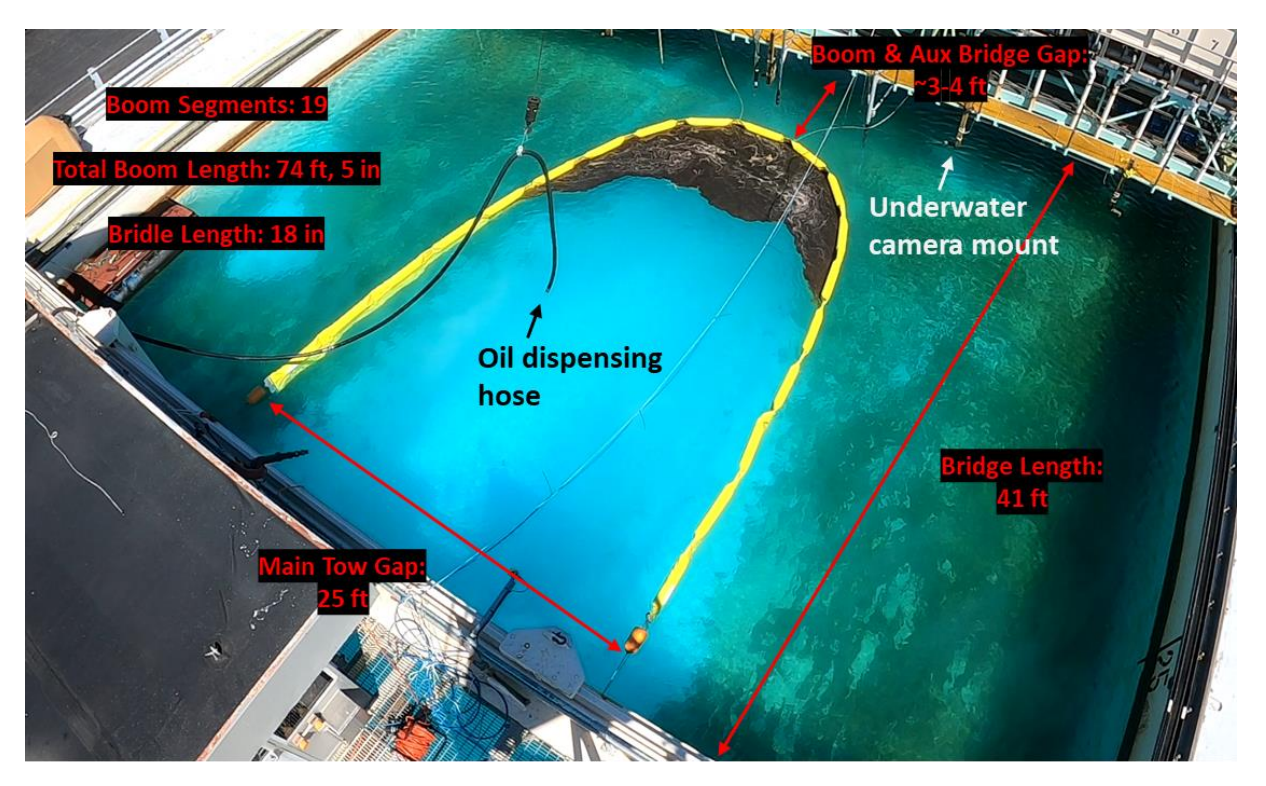


Fig. 6 Boom test setup at Ohmsett.

Looking down and North towards the auxiliary bridge from the main bridge crow's nest; half-size Elastec Foam boom.

Table 3. Boom lengths and gaps

Scale	Length (m)	Gap (m)	Boom	
Full	45.7	15.2	All	
60%	27.4	9.1	Elastec Airmax	
Half	22.9	7.6	Elastec Foam, Abasco Inflatable	
33%	15.2	5.1	Elastec Airmax	
Quarter	11.4	3.8	Elastec Foam, Abasco Inflatable	

Three underwater cameras were positioned to collect video of the apex of the boom catenary. One Kongsberg SD pan-tilt-zoom (PTZ) camera was located on the main bridge in the center, a second Kongsberg HD PTZ camera was located on the auxiliary bridge to the East side of the apex, and a GoPro HD was located on the west side of the apex. The auxiliary bridge was placed a short distance behind the apex of the boom. The auxiliary bridge position was adjusted for each boom to maintain this spacing. During the first set of tests (August) the camera on the main bridge did not yield useable video as in most cases the water clarity was not sufficient to view oil entrainment at that distance. Therefore, for the second set of tests (December) this camera was moved to the west side of the apex and the GoPro that had been there was moved to the center of the apex.

Three water flow sensors were installed in an attempt to measure the currents at various locations in the tank. The sensors used were: Vector, Vectrino, and Vectrino Profiler; all from Nortek. All three are acoustic doppler sensors that provide 3D vector velocity measurements. These were attached temporarily to the auxiliary bridge using 80/20 T-slot framing components. Unfortunately, the resulting measurements were not usable. First, it was not possible to mount the sensors stiffly enough to prevent vibration as the bridge moved so that there was significant oscillation in the sensors. Second, the available locations for mounting were limited as the sensors needed to be mounted close to the auxiliary bridge to keep them as firmly fixed as possible and the auxiliary bridge spacing needed to be set to optimize the camera views. The locations behind the boom where the sensors were installed were very turbulent and resulted in readings that were unusable as the speed increased. The only sensor that provided usable readings was the one mounted near the side of the tank on the auxiliary bridge, and this provided readings that matched the tank speed as indicated on the control system.

2.3. Test Procedure

Testing for each boom type and scale and oil type followed the same general procedure. The complete list of tests is listed in Table 4. Each series of tests started with a test run (no oil) to confirm that the auxiliary bridge spacing was correct (close enough to the boom apex for good camera angles), the boom was properly rigged, and all data collection instrumentation was functioning correctly. The test run was followed by series of preload test runs as prescribed by the ASTM standard F2084. Preload tests "determine the minimum volume of test fluid necessary for a containment boom to display loss by entrainment, and simultaneously determine the volume of test fluid a boom holds until the addition of fluid has a 'minimal' effect on the first loss tow speed" (Standard Guide for Collecting Containment Boom Performance Data in Controlled Environments, 2018). According to ASTM F2084, there is a volume at which the addition of test fluid to the preload will have minimal or no effect on the first loss tow speed (entrainment speed) and that it is this volume that should be used for the subsequent entrainment tests. The final three tests in each series were entrainment tests using the volume of oil determined by the preload tests. The entrainment tests proceeded past first loss until gross loss was observed. The underwater cameras were used to visually observe first and gross loss, and the bridge speed at those points was recorded.

Table 4. Condensed list of tests

Test #s	Date	Boom	Oil Type
1 – 11	17-18 Aug	Elastec Foam Full	Hydrocal
12 – 22	19-Aug	Elastec Foam Half	Hydrocal
23 – 31	22-Aug	Elastec Foam Qtr	Hydrocal
32 – 40	23-Aug	Abasco Qtr	Hydrocal
41 – 49	24-Aug	Abasco Half	Hydrocal
50 – 58	25 - 26 Aug	Abasco Full	Hydrocal
59 – 67	29 - 30 Aug	Airmax Full	Hydrocal
68 – 76	30-Aug	Airmax 60%	Hydrocal
77 – 85	31-Aug	Airmax 33%	Hydrocal
86 – 94	7-Dec	Elastec Foam Full	Calsol
95 – 103	8-Dec	Elastec Foam Half	Calsol
104 – 111	9-Dec	Elastec Foam Qtr	Calsol
112 – 114	12-Dec	Airmax 60%	Calsol
115 – 117	13-Dec	Airmax 33%	Calsol

The ASTM standard specifies starting the test at a speed of approximately half of the expected entrainment speed (0.5 knots (kts)) and then increasing the speed by 0.1kt every 10 seconds until first loss is observed. We initially followed the recommended 10-second increment but observed that more time was needed at each time increment for the boom and oil to reach a new equilibrium. Each time the speed is increased the oil compresses further into the boom's apex, and this compression generally required greater than 10 seconds. Therefore, in subsequent tests we increased the interval between each speed change to at least 20 seconds to allow for the boom and oil to reach equilibrium. The starting speed, speed increments, and expected max speed were scaled along with the scale models since according to page 22 of (Baker et al., 2019) speed scales with the square root of scale:

$$U_m = U_f \sqrt{R}$$
, $U_m = scale\ model\ speed$, $U_f = full\ scale\ speed$, $R = scale\ ratio$

The specific values used are in Table 5; values were rounded to the nearest increment.

Table 5. Speed ranges for each scale (all speeds in knots)

Scale	Starting speed	~Top speed	Increment
100%	0.5	1.2	0.1
60%	0.4	0.95	0.1
50%	0.35	0.85	0.05
33%	0.3	0.60	0.05
25%	0.25	0.60	0.05

2.4. Physical Testing Results

2.4.1. ASTM Preload Tests

ASTM F2084 provides a graph of first loss speed versus preload volume that is repeated here in Fig. 7. The expectation is that the first loss speed will decrease with increasing amounts of oil until it levels off at which point the speed is constant regardless of the increase in amount of oil. These are not the results that we observed. We conducted 6-8 preload tests of each boom system at each scale (9 total booms tested). In all preload tests the first loss speed seemed to be independent of preload volume. See Fig. 8, Fig. 9, and Fig. 10 for full size, half size, and quarter size booms respectively. The lines connect the preload test data, the markers alone are the individual entrainment tests (three for each boom type and size). The colors and marker type indicate the boom system. These figures show that the preload volume versus first loss tow speed did not follow the curve predicted in the ASTM standard. In all cases there is no inverse relationship between increasing preload volume and first loss speed. Although contrary to the ASTM F2084 graph (Fig. 7), this lack of decrease in first loss speed with increase in preload oil volume is consistent with other results obtained by BSEE at Ohmsett in BSEE Project 7022 (unpublished).

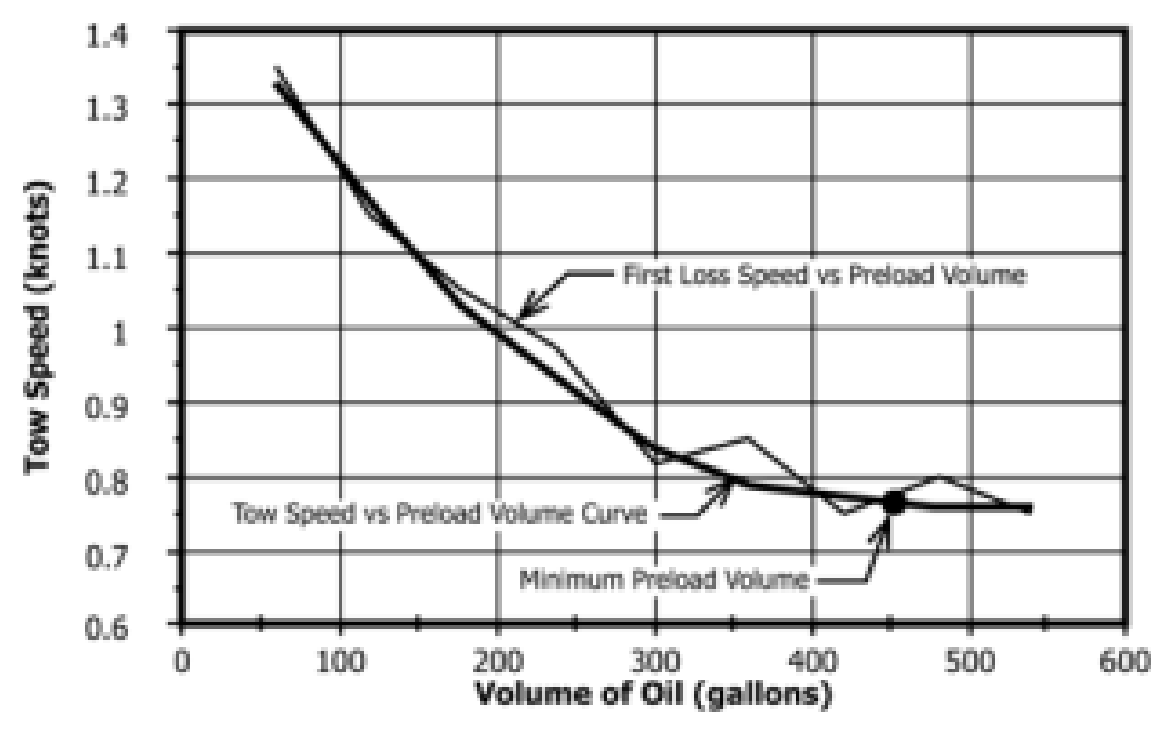


Fig. 7 Boom preload determination test, first loss speed vs. preload volume (ASTM F2084).

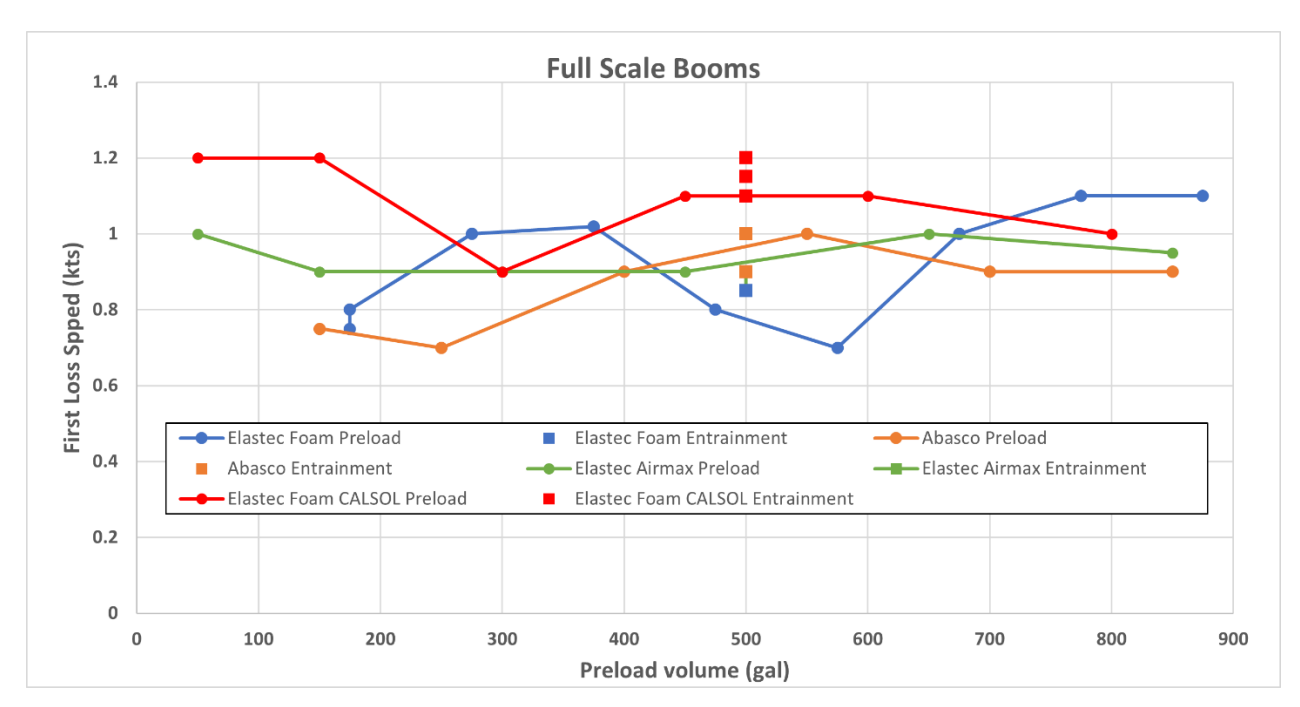


Fig. 8 First loss results for all full-scale booms

First loss speed (kts) plotted vs. preload oil volume (gallons).

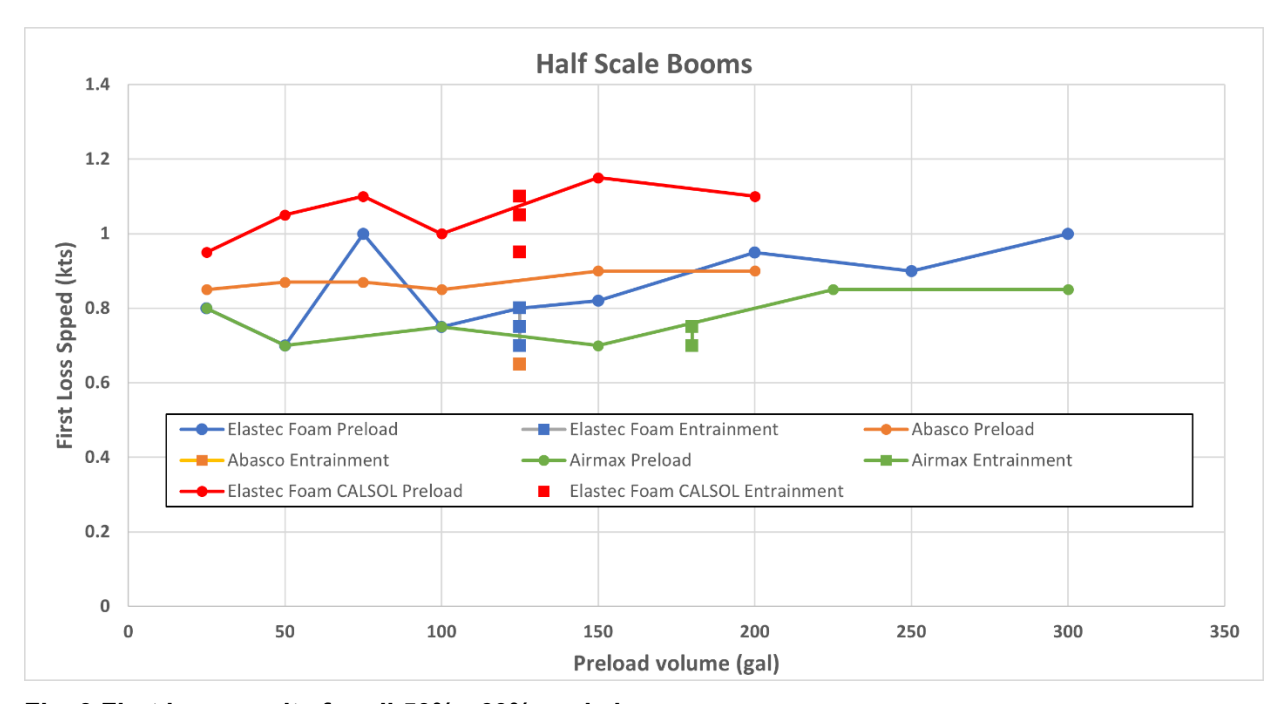


Fig. 9 First loss results for all 50% - 60% scale booms.

First loss speed (kts) plotted vs. preload oil volume (gallons).

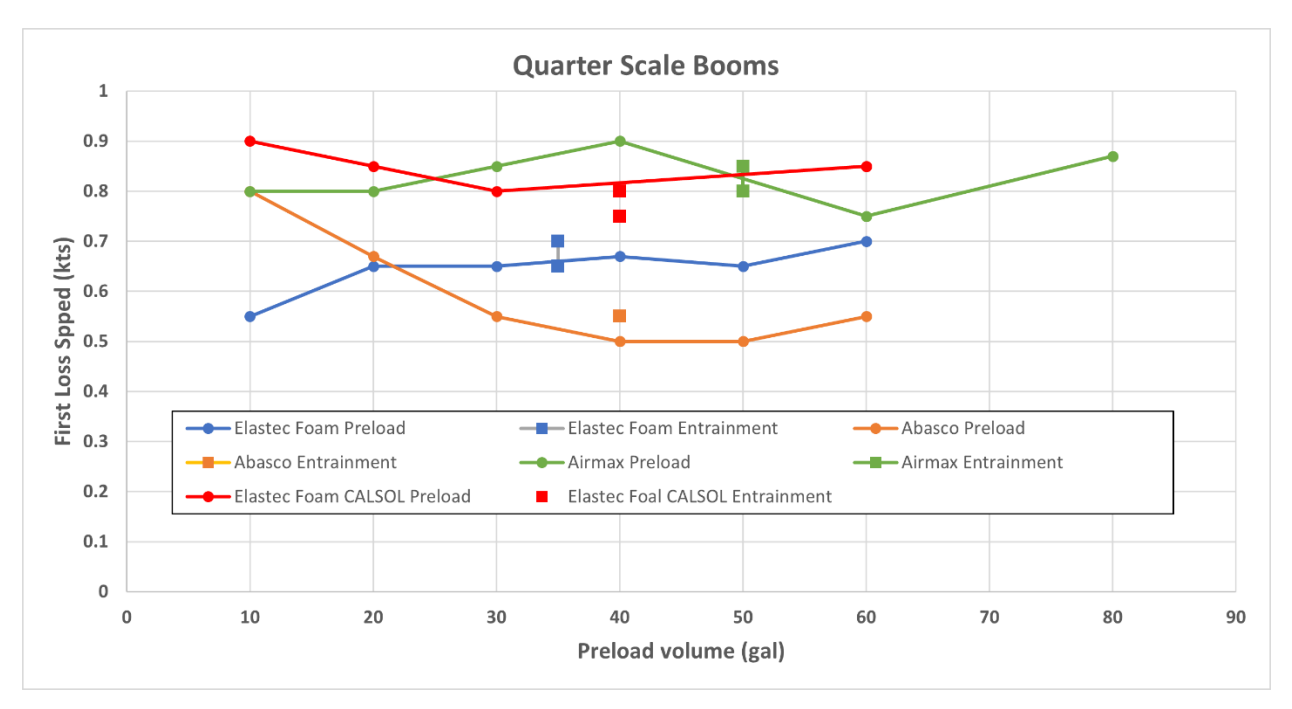


Fig. 10 First loss results for all 25% - 33% scale booms. First loss speed (kts) plotted vs. preload oil volume (gallons).

Based on our observations, sufficient oil is important to ensure that first loss can be easily observed without losing a significant volume of the oil. However, too much oil is problematic because it becomes impossible to manage. We used water sprays to keep the oil contained in the boom while loading the oil and while waiting for a run to start, but there is an upper limit to the volume of oil that can be contained. In our experience we found that using 1.893 cubic meters (m³) (500 gallons) for the full-sized booms worked well. This equates to filling the boom area about 50 percent of the catenary length to a depth of 2.5cm (1 inch) of oil (see Fig. 11 and Fig. 12). As the entrainment run commences, the oil compresses into the apex of the boom as seen in Fig. 13. At this compression the estimated depth is greater than 11.4cm (4.5 inches) using the calculations shown in Fig. 14. The red area is calculated by numerical integration of the catenary curve. The oil thickness is calculated based on the volume of 500 gallons of oil spread evenly across the red surface.



Fig. 11 Full-size boom, 500 gallons of oil at start of test. 50% line is $\sim\!50\%$ of the catenary length.

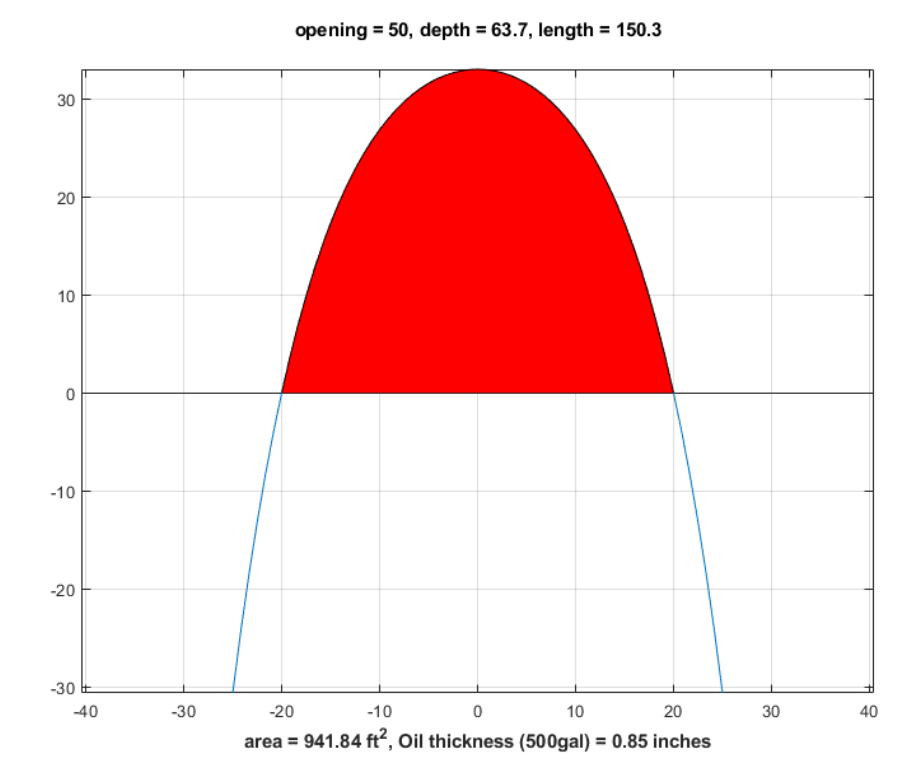


Fig. 12. Calculated catenary shape, oil area (red) and thickness, 500 gallons of oil.

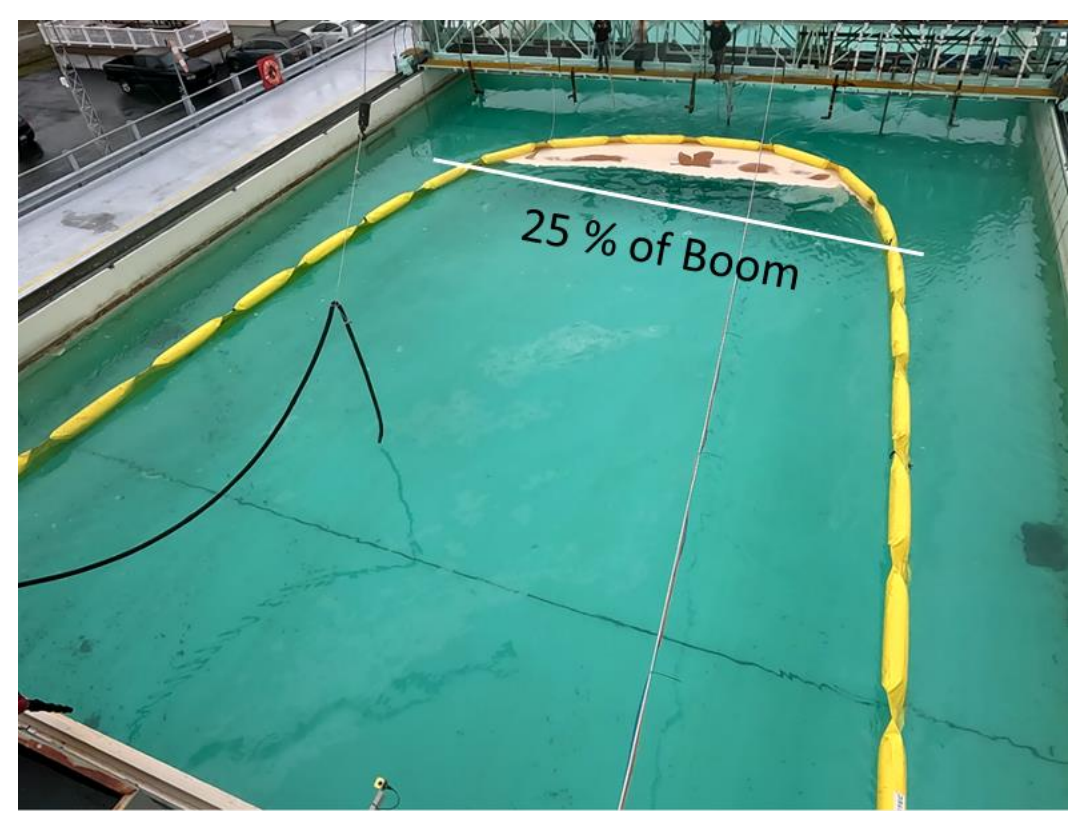


Fig. 13 The 500 gallons of oil compressed into the apex during the entrainment run. 25% line is $\sim\!\!25\%$ of the catenary length.

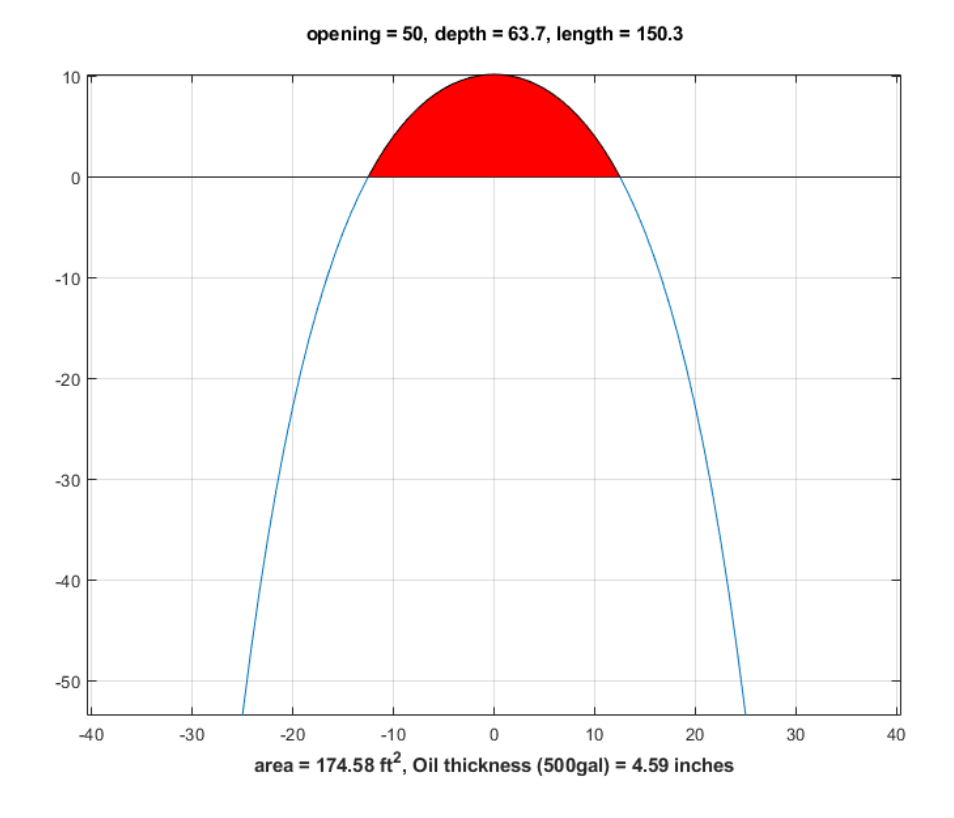


Fig. 14 The calculated oil thickness for the 500 gallons of oil compressed into the apex.

2.4.2. Entrainment Results

After the preload tests a series of three entrainment tests were conducted; this was done for each boom type and size. The first loss and gross loss speeds for the three tests were averaged and are tabulated in Table 6. The videos were reviewed after the testing, using both underwater camera views, to judge more accurately the first and gross loss speeds. All video views were important as it was not always possible to see the entrainment clearly on one video or the other. These post-test results are what are presented below. Pictures of entrainment for each boom are contained in Appendix F.

The assumption in (Baker et al., 2019) is that the speed of entrainment will scale with increases (or decreases) in boom scale size according to the square root of the scale factor. Table 6 contains the average speed of the three entrainment tests for first loss and gross loss for all of the boom systems at each scale and with each oil. Although we observed a decreasing trend in speed, the data did not exactly follow the square root factor. In Fig. 15, we plot the three first loss speeds vs. boom scale for each of the three boom systems, plus the one full system tested with Calsol. In each case, the speeds are normalized to 1 at the full scale. The dashed red line is the theoretical decrease with decreased scale (square root of scale factor); the dashed green line is a theoretical curve using the cube root of the scale factor. It is unknown why the Airmax 33 percent scale number is so off compared to the others; the videos were checked again and that did seem to be the correct entrainment speed.

Table 6 First and gross loss results for all booms (average of 3 trials each)

Boom	Draft	Oil Type	Draft Scale	First Spd (kts)	Gross Loss Spd (kts)
Elastec full average	25	Hydrocal	1.00	0.92	1.12
Elastec half average	13	Hydrocal	0.52	0.75	0.91
Elastec qtr average	6.5	Hydrocal	0.26	0.67	0.78
Abasco full average	25	Hydrocal	1.00	0.97	1.13
Abasco half average	12	Hydrocal	0.48	0.65	0.83
Abasco qtr average	7	Hydrocal	0.28	0.55	0.65
Airmax full average	24	Hydrocal	1.00	0.88	1.08
Airmax 60% average	14	Hydrocal	0.58	0.73	0.95
Airmax 33% average	8	Hydrocal	0.33	0.82	0.95
Elastec full average	25	Calsol	1.00	1.13	1.32
Elastec half average	13	Calsol	0.52	0.95	1.15
Elastec qtr average	6.5	Calsol	0.26	0.75	0.85
Airmax 60% average	14	Calsol	0.60	0.93	1.05
Airmax 33% average	8	Calsol	0.33	0.80	0.85

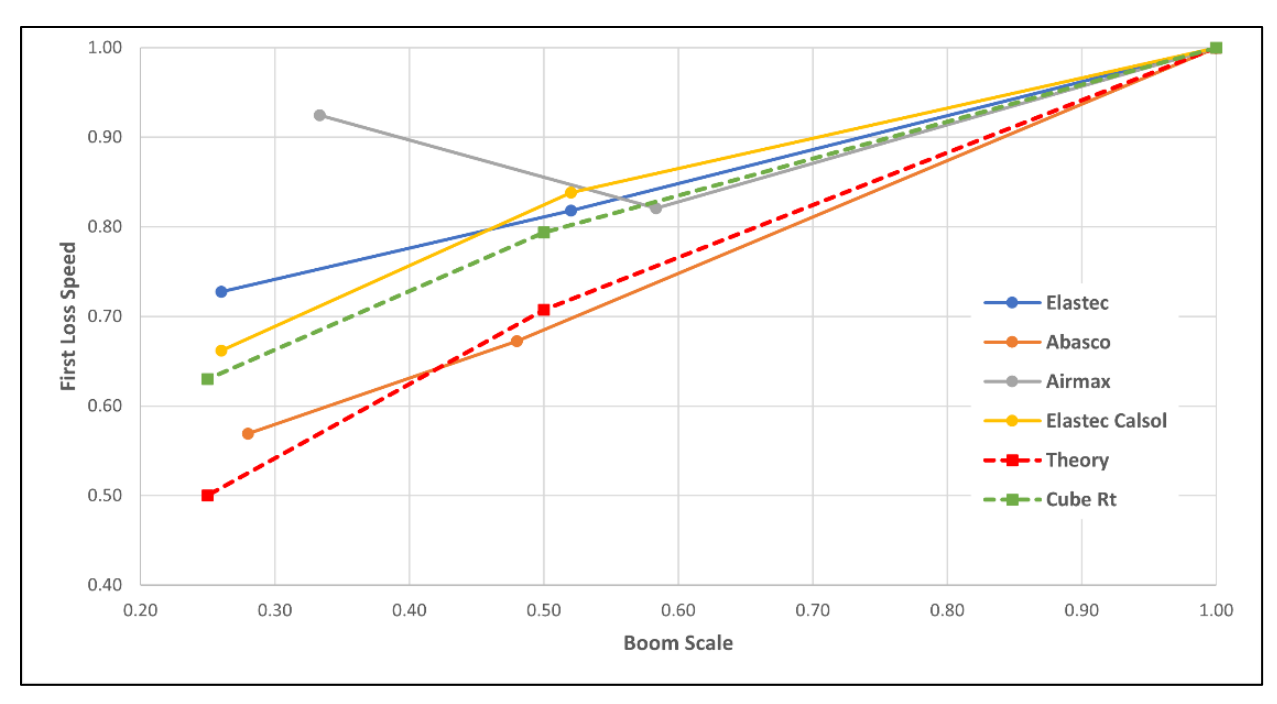


Fig. 15 First loss speeds plotted by boom type and scale. All full speeds normalized to one at full-scale.

In order to see how this might work in practice, we have reversed this in Fig. 16. Here we start with the smallest scale and then extrapolate to the larger scales and then estimate the error at each step by comparing to the actual averaged first loss speed observed. We use the smallest size boom in each grouping as the starting point (so scale is 1), and then the larger sizes are ~2 or 4 times larger (exact scale is calculated based on the measured drafts of the larger compared to the smallest booms). The measured first loss speeds are plotted vs. the boom scale factor with each boom system a different color. The dashed lines in the same color are the theoretical scaled speeds (the square root of the scale factor multiplied by the measured first loss speed of the smallest boom). For each boom scale the error between the actual first loss speed and the theoretical scaled speed is calculated; this is tabulated in Table 7.

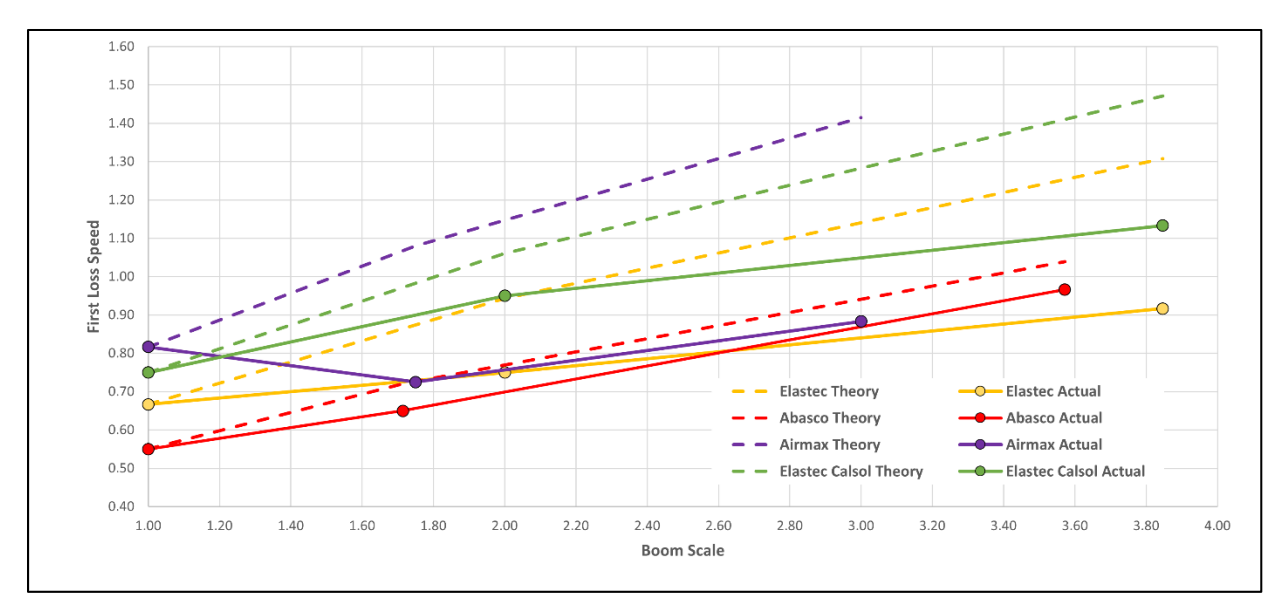


Fig. 16 First loss speed vs. boom scale.Extrapolated from the smallest size boom, compared to square root scaling.

Table 7. Tabulated data and error estimates for extrapolated first loss speeds using square root of scale factor

Boom System	Draft	Oil Type	Draft Scale	Sqrt scale	Scaled speed	First Loss Spd (kts)	Error (kts)	% error
Elastec qtr average	6.5	Hydrocal	1.00	1.00	0.67	0.67	0.00	
Elastec half average	13	Hydrocal	2.00	1.41	0.94	0.78	0.16	17
Elastec full average	25	Hydrocal	3.85	1.96	1.31	0.92	0.39	30
Abasco qtr average	7	Hydrocal	1.00	1.00	0.55	0.55	0.00	
Abasco half average	12	Hydrocal	1.71	1.31	0.72	0.65	0.07	10
Abasco full average	25	Hydrocal	3.57	1.89	1.04	0.97	0.07	7
Airmax 33% average	8	Hydrocal	1.00	1.00	0.82	0.82	0.00	
Airmax 60% average	14	Hydrocal	1.75	1.32	1.08	0.73	0.36	36
Airmax full average	24	Hydrocal	3.00	1.73	1.41	0.88	0.53	38
Elastec qtr average	6.5	Calsol	1.00	1.00	0.75	0.75	0.00	
Elastec half average	13	Calsol	2.00	1.41	1.06	0.95	0.11	10
Elastec full average	25	Calsol	3.85	1.96	1.47	1.13	0.34	23

Since the predicted square root scaling does not match well (the first loss speed does not increase with scale as much as theory predicts), we have also plotted the data against a cube root scaling (the cube root of the scale factor multiplied by the measured first loss speed of the smallest boom). This is plotted in Fig. 17 and tabulated in Table 8. The cube root scaling gives much better results, with errors less than 15 percent (except for the anomalous Airmax boom).

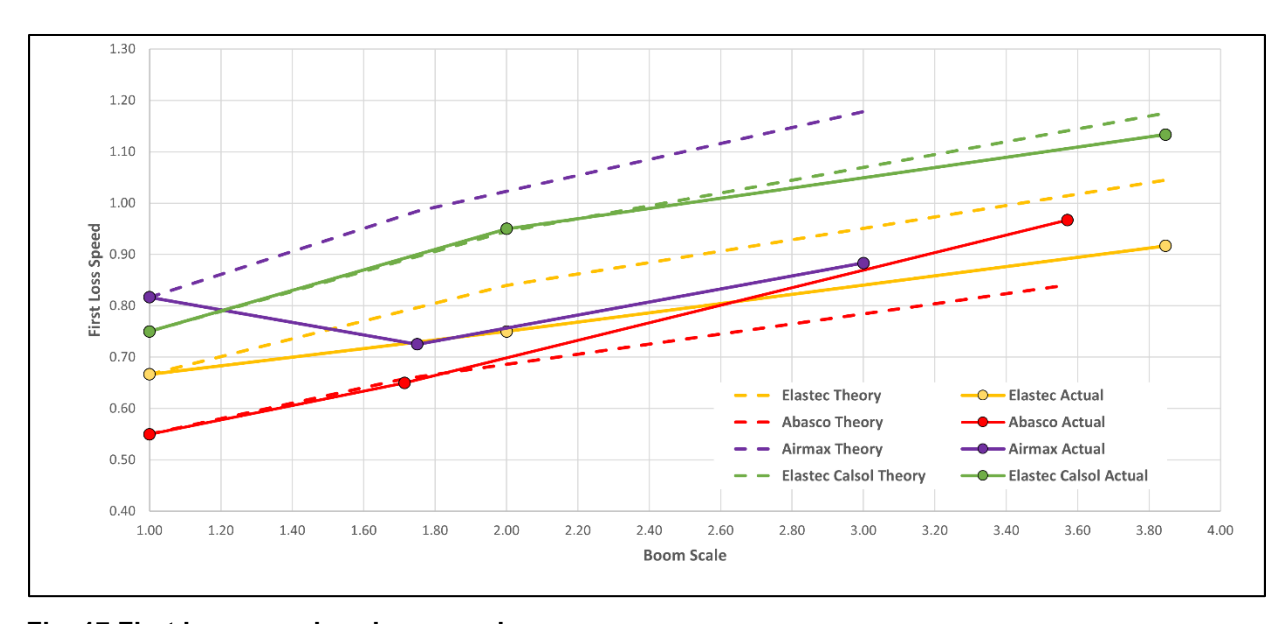


Fig. 17 First loss speed vs. boom scale. Extrapolated from the smallest size boom, compared to cube root scaling.

Table 8 Tabulated data and error estimates for extrapolated first loss speeds using cube root of scale factor.

Test	Draft	Oil Type	Draft Scale	Cube rt scale	Scaled speed	First Spd (kts)	Error	% error
Elastec qtr average	6.5	Hydrocal	1.00	1.00	0.67	0.67	0.00	
Elastec half average	13	Hydrocal	2.00	1.26	0.84	0.78	0.06	7
Elastec full average	25	Hydrocal	3.85	1.57	1.04	0.92	0.13	12
Abasco qtr average	7	Hydrocal	1.00	1.00	0.55	0.55	0.00	_
Abasco half average	12	Hydrocal	1.71	1.20	0.66	0.65	0.01	1
Abasco full average	25	Hydrocal	3.57	1.53	0.84	0.97	0.13	15
Airmax 33% average	8	Hydrocal	1.00	1.00	0.82	0.82	0.00	_
Airmax 60% average	14	Hydrocal	1.75	1.21	0.98	0.73	0.26	26
Airmax full average	24	Hydrocal	3.00	1.44	1.18	0.88	0.29	25
Elastec qtr average	6.5	Calsol	1.00	1.00	0.75	0.75	0.00	
Elastec half average	13	Calsol	2.00	1.26	0.94	0.95	0.01	1
Elastec full average	25	Calsol	3.85	1.57	1.18	1.13	0.04	4

2.4.3. Weather

The weather data (temperature, pressure, wind speed and direction) for each of the test days is shown in Appendix G. Weather was not a factor in any of the testing.

3 Computational Fluid Dynamics Modeling

3.1. CFD Plan

3.1.1. Background

A numerical simulation of the three boom designs was conducted with a CFD solver. The use of a numerical solver allows for detailed inspections of the fluid flow and interaction between the oil, water, and boom, which are not possible without a considerable increase in the cost of the physical experiments. An added benefit of a numerical solution is that there are some additional results available from the CFD simulations that cannot be practically determined in most test environments (e.g., velocity vectors, water surface heights, and volume of oil captured).

In the public literature a number of CFD tools have been used to perform analyses of oil boom containment, with ANSYS Fluent (Amini et al., 2008; Amini & Schleiss, 2009; Baker et al., 2019; Kwangu et al., 2013; Wang et al., 2012; Zhang et al., 2002) and OpenFOAM (Baker et al., 2019; Bjørvik, 2015; Gong et al., 2014) being used significantly. Of the publicly available literature only Baker (Baker et al., 2019) is recent, other work is over ten years old. Based on Serco's extensive experience with Fluent for multiphase flows, that numerical tool was selected to use for this work. A state-of-the-art workstation with 32 central processing unit (CPU) cores was used for the calculations.

When collecting oil from calm water there are three primary methods of failure: entrainment, drainage, and critical accumulation (Baker et al., 2019; Gong et al., 2014). Entrainment failure occurs with lower viscosity oils when the velocity at the oil-water interface becomes high enough to cause interface instabilities. This leads to droplets of oil peeling off the oil mass and passing underneath the boom skirt (see Fig. 18). Drainage failure, which is a more significant amount of oil lost than entrainment, occurs when oil passes under the boom along with water (see Fig. 19). This is possible with booms that have a small draft, that is not deep enough compared to the thickness of the oil on the water surface. Critical failure occurs during the collection of highly viscous oils where the collected oil behaves as a non-Newtonian fluid and can suddenly pass under the boom due to insufficient circulation within the oil slick (Gong et al., 2014). The oil planned to be used for the Ohmsett testing is not viscous enough for this failure method. Operation of booms in seas where there are waves can result in other failures (e.g., splashover, submergence, planing, and critical) (Zhang et al., 2002). These failure modes will not be discussed in this report as all testing for this effort will be in calm water.

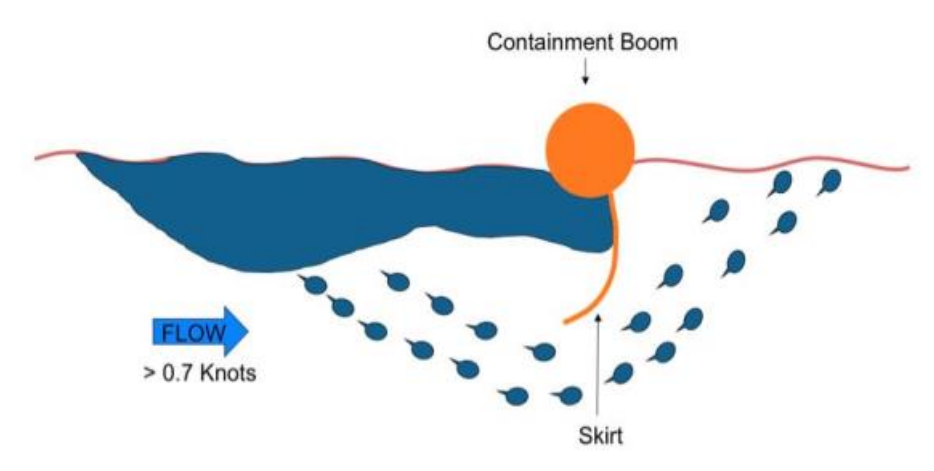


Fig. 18 Entrainment failure mode. (ACME Environmental from (Baker et al., 2019)).

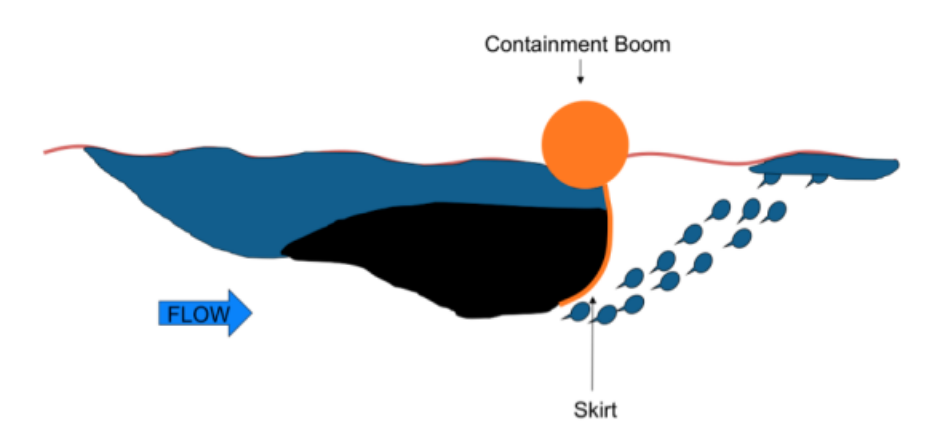


Fig. 19 Drainage failure mode. (ACME Environmental from (Baker et al., 2019)).

3.1.2. Approach

The commercial software package ANSYS Fluent (2022R1) was used to simulate the multiphase flow past the three oil boom designs. The solver is a finite volume method that calculates the solution to the Navier-Stokes equations based on a collection of cells, with the vertices of each cell based on a series of grid points. The primitive variables (e.g., temperature, and velocity) are solved for within each cell.

A Volume of Fluid (VOF) method was used to accurately track the three phases in the simulation: air, oil, and water. The VOF method allows for the development of oil droplets at the oil-water interface (if they exist). It also captures the movement of the water surface, including the collection of water upstream of the boom (e.g., a headwave), which can rise above the quiescent free surface level and onto the boom. The VOF method is such that it can track the movement of the initial layer of oil on the surface of the water and the movement of the oil under the water surface as well as past the boom skirt, if failure occurs. While not expected to occur at the tow speeds of up to one knot, if waves were generated such that they would crest over the boom (i.e., splashover failure) this would also be captured with the solver. It should be

noted that this is one of the few CFD analyses that simulates three fluids in a single simulation (i.e. air, water, and oil). The majority of prior simulations, neglected the air in the simulation.

While the CFD solver can be used to simulate the oil/water flow approaching the boom some assumptions are made to reduce the calculation time. The major assumptions for this work are:

- 1. The air, oil, and water are incompressible fluids.
- 2. The oil is modeled as a Newtonian fluid.
- 3. Critical failure is not expected for these simulations.
- 4. The boom geometry is modeled as a single, rigid boom without linkages. Inflatable booms are comprised of segments to prevent failure of the entire boom if one segment leaks. However, the geometry is constant along the entire length.
- 5. The shape of the boom skirt is fixed along the length of the boom. The skirt will deflect based on hydrodynamic forces as it is towed through the water. While the dynamic deflection of the skit could be determined with a coupled fluid-structure model the added complexity would not improve the results.
- 6. The boom is modeled with a fixed orientation. The shape of the boom is anticipated to be catenary-shaped. This was confirmed during the physical testing.
- 7. The vertical position of the boom is fixed in the water, i.e. no heave or pitch. This was confirmed during the physical testing.
- 8. The symmetry plane along the axis parallel to the tow direction is utilized so that only half the boom is modeled. This provides a significant cost savings in the calculation time.
- 9. The turbulence model used is the Stress Blended Eddy Simulation. This is a hybrid RANS-LES turbulence model. The benefits of this model will be discussed in more detail below.

Of these assumptions, one that plays a significant role in an accurate CFD simulation is the turbulence model. There are three main types of turbulence models: Direct Numerical Simulation (DNS), Large Eddy Simulation (LES), and Reynolds-Average Navier-Stokes (RANS), with different levels of complexity within each of these main types. In the solution of the Navier-Stokes equations a DNS solver will resolve all scales of the flow explicitly and no turbulence model is needed. For high Reynolds number¹ flows, this is typically not practical due to very refined grids that lead to extremely long calculation times. The next level of sophistication is a LES. This will directly calculate the flow away from the wall but uses a near-wall turbulence model for the boundary layer. This allows for an accurate calculation of the flow structures that can significantly affect the flow, while using well established turbulence models for the boundary layer. The next major demarcation in turbulence model is the one that has seen the most usage due to a balance of accuracy with lower calculation time is RANS.

A RANS model that is often used in marine type flows is Menter's SST turbulence model (Menter, 1994). This combines a turbulence model that is well-suited to wall bounded flows $(k-\omega)$, while using another turbulence model $(k-\varepsilon)$ for shear layers and recirculating flows.

20

¹ The Reynolds number is the ratio of inertial forces to viscous forces within a fluid which is subjected to relative internal movement due to different fluid velocities. The Reynolds number can be used as a guide to determine expected flow patterns and laminar versus turbulent flow.

However, there is a concern with accurately capturing entrainment failures, where droplets of oil leave the captured oil mass and pass under the skirt. A RANS model may not be able to capture this fine scale movement of fluid and a more accurate turbulence model is probably warranted. Rather than move to a LES model, which can have significant increases in calculation time associated with it, a hybrid RAN-LES model was used.

The turbulence model is the Stress-Blended Eddy Simulation (SBES) (Menter, 2016). SBES is an improved RANS-LES hybrid model that captures the turbulence shear in the thin boundary layer with RANS and the vigorous turbulence transport in the shear layer away from the wall via LES.

3.1.3. Initial Conditions

The CFD modeling and analysis is a three-dimensional analysis that replicates the experimental testing. The CFD model was developed from a computer-aided design (CAD) model for each of the three booms. This model is a collection of grid points that surround the boom as well as upstream and downstream of the boom. The boom is stationary, and the water moves past the boom.

The location of the bottom of the tank in the computational model should not affect the results as long as it is a depth of at least four times the draft (Baker et al., 2019). For the experimental test the depth of the tank was 2.4m. The width is 20m and the length is 203m. The largest draft of the boom is for the full-scale booms and is 0.61m. Thus, a slight affect due to the interaction of the tank bottom is possible. The results will be examined to determine if there is any interaction.

For the Elastec Foam boom design a CFD model was generated for full, 50 percent, and 25 percent scales. The Elastec Airmax Inflated boom and Abasco Air-Inflated Ocean boom were analyzed at full scale only.

The setup and some initial verification of the CFD models for the booms was conducted prior to the experimental testing. The towed shape of the boom was observed during the physical testing and matched the expected catenary shape pretty well thus the CFD modeling was all executed with the booms in the catenary shapes. The CFD analysis was initialized with a preload volume of oil, similar to the experiment. The oil was evenly spread on top of the water inside the boom and then the simulation started with a velocity of 0.5kts (for full-scale). The smaller scale simulations were started with a lower initial velocity. To match the physical experiments, the velocity was increased by 0.1 knots every 10 to 15 seconds. The time step is small enough to ensure the flow characteristics are accurately captured. This continued until entrainment or drainage failure was achieved (expected to be around 1.0 to 1.1 knots for the full-sized booms).

3.2. CFD Simulation and Results

3.2.1. Model Development

A CAD model for each of the booms was electronically created based on the physical booms. The X direction increases in the direction the boom is moved with the X origin at the leading edge of the boom. The Y direction is positive towards the symmetry plane with y = 0 at the

centerline, and Z is positive up with Z=0 at the base of the floation. Diagrams of the floats are shown in Fig. 20 and Fig. 21. To visualize the difference in scales the three different scales for the Elastec Foam boom are provided in Fig. 22. To reduce the number of grid points, which will reduce the simulation time, a symmetry plane is used. This symmetry plane is through the apex of the boom and is along the direction of travel for the boom. The computational domain extends from this centerline plane normal to the tank wall. This reduces the number of grid points by a factor of two. The half-booms used for the analysis are shown in Fig. 23.

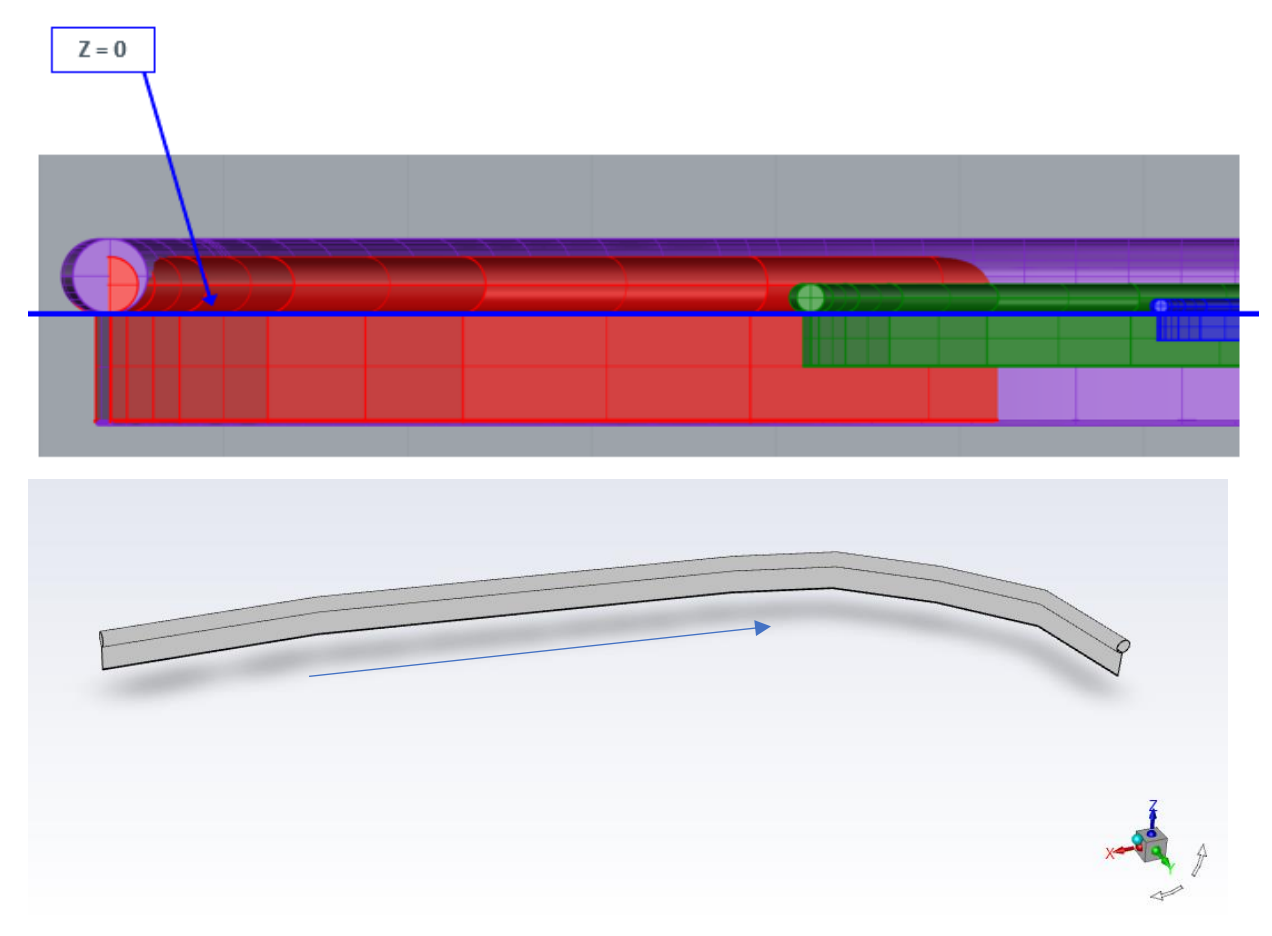


Fig. 20 CAD boom models.CAD model of all booms with water surface shown at Z = 0 (top). Orientation of the boom (bottom). Flow is in the negative X direction (arrow).

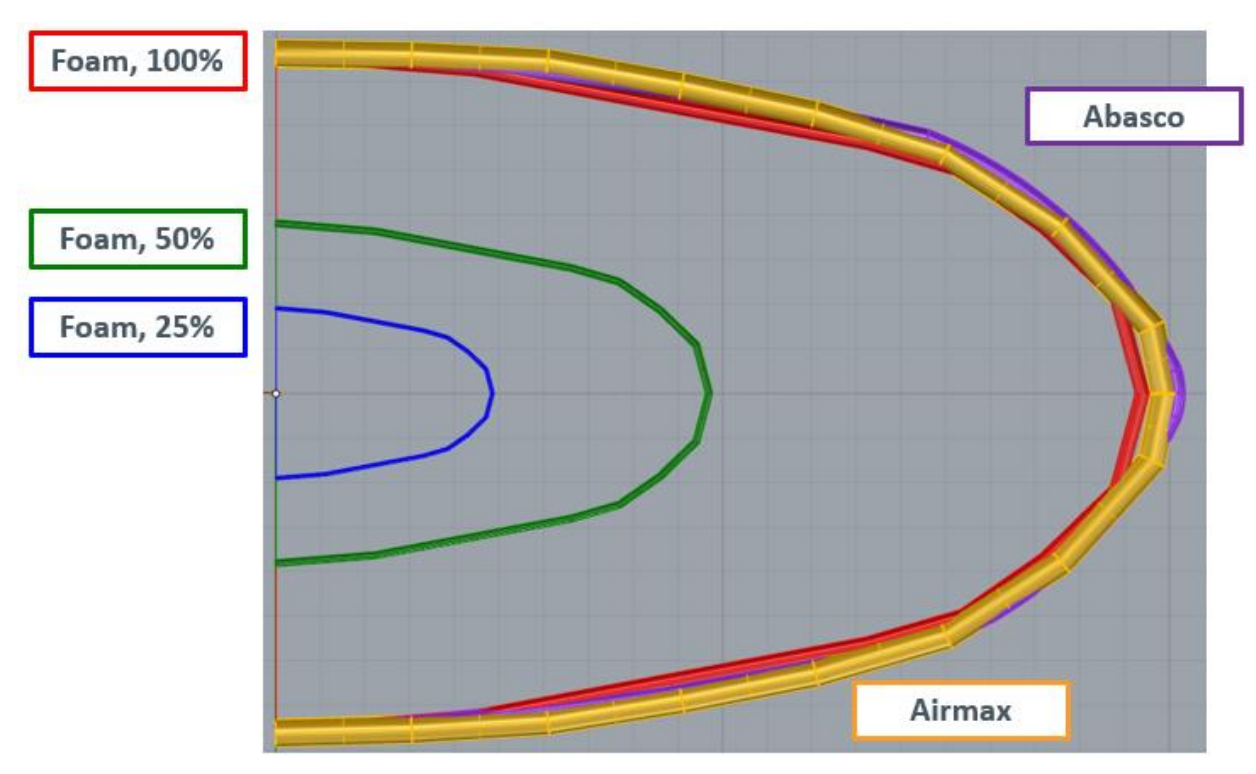


Fig. 21 CAD geometry of all booms, view from above.

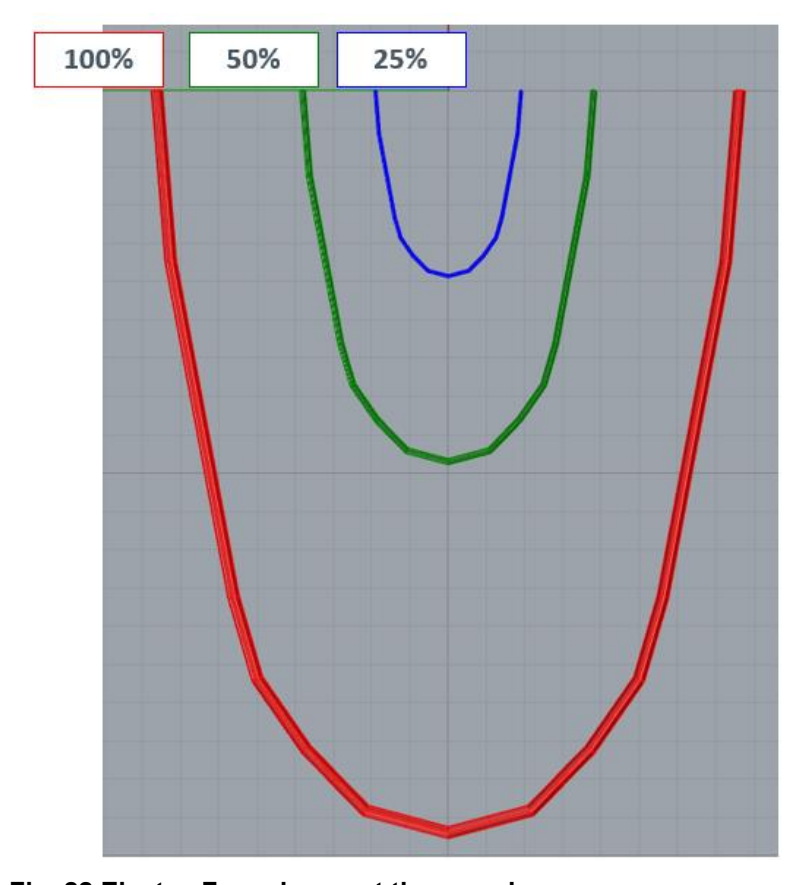


Fig. 22 Elastec Foam boom at three scales.

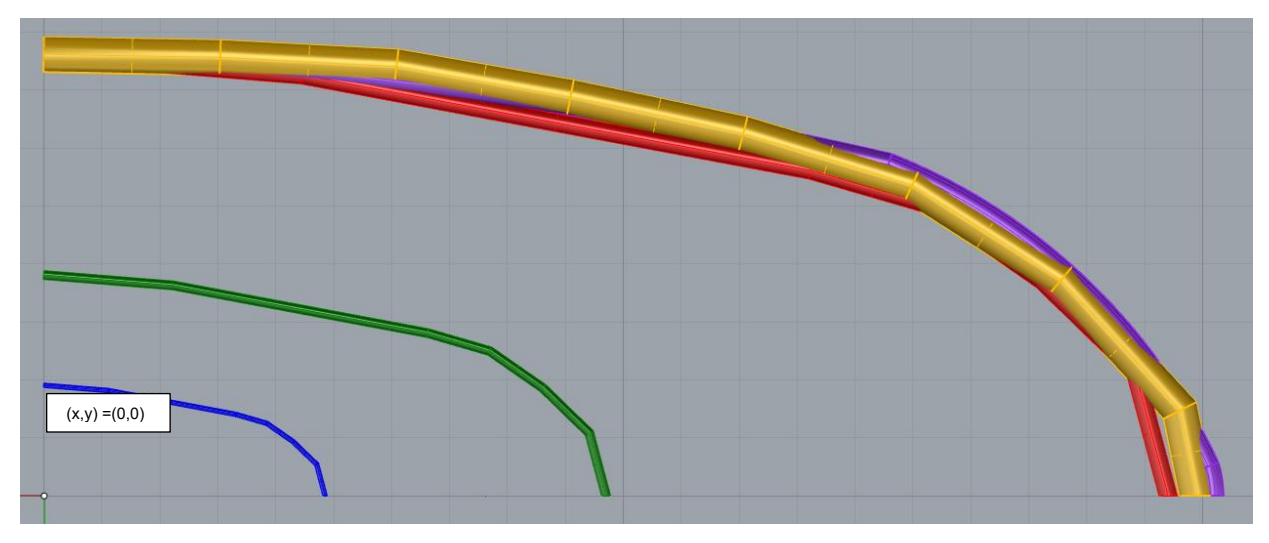


Fig. 23 Geometric models used for CFD analyses; symmetry plane portion removed.

3.2.2. Grid Development

The commercial software Pointwise was used to develop a hybrid grid with both structured and unstructured blocks. The structured blocks are immediately surrounding the boom and the unstructured blocks are used everywhere else. Solutions on the hexahedral cells in the structured grids are typically more accurate in boundary layer regions, which are surrounding the boom. There are also finer controls available in the grid generation for structured grids, which is important to accurately capture the movement of the oil and the air/water/oil interfaces.

A hybrid grid was generated that maximized the use of structured and unstructured grids. On the surface of the boom and skirt, structured grids are used. The spacing is approximately 0.01 to 0.025m, depending on the direction on the surface. A portion of the surface grid for the Elastec Foam simulation is shown in Fig. 24. These surface grids are extruded normally to provide tight grid spacing near the booms to capture fluid interactions with the boom. The extrusion normal to the surface varies from 0.25 millimeter (mm) (25 percent scale) to 1mm (100 percent scale). A grid surface is placed along the z = 0.03 plane, which is the surface of the water when the boom is at rest. This grid surface is replicated vertically up and down with a spacing normal to this surface of 2mm. This tight spacing is used to accurately capture the thin layer of oil on the water surface (12.7mm). The grid spacing for the different models is presented in Table 9.

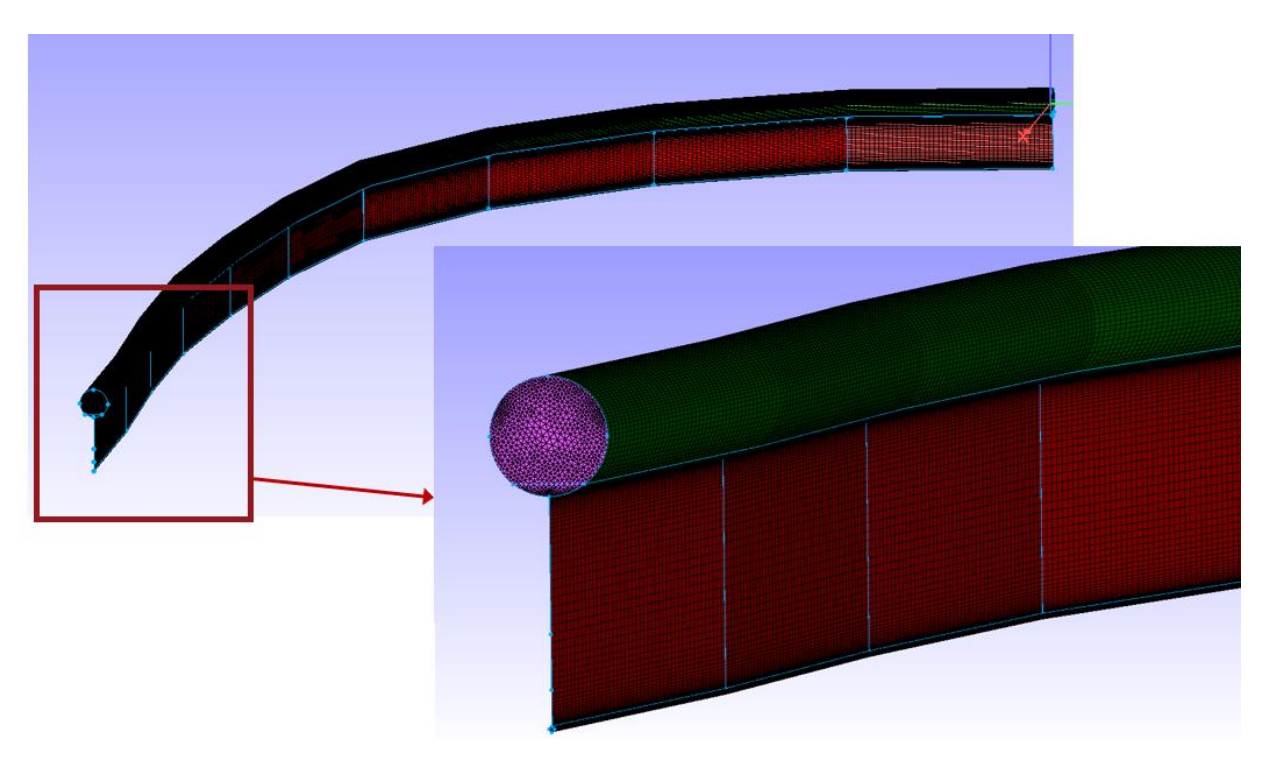


Fig. 24 Surface grid for full-scale Elastec Foam boom.

Table 9. Grid cell counts and spacing for different booms

Boom	Scale	Cell Count	Cell Spacing Normal to Boom (mm)	Cell Spacing Normal to Water Surface (mm)
Elastec Foam	100%	26.3 M	1	2
Elastec Foam	50%	23.7 M	0.5	5
Elastec Foam	25%	24.1 M	0.25	5
Abasco	100%	20.9 M	1	2
Elastec Airmax	100%	23 M	1	5

The size of the tank at Ohmsett is 2.4m deep, 20m wide, and 203m long. The CFD simulation is conducted by having the boom stationary and having the water flow past the boom. This is analytically the same as having the boom move through water. Since a symmetry plane is used the width of the computational domain is 10m and the depth is the same as the tank, 2.4m. The inlet boundary is upstream of the leading edge of the boom approximately twenty times the full-scale draft. The outlet boundary is approximately a distance of thirty times the full-scale draft from the apex. The full-scale draft is 0.61m. An overall view of the computational domain is given in Fig. 25.

A visual representation of the grid spacing and organization is provided in Fig. 26 through Fig. 30. This is the grid for the Elastec Foam but is representative of other grid spacings. The darker the green, the smaller the spacing of the grid cells. Large grid cells are easily seen in green. The grid size is represented by the size of the triangle or rectangle. The grid sizes for all three Elastec Foam scales are similar. Normally, the number of grid cells that will be needed to

analyze the flow past a shape is proportional to the size. Thus, one might expect the 50% scale boom to require half the number of grid points of the full scale boom. However, the number of grid points is similar as the air/water interface must be well discretized to accurately simulate the movement of the oil. Also, as the size of the boom decreases the spacing normal to the boom surface decreased to capture the curvature of the boom, which resulted in more grid points.

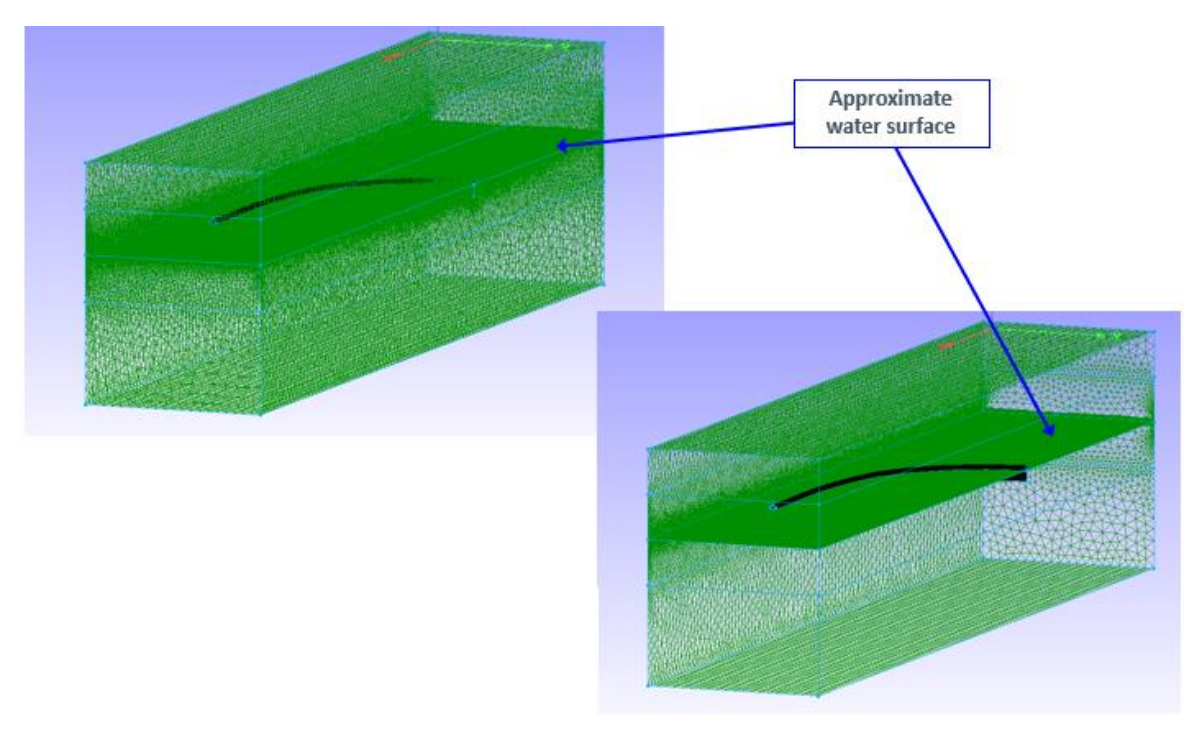


Fig. 25 Computational domain for Elastec Foam with water surface.

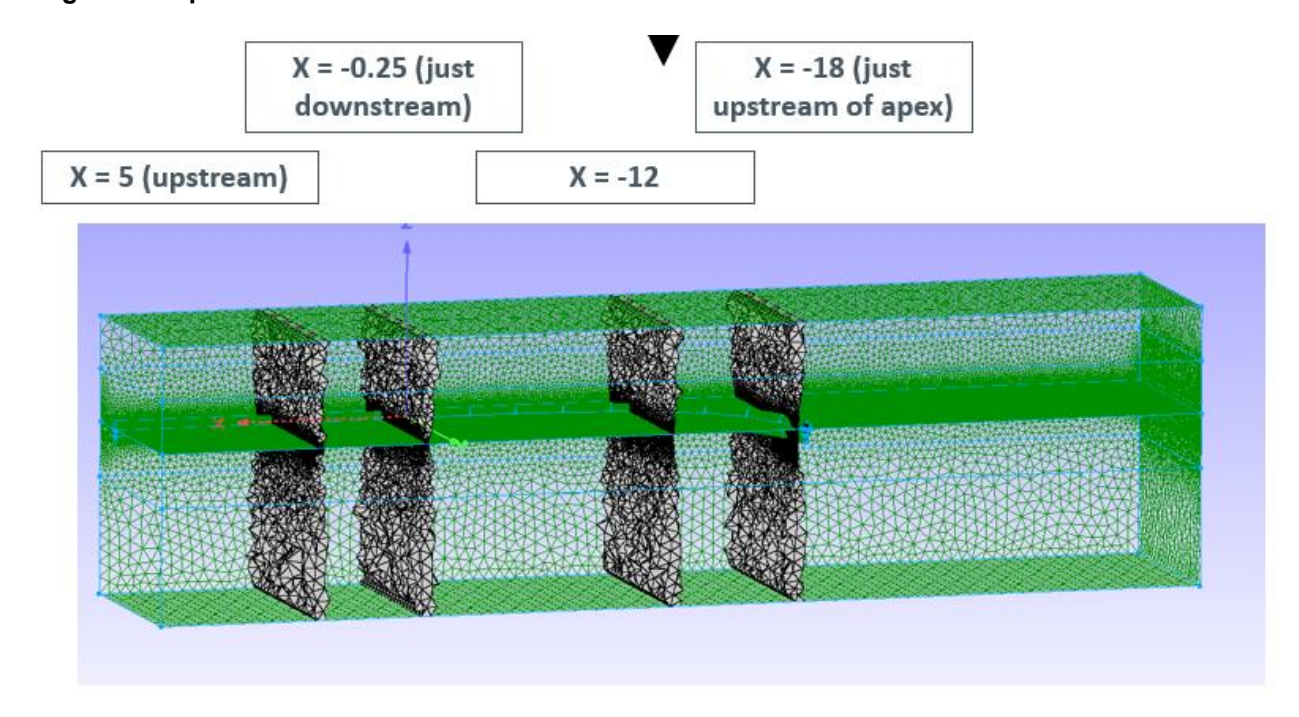


Fig. 26 Selections for cuts in the X direction.

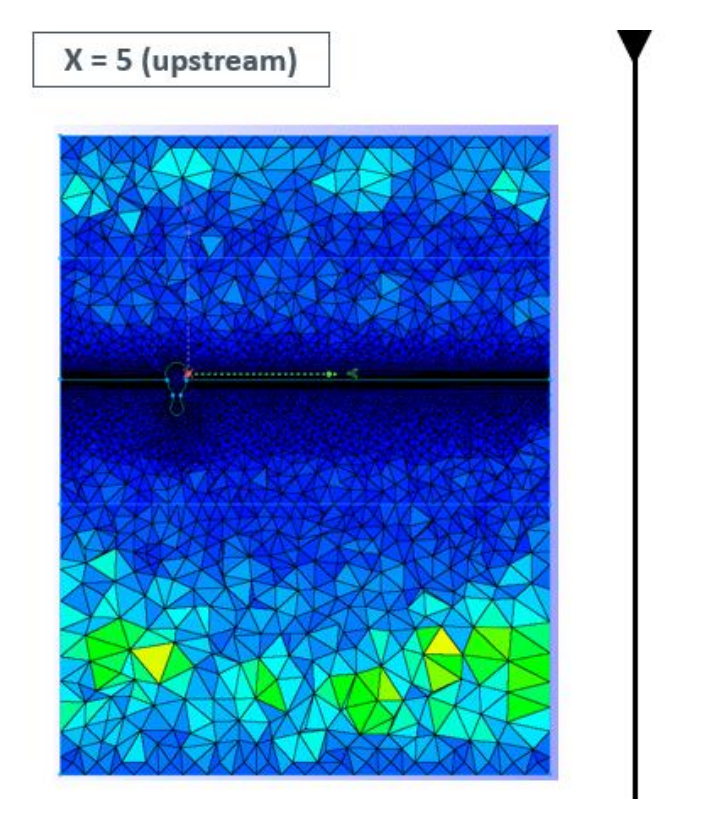


Fig. 27 Two X-cuts for the Elastec Foam grid.

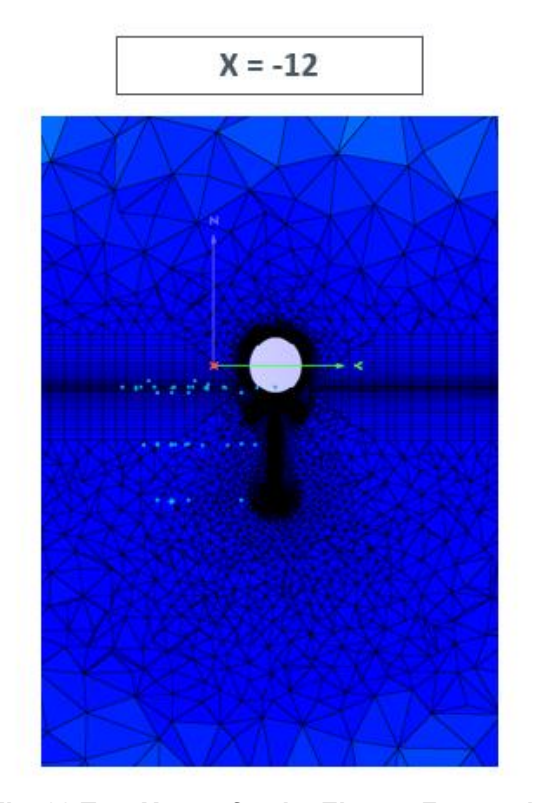
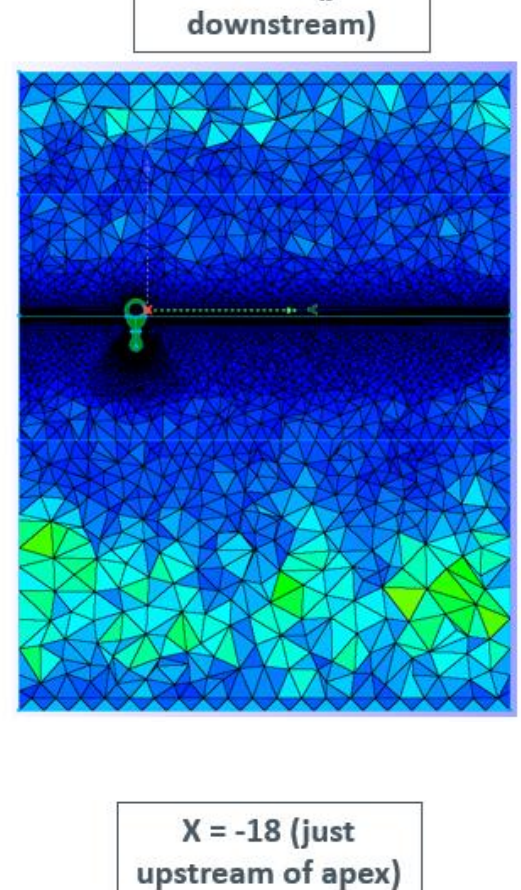
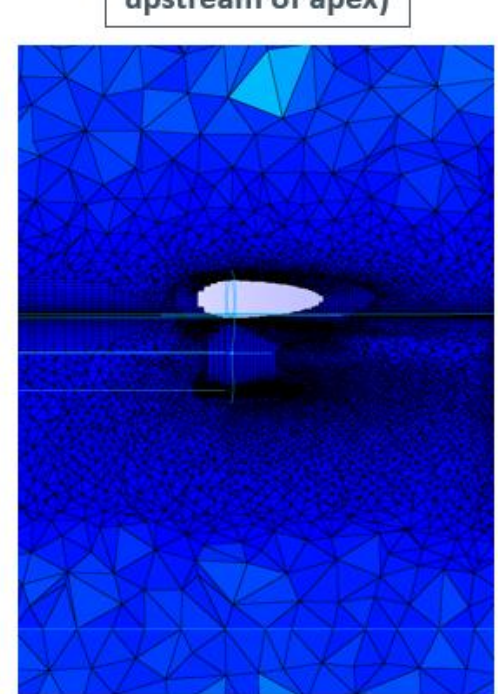


Fig. 28 Two X-cuts for the Elastec Foam grid.



X = -0.25 (just



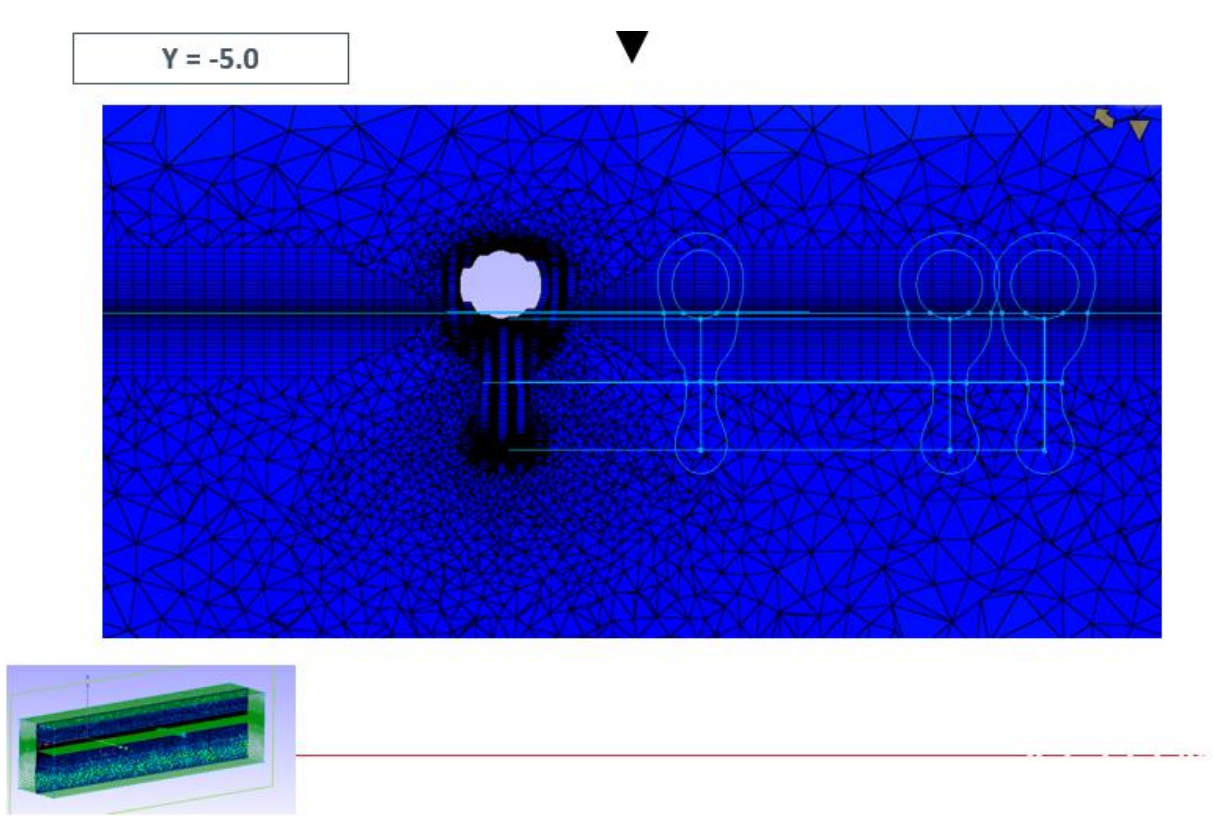


Fig. 29 Y= -5.0 cut for Elastec Foam grid.

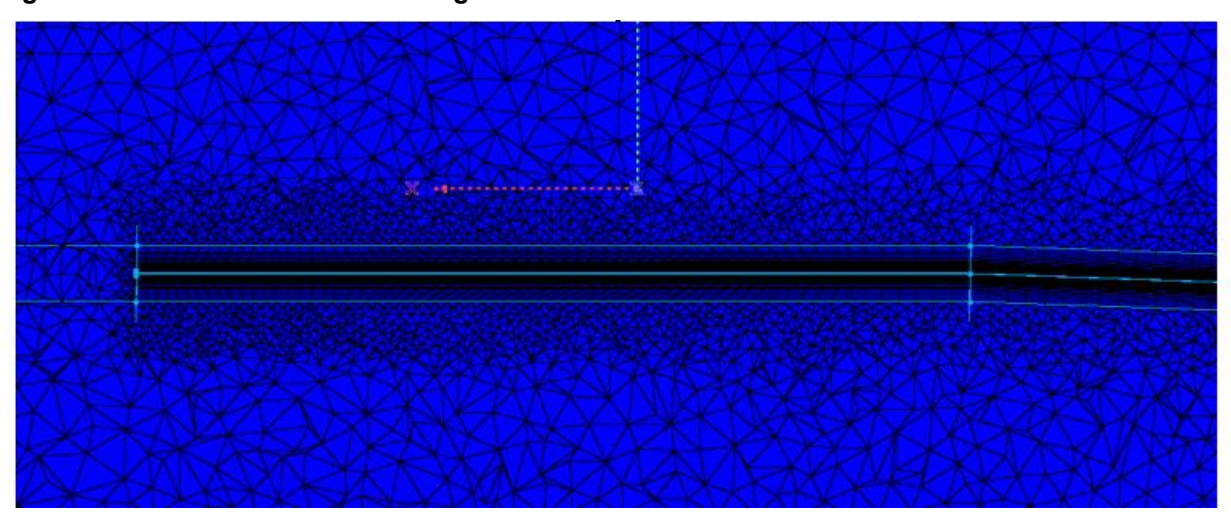


Fig. 30 Z = -0.25 cut (middle of skirt) as viewed from below.

3.2.3. Boundary Conditions

The water moves past a fixed boom, which allows for a smaller computational domain. The inlet boundary is placed a distance upstream of the boom that is approximately twenty times the full-scale draft. The outlet boundary is downstream of the boom by approximately thirty times the full-scale draft. One side of the domain will be modeled with a symmetry boundary condition. The other side of the domain will be modeled with either a pressure outlet boundary condition (for the part of the domain above the water line) or a solid wall boundary condition (to represent

the wall of the tank). Since the boom will be towed during the experiment the waves that develop from the passing boom will reach the tank walls and reflect without affecting the boom operation as the boom will have already moved upstream. The boundary conditions for the computational domain are shown in Fig. 31. The draft of each boom (defined as the height of the skirt) is:

Elastec Inflatable, 100% 0.61m
Elastec Foam, 100% 0.61m
Elastec Foam, 50% 0.30m
Elastec Foam, 25% 0.15m
Abasco Air-inflated, 100% 0.61m

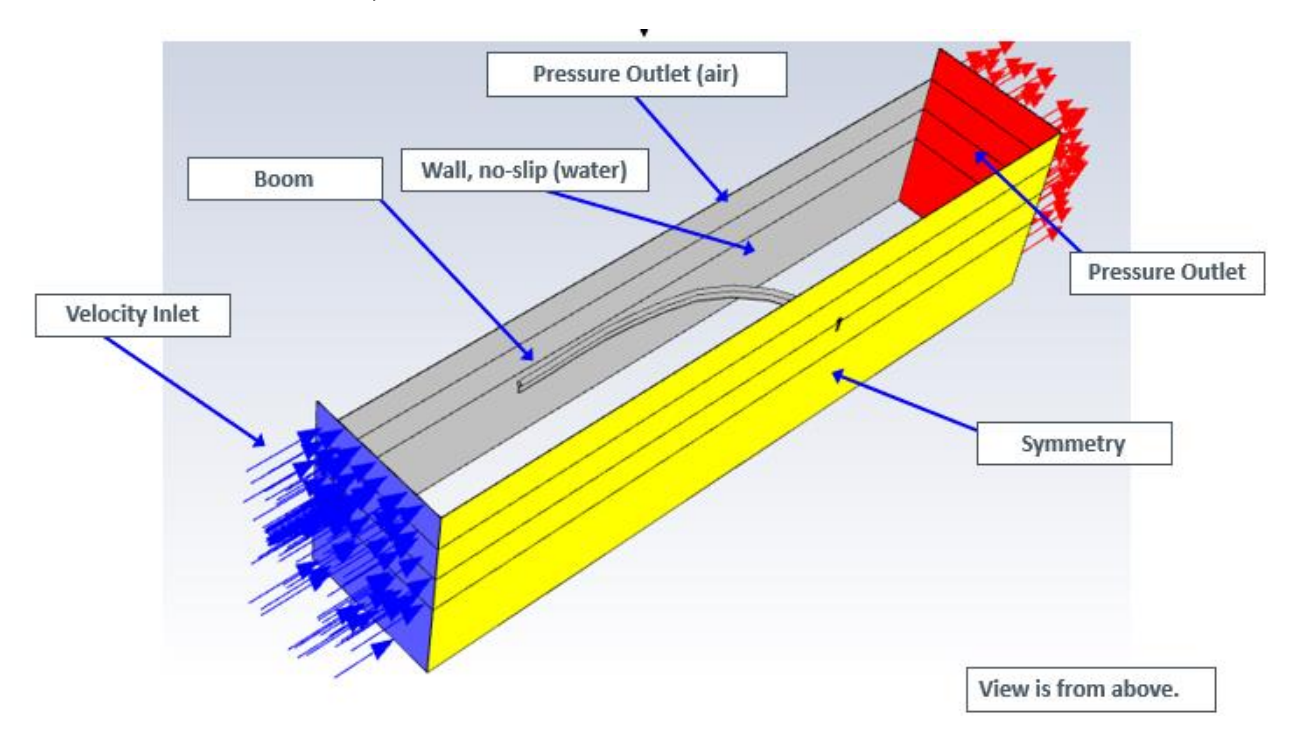


Fig. 31 Boundary conditions.

3.2.4. Initial Conditions

The initial velocity for each simulation is given in Table 10. Each analysis started with a preload of oil that roughly covers the interior of the boom.

Table 10 Initial velocity and speed increments for each scale boom

Scale	Starting Speed (kts)	Expected Top Speed (kts)	Speed Increment (kts)
100%	0.5	1.2	0.1
50%	0.35	0.85	0.05
25%	0.25	0.60	0.05

The oil used in the simulation is Hydrocal 300. At a temperature of 20 degrees centigrade (°C) (68 degrees Fahrenheit (°F)) this oil has a density of 910 kilograms per cubic meter (kg/m³), kinematic viscosity of 1.9E-4 square meters per second (m²/s), and dynamic viscosity of 0.1729

kg/(m·s). This data is based on Fig. 32. Note, that this value is slightly lower than the viscosity of the Hydrocal oil as measured after the physical testing (~0.2 kg/(m-s). For the full scale boom a preload of 1.89m³ (500 gallons) of oil is used, to match the experimental test. At smaller scales smaller amounts of oil is used: 0.473m³ (125 gallons) at 50 percent scale and 0.132m³ (35 gallons) at 25 percent scale. The amount of oil in the simulation is halved to account for only modeling the starboard side of the boom through symmetry. The initial thickness of oil is 12.7mm (0.5 inch). The oil is added in three different locations, as shown in Fig. 33. The small inset figure shows the different phases of the oil and water, with water in blue and oil in red. These unrealistic initial load areas were used to make the application of the oil into the scenario easier; as the simulation progresses the oil spreads out and pushes up against the boom to match the physical testing observations.

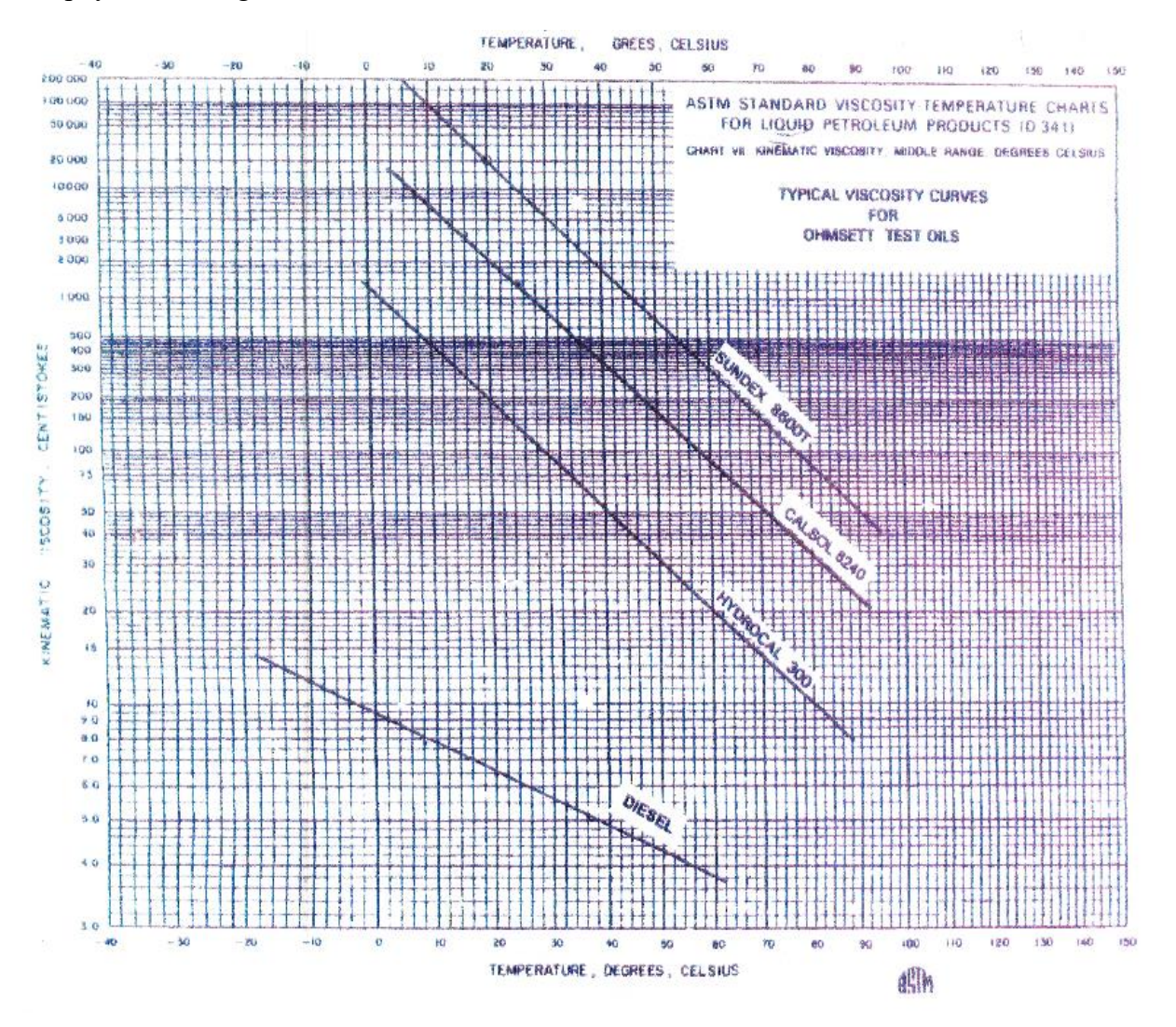


Fig. 32 Viscosity curves for Hydrocal 300 and Calsol 8240.

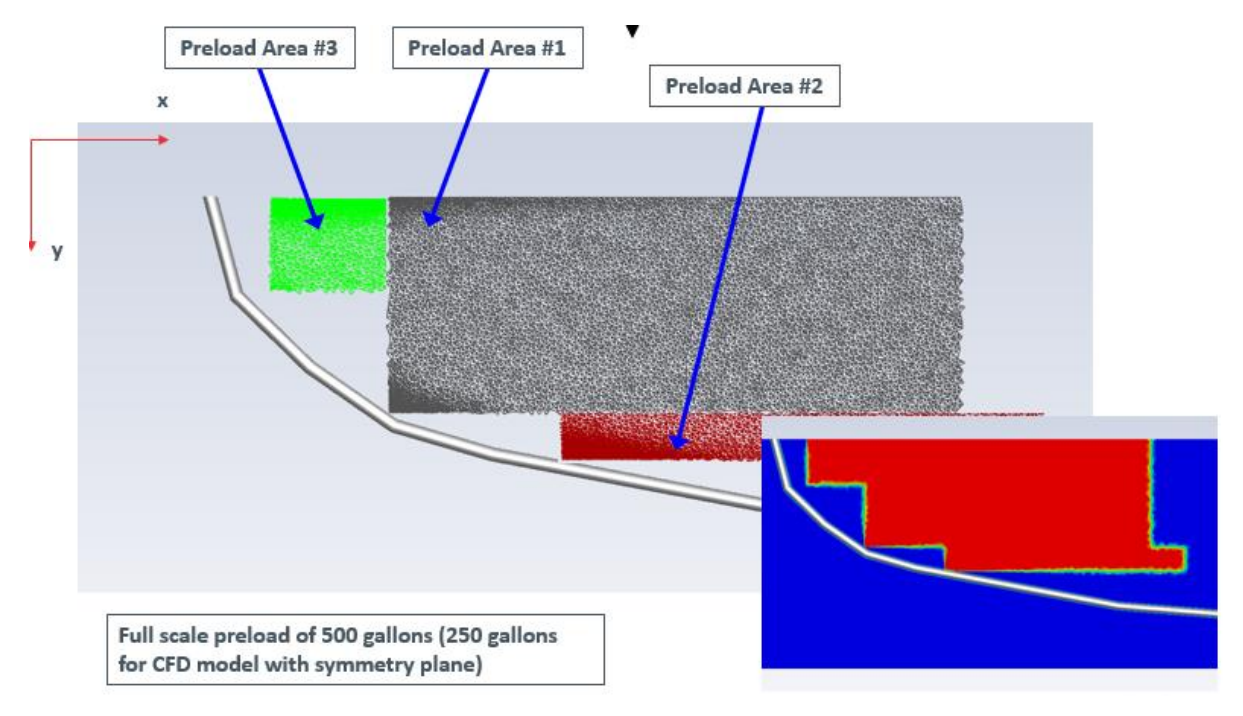


Fig. 33 Initial condition for oil (Baker et al., 2019).

The different scenarios are listed in Table 11. The top speed is the estimated speed at which entrainment will occur. The top speed is based on Froude scaling for when the 100 percent scale boom is expected to experience entrainment.

Table 11 Different simulations as well as the estimated top speed

Case Number	Boom	Scale	Oil Type	Preload Amount (gal)	Est. Top Speed (kts)
1	Elastec Foam	100%	Hydrocal 300	250	1.2
2	Elastec Foam	50%	Hydrocal 300	62.5	0.7
3	Elastec Foam	25%	Hydrocal 300	17.5	0.5
4	Abasco	100%	Hydrocal 300	250	1.2
5	Elastec Airmax	100%	Hydrocal 300	250	1.2

3.2.5. CFD Results

This section provides the results from the CFD simulations. There are a number of planes that results will be shown for. The four most common planes are shown in Fig. 34 relative to the boom.

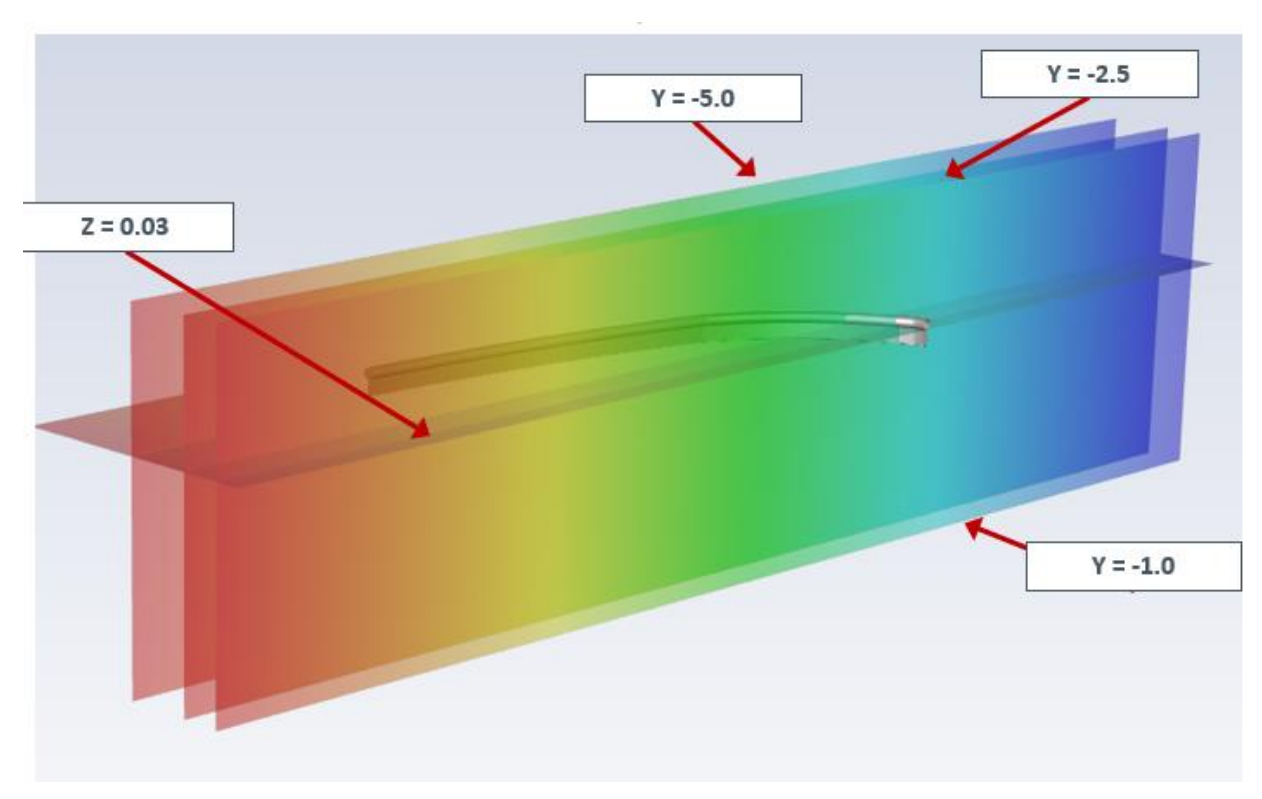


Fig. 34 Iso-surfaces for results.

3.2.5.1. Elastec Foam, 100%

The initial condition of the oil is given in Fig. 35. There is an initial "start-up" period where the flow moves at 0.5 knots but the oil is not against the boom yet. This "start-up" period is experienced in the experimental test as well though the initial condition of the oil is different since the oil is added in a haphazard fashion to inside the boom.

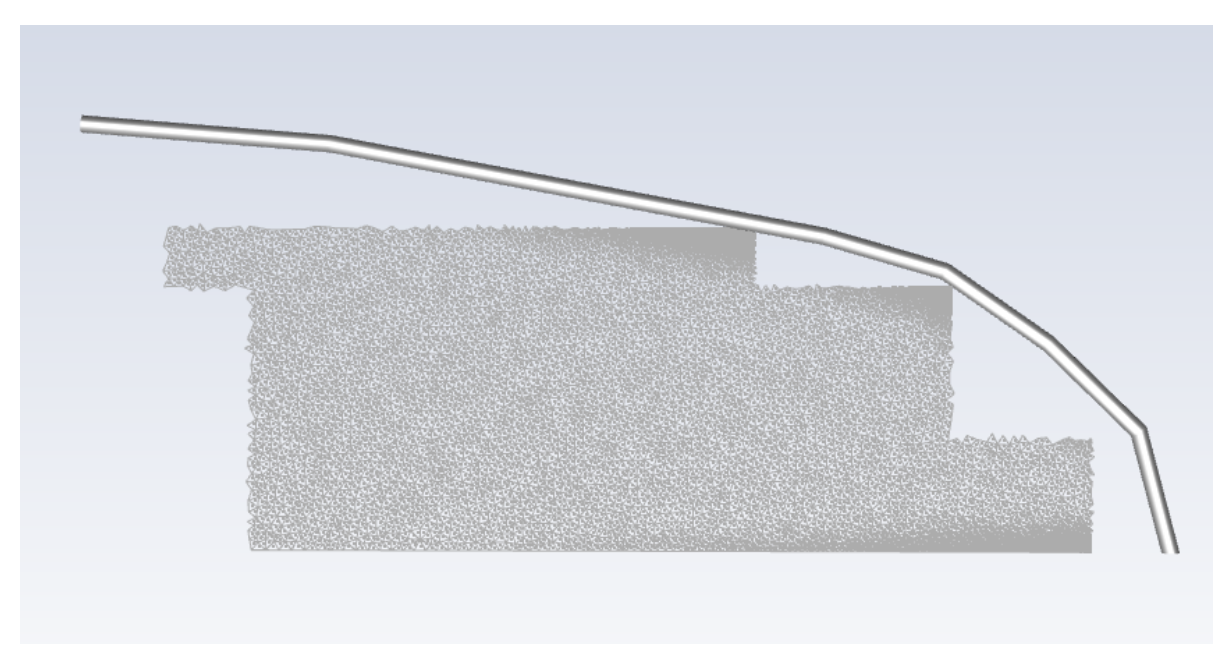


Fig. 35 Elastec Foam, 100%. Initial condition of oil at Z = 0.035, as viewed from above.

The results of the oil during this initial period are not important as the main focus is to get the oil up against the boom. No entrainment is expected until at least 0.9 knots, so the transition from 0.5 to 0.9 knots will roughly follow the experiment. Fig. 36 shows the dispersion of oil after some time at 0.5 knots. In this figure each grid cell that has oil in it is colored pink for viewing. The areas that are darker are where the size of the grid cells is much smaller, so when the edges of the grid cell are colored it appears as a solid cell with that coloring. In this picture the oil is starting to collect along the boom, but additional time is required to have the oil pressed along the boom.

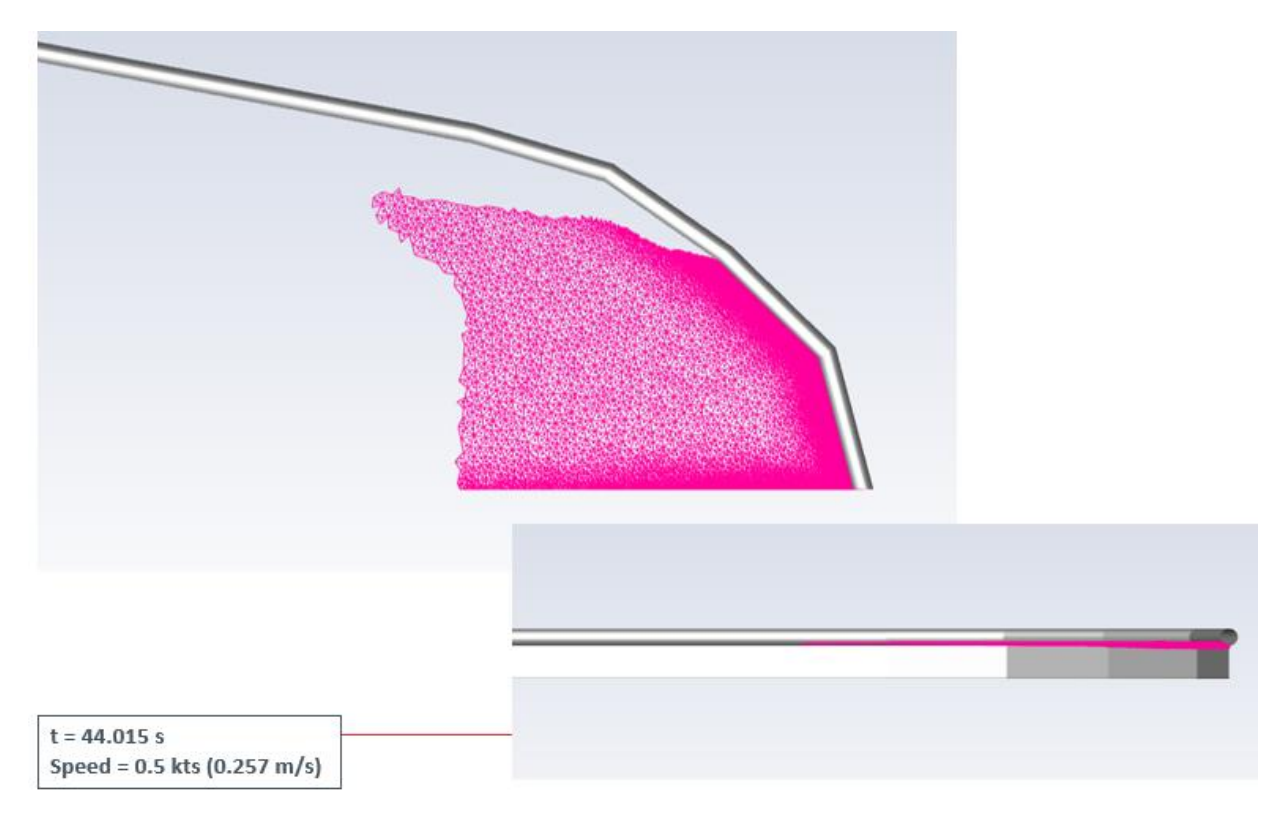


Fig. 36 Elastec Foam, 100%. Oil in the domain after 44.015 s at a speed of 0.5 knots.

Just prior to increasing the speed from 0.5 knots to 0.6 knots the velocity and phase at different simulation planes are provided in Fig. 37 and Fig. 38. For the velocity plots the dark blue region represents a region of lower velocity. The lower velocity upstream of the boom apex is expected as the flow is blocked by the boom. Similarly, just behind the apex of the boom is a region of low velocity. For the plots of phase, the air is represented by a value of 0 (blue), the water by a value of 1 (green), and the oil by a value of 2 (red). Fig. 39 is a similar plot, showing all cells (in yellow color) that have oil. Again, the darker yellow is indicative of smaller cell sizes not more oil in each cell.

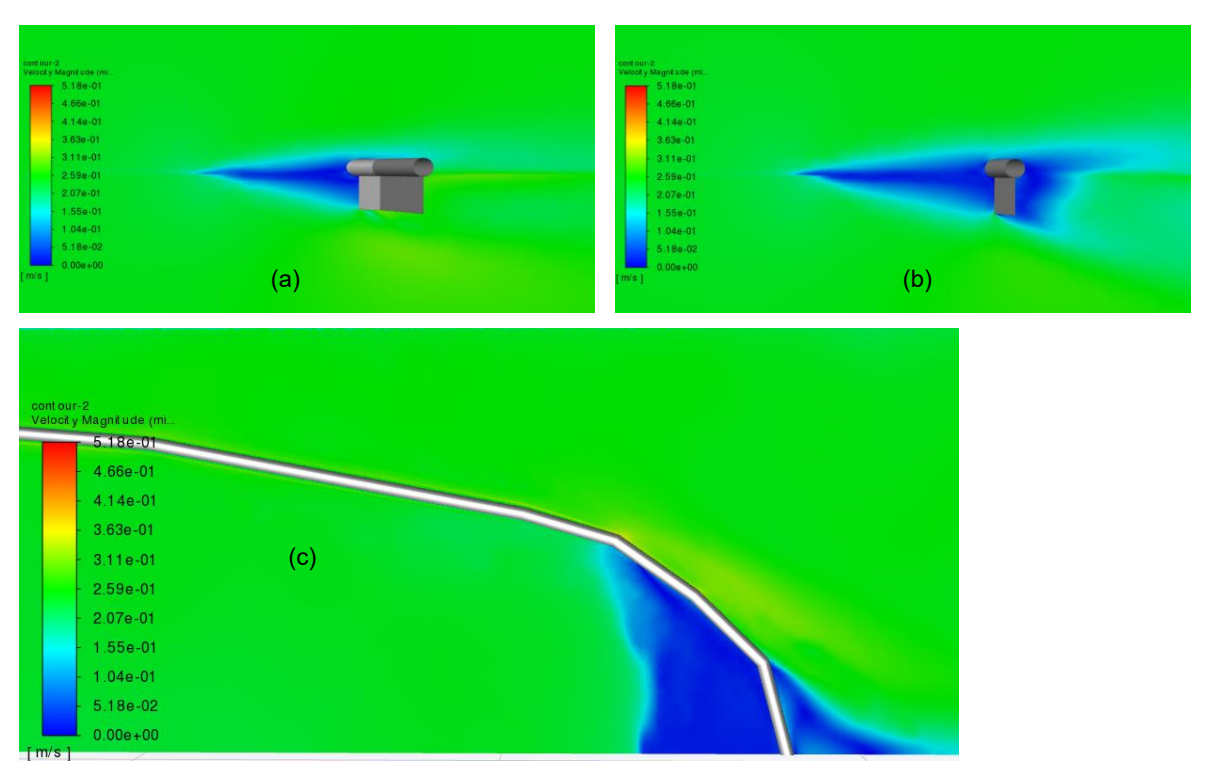


Fig. 37 Elastec Foam, 100%. Velocity on (a) y = -2.5, (b) y = -1.0, and (c) z = 0.03 planes at 0.5 kts.

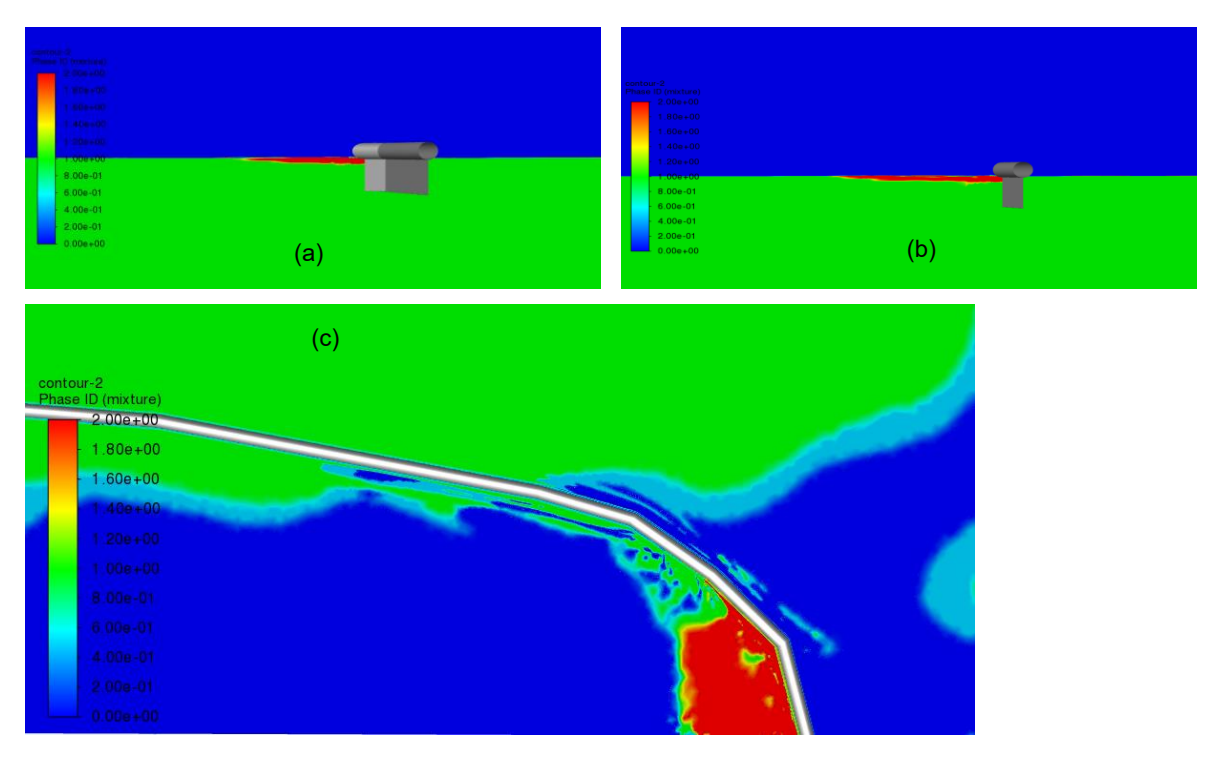


Fig. 38 Elastec Foam, 100%. Phase on (a) y = -2.5, (b) y = -1.0, and (c) z = 0.03 planes at 0.5 kts.

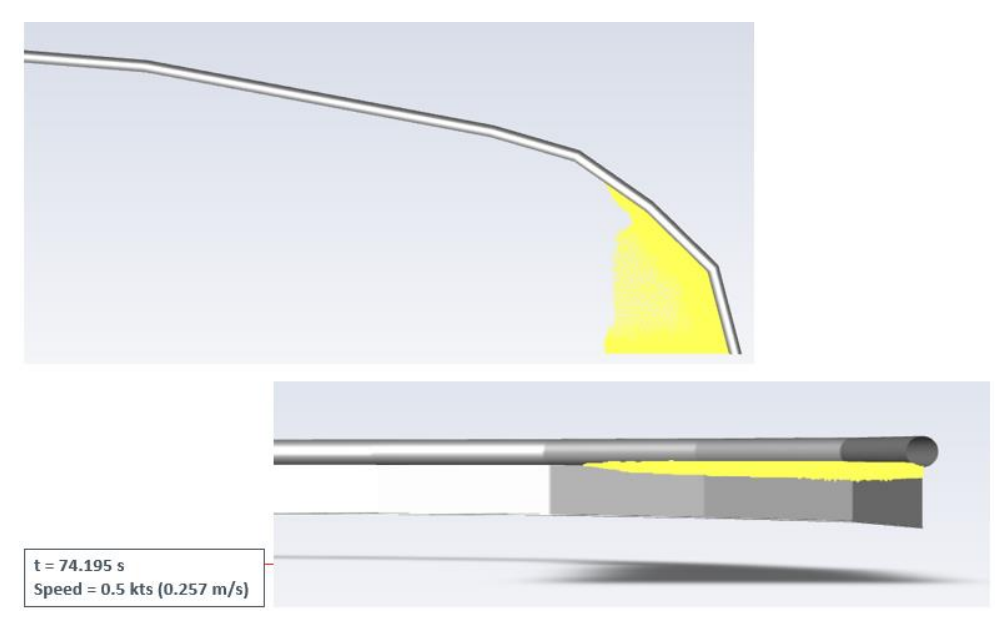


Fig. 39 Elastec Foam, 100%. Cells with oil at 74.195 s at 0.5 kts.

The simulation was continued at 0.5 knots until the oil rested against the boom as was seen during the experiment. From that point forward the velocity was increased by 0.1 knots every 10 to 20 seconds. At 176.185 sec into the simulation, at a speed of 0.8 knots the oil in the domain is shown by coloring the cells pink. This is seen in Fig. 40. Here the oil is resting against the boom, as is expected. This qualitatively matches the experimental results, as shown in Fig. 41. At a higher speed, which will be determined by the simulation, entrainment will occur.

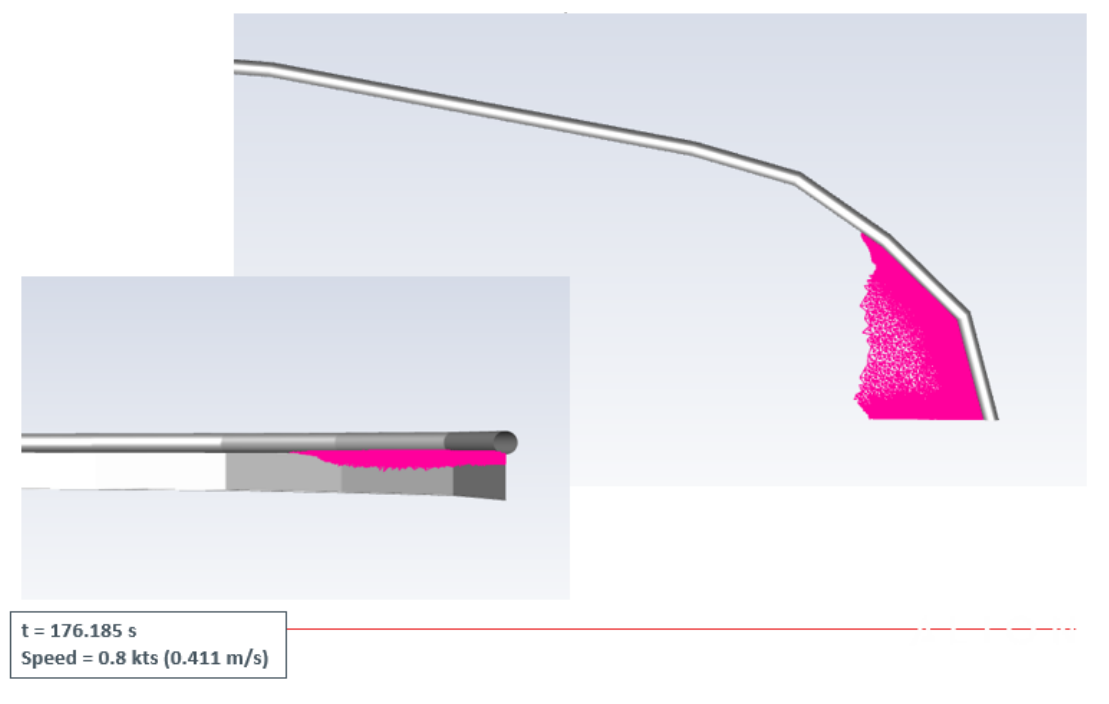


Fig. 40 Elastec Foam, 100%. Cells with oil at 176.185 s and 0.8 kts.

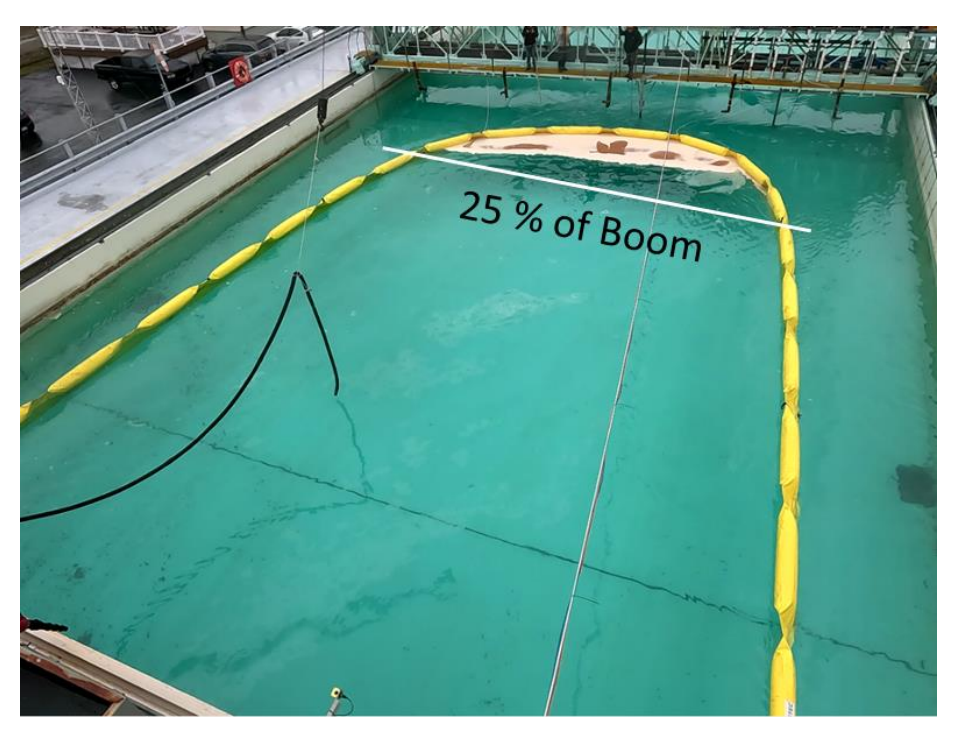


Fig. 41 The 500 gal of oil compressed into the apex during the entrainment run. 25% line is ~25% of the catenary length. At the start of the run, the oil filled about 50% of the catenary length. The oil depth is estimated at 11.4cm based on the surface area.

At a simulation time of 201.27 seconds the velocity was increased from 0.9 to 1.0 knots. The volume of oil in the domain at that time is provided in Fig. 42. First loss has not been observed yet. At 236.07 seconds with a velocity of 1.0 knots gross loss was observed. The velocity at three different planes is shown in Fig. 43. In the plot for y = -1.0 the low-speed flow is seen going underneath the boom. This is the plane near the boom apex, where entrainment is expected. The phases on the same planes are plotted in Fig. 44, where droplets of oil are seen going underneath the boom, which is the definition of entrainment. A better depiction is seen in Fig. 45, where all cells that have oil are colored pink. A speed of 1.0 knots matched the results seen experimentally.

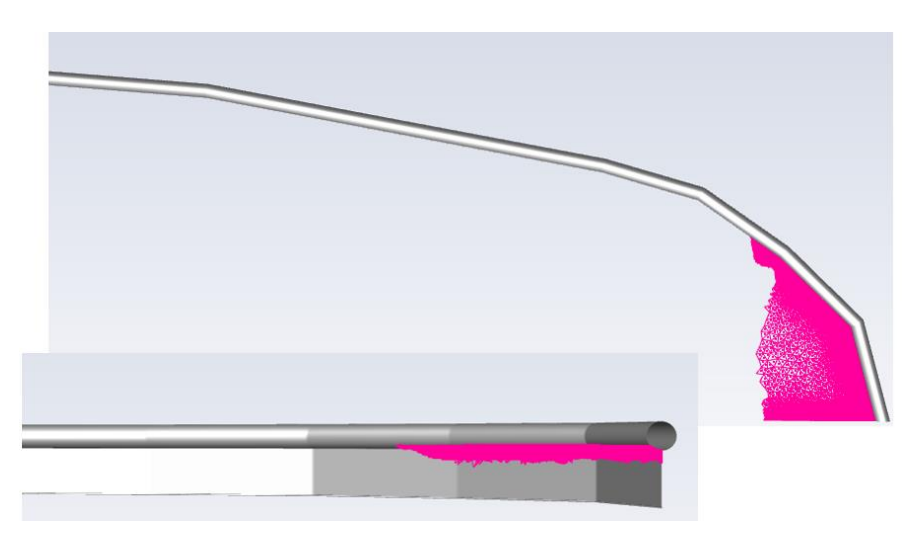


Fig. 42 Elastec Foam, 100%. Cells with oil at 201.27 s and 0.9 kts.

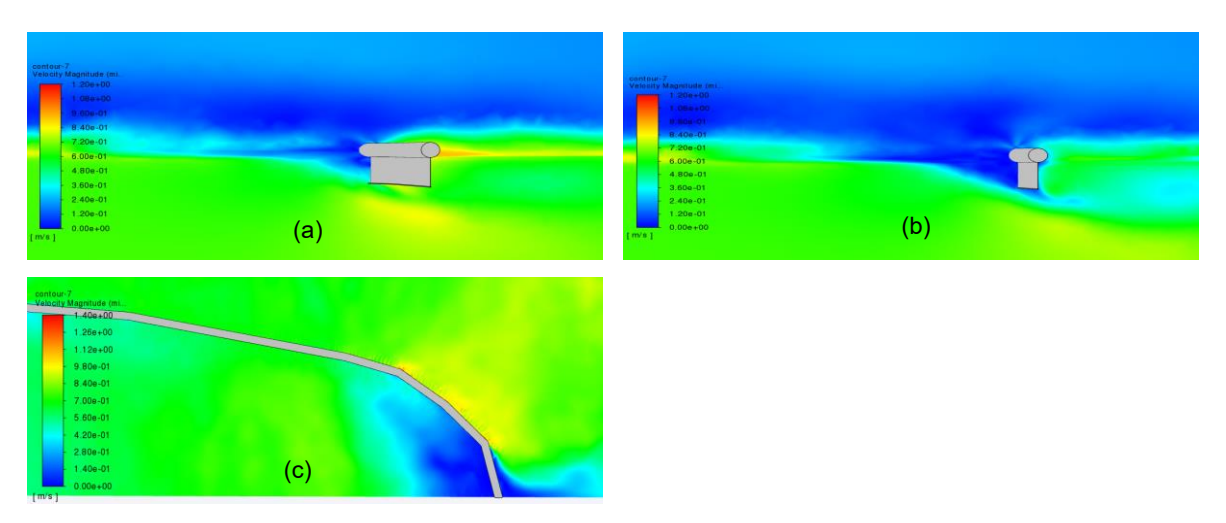


Fig. 43 Elastec Foam, 100%. Velocity on (a) y = -2.5, (b) y = -1.0, and (c) z = 0.03 planes at 1.0 kts.

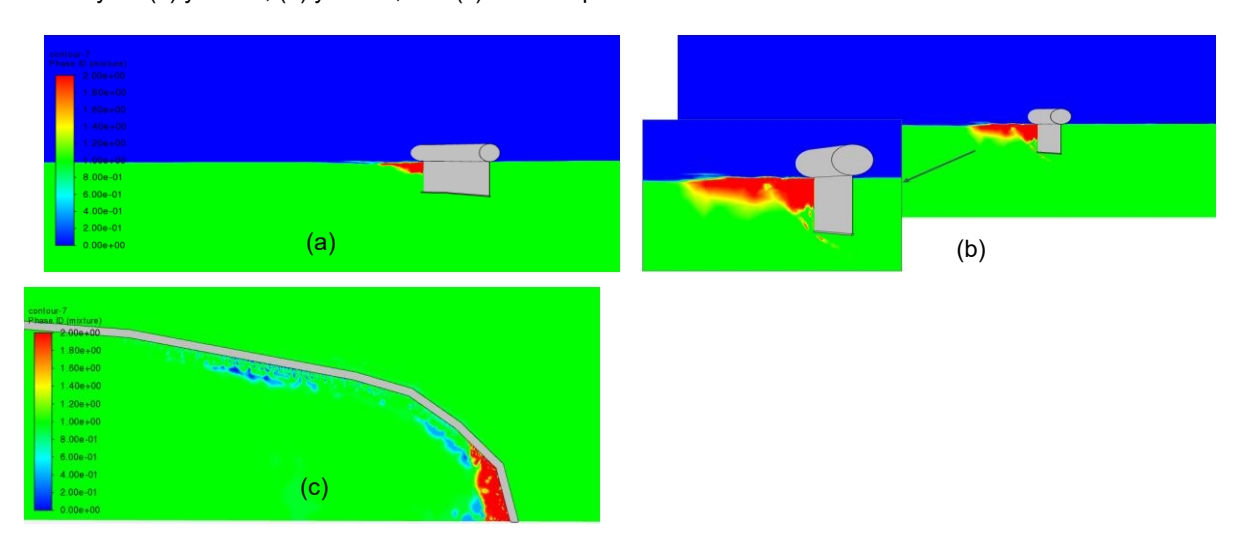


Fig. 44 Elastec Foam, 100%. Phase on (a) y = -2.5, (b) y = -1.0, and (c) z = 0.03 planes at 1.0 kts.

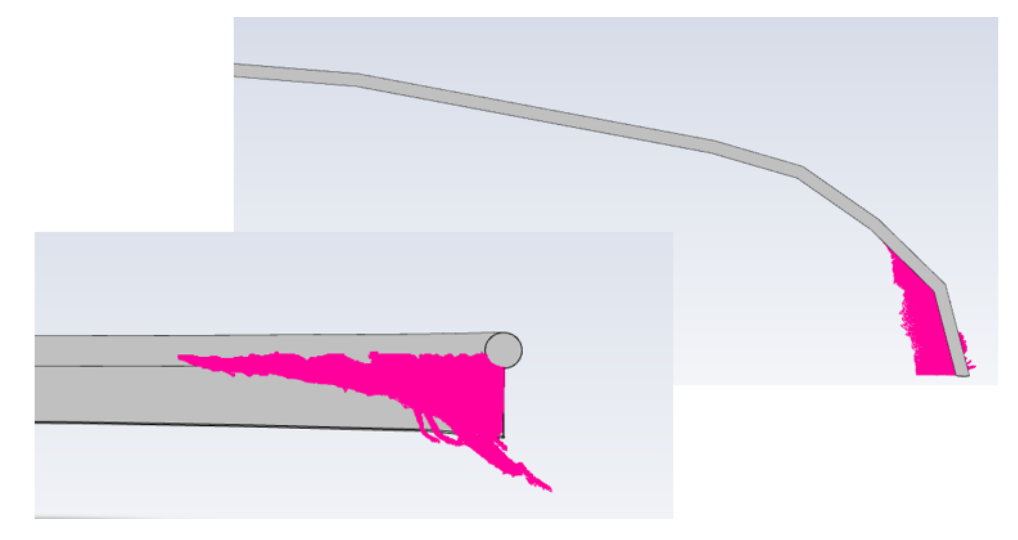


Fig. 45 Elastec Foam, 100%. Cells with oil at 236.07 s and 1.0 kts.

3.2.5.2. Elastec Foam, 50%

To understand if the CFD analysis can accurately predict the behavior of the oil collection booms at smaller scales the Elastec Foam at 50% scale was analyzed. Using the experimental test as a guideline the starting speed of the calculation is 0.35 knots. Entrainment was shown during the experiment at 0.85 knots and a similar speed is expected for the numerical simulation. It should be noted that scaling the top speed of the full-scale boom down to the half scale (Baker et al., 2019) results in a top speed of 0.68 knots, which is lower than what was seen experimentally.

The prediction of oil in the domain at 82.66 sec and 0.65 knots is provided in **Fig**. 46The oil is starting to collect near the apex of the boom, but entrainment is not expected soon based on the experimental results. At 88.30 sec the inlet velocity was increased from 0.65 to 0.725 knots. This new speed is still below the expected entrainment of 0.85 knots. However, oil loss over the boom was seen, see Fig. 47. The simulation was run for a few more seconds and the loss over the boom continued, as shown in Fig. 48. It is surmised that the abrupt increase at the velocity inlet accelerated the flow, which results in a small disturbance in the water that results in the oil going over the boom. This was not seen in the full-scale simulations as the boom was larger and the small disturbance was not significant enough to cause the oil to go over the boom. A future analysis that ramps up the inlet velocity in smaller increments (e.g. 0.01 knots instead of 0.05+knots) could be conducted to see if the oil does not go over the boom.

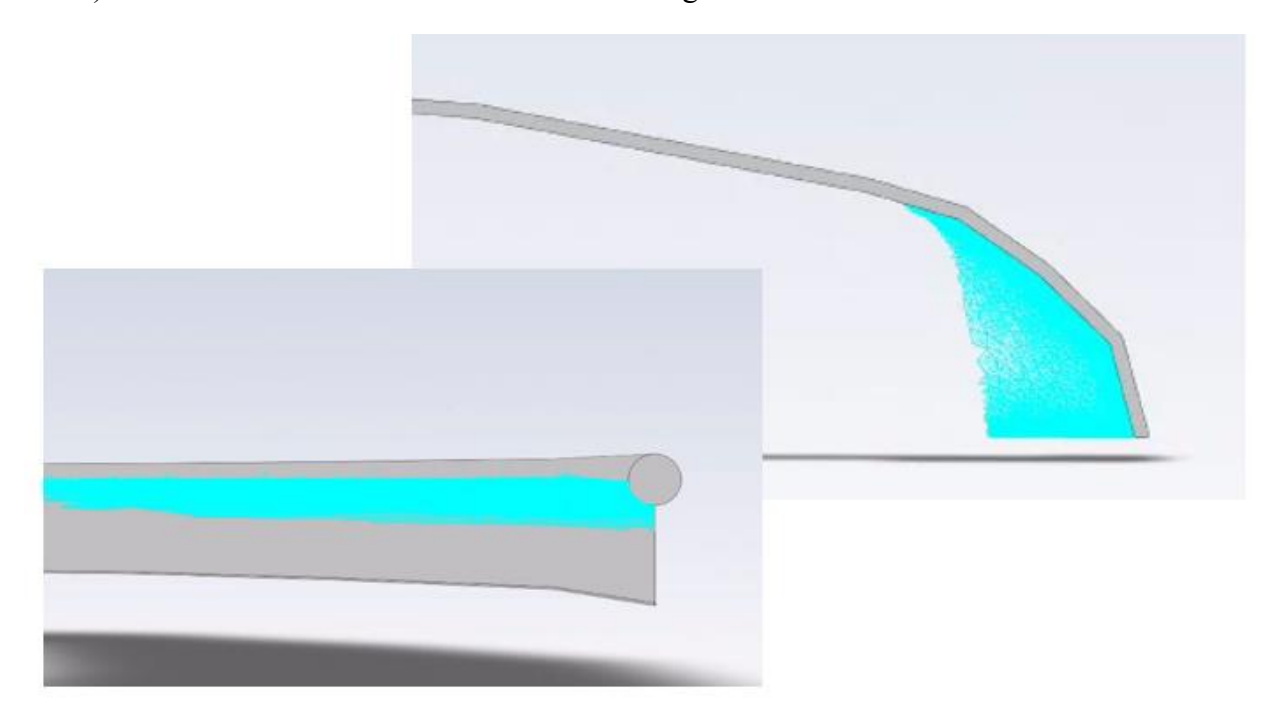


Fig. 46 Elastec Foam, 50%. Cells with oil at 82.66 s and 0.65 kts.

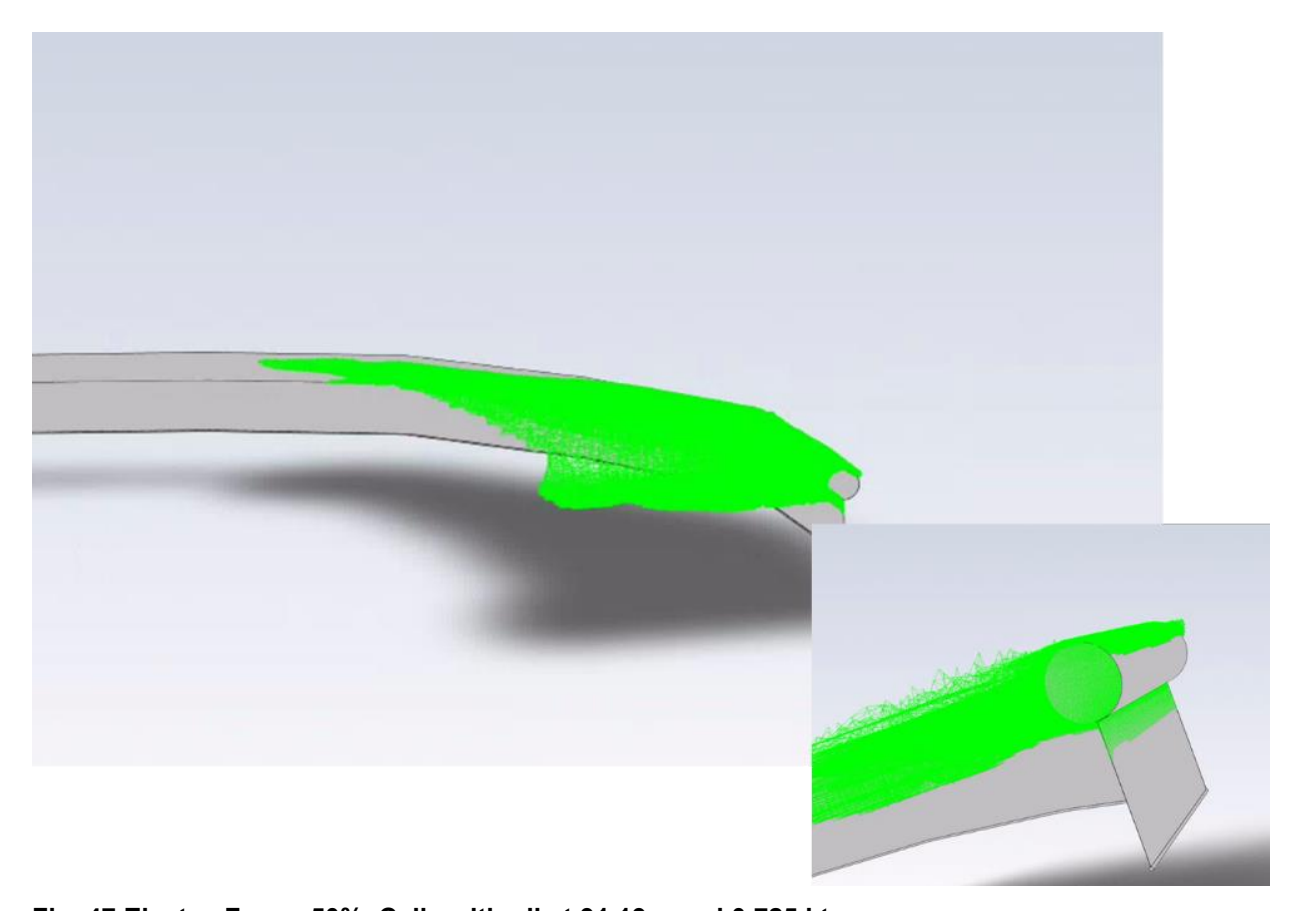


Fig. 47 Elastec Foam, 50%. Cells with oil at 91.19 s and 0.725 kts.

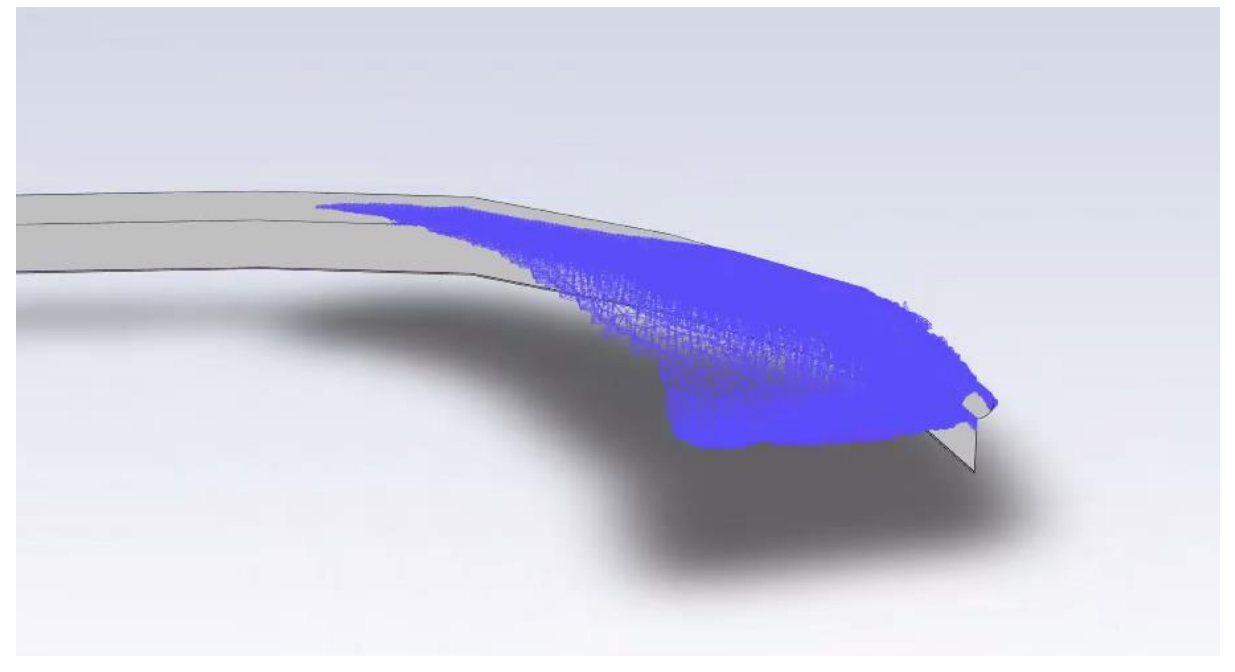


Fig. 48 Elastec Foam, 50%. Cells with oil at 93.09 s and 0.725 kts.

3.2.5.3. Elastec Foam, 25 percent

The next simulation was the Elastec Foam boom at a 25% scale. The starting speed of the simulation was 0.25 knot with a volume of 17.5 gallons of oil. Experimentally, entrainment was seen at 0.67 knots.

The numerical prediction of oil at 53.37 seconds into the simulation, where the inlet speed is 0.50 knots is provided in Fig. 49. At this point in the analysis the oil is against the oil boom, as would be expected. The water height at this time is given in Fig. 50, where the depression is due to the oil floating on the water. Next, the oil at 60.865 seconds, with an inlet velocity of 0.55 knots is in Fig. 51. It is evident from this graphic that the oil has passed over the boom, similar as to the Elastec Foam 50% simulation. The water level at this time is shown in Fig. 52. The depression in the water is seen both upstream and downstream of the boom, reflective of the oil on both sides of the boom. The oil failed over the boom just prior to the speed at which entrainment was seen in the experiment. As this failure happened for both the 50% and 25% scale boom it is assumed that the abrupt increase in velocity from 0.50 to 0.55 knots cased a non-physical disturbance that results in failure of the oil over the boom. A smaller increase for the inlet velocity as entrainment is approached could prevent this non-physical disturbance and prevent what is perceived as an artificial failure of oil over the boom. Additional analysis would be required to confirm is this would mimic the real-world behavior and have entrainment predicted, vice failure over the boom.

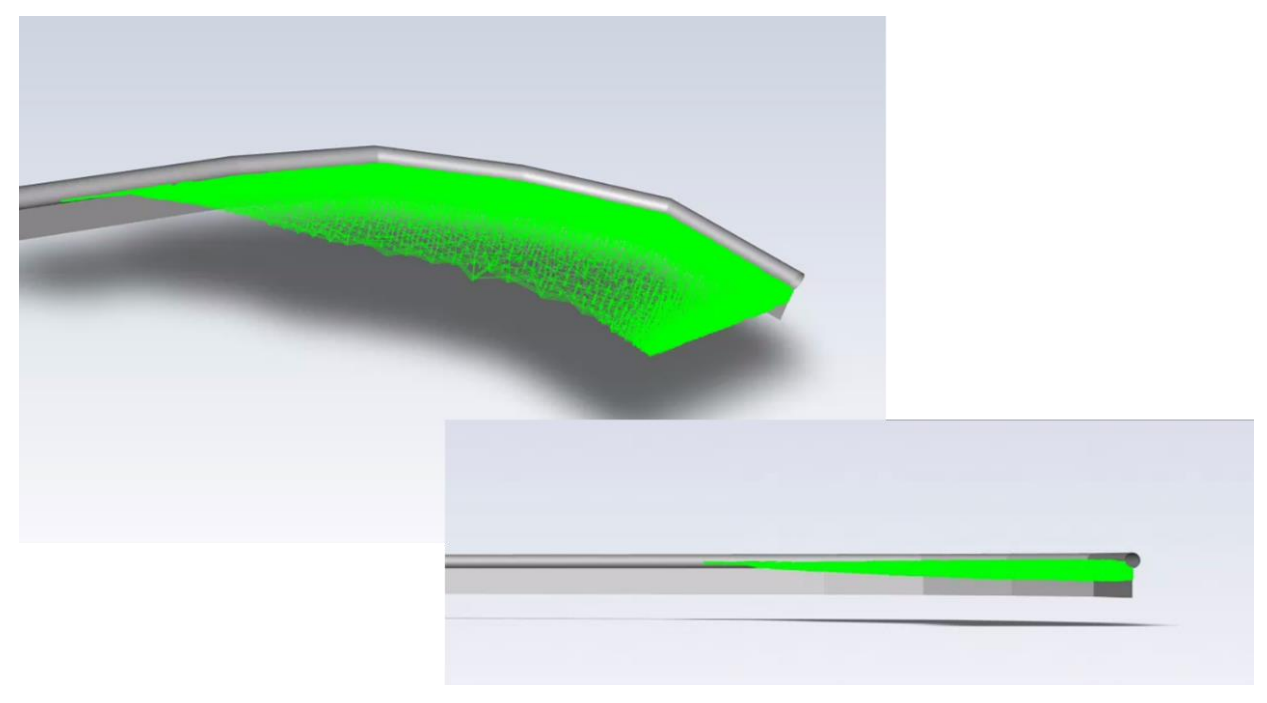


Fig. 49 Elastec Foam, 25%. Cells with oil at 53.37 s and 0.50 kts.

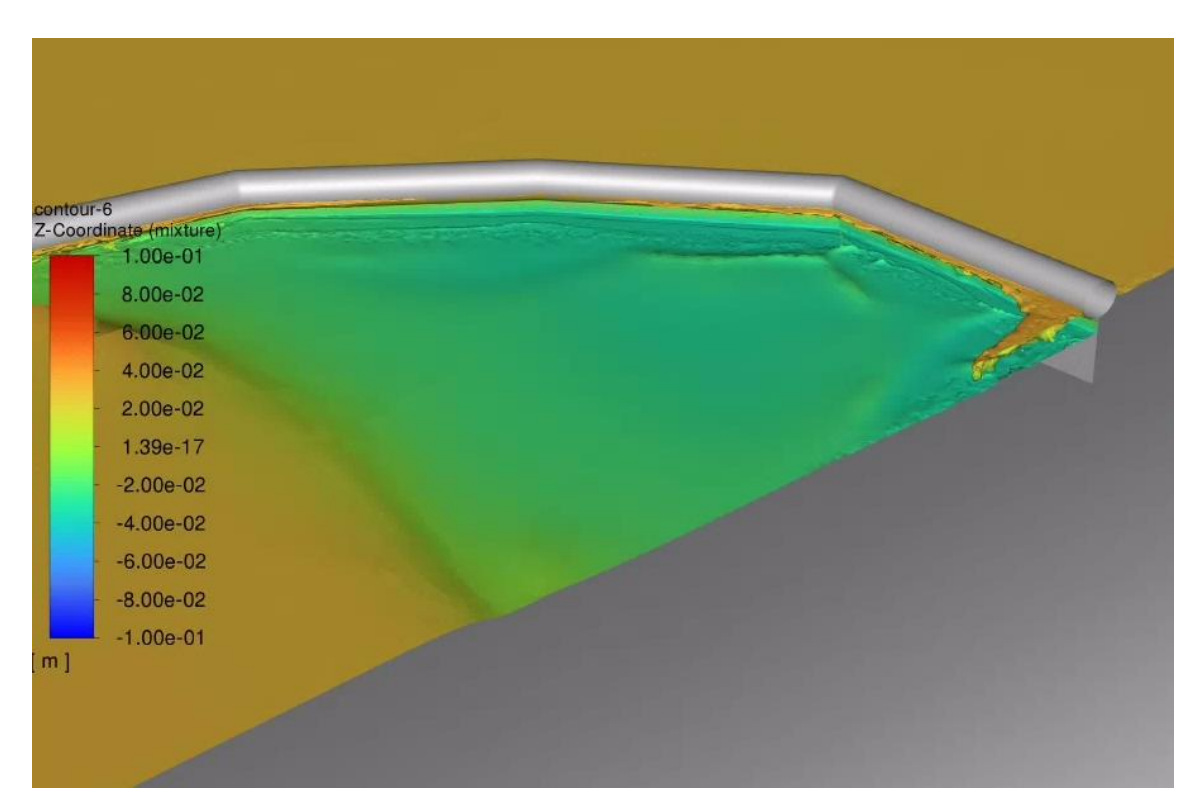


Fig. 50 Elastec Foam, 25%. Water surface colored by height at 53.37 s and 0.5 kts.

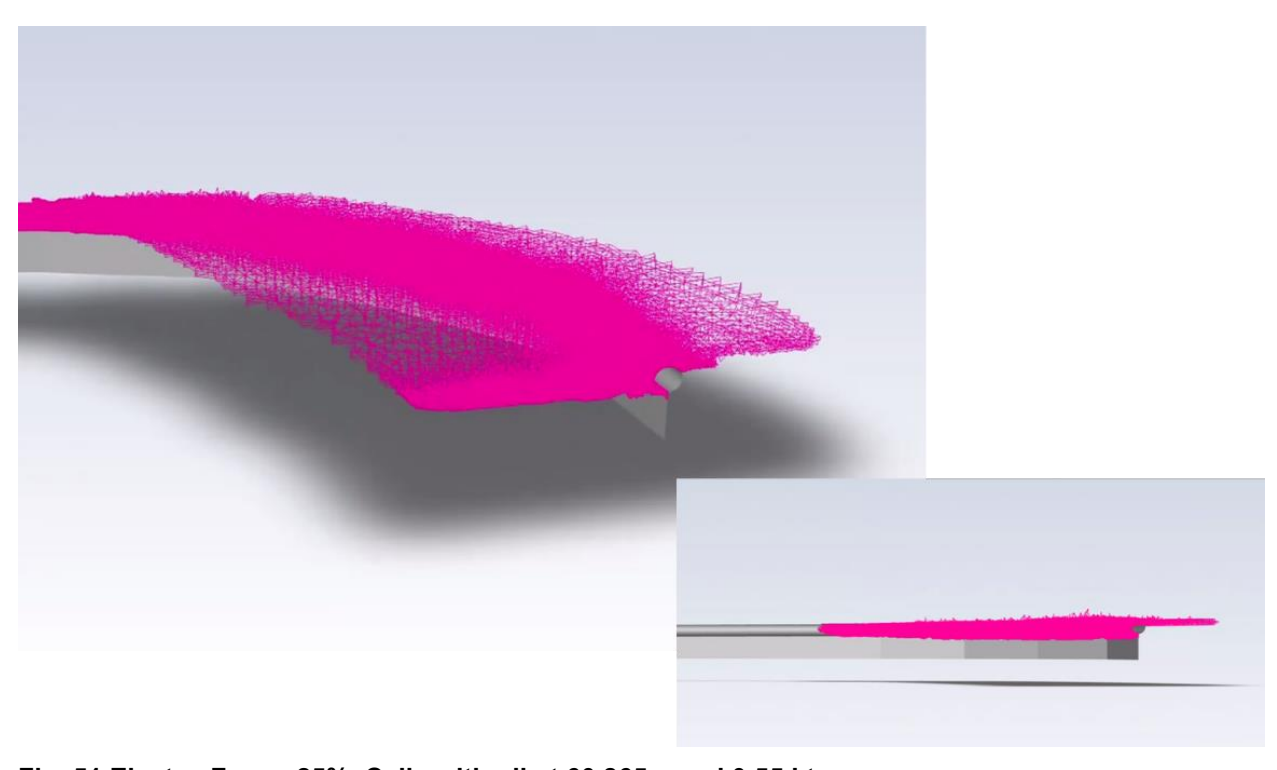


Fig. 51 Elastec Foam, 25%. Cells with oil at 60.865 s and 0.55 kts.

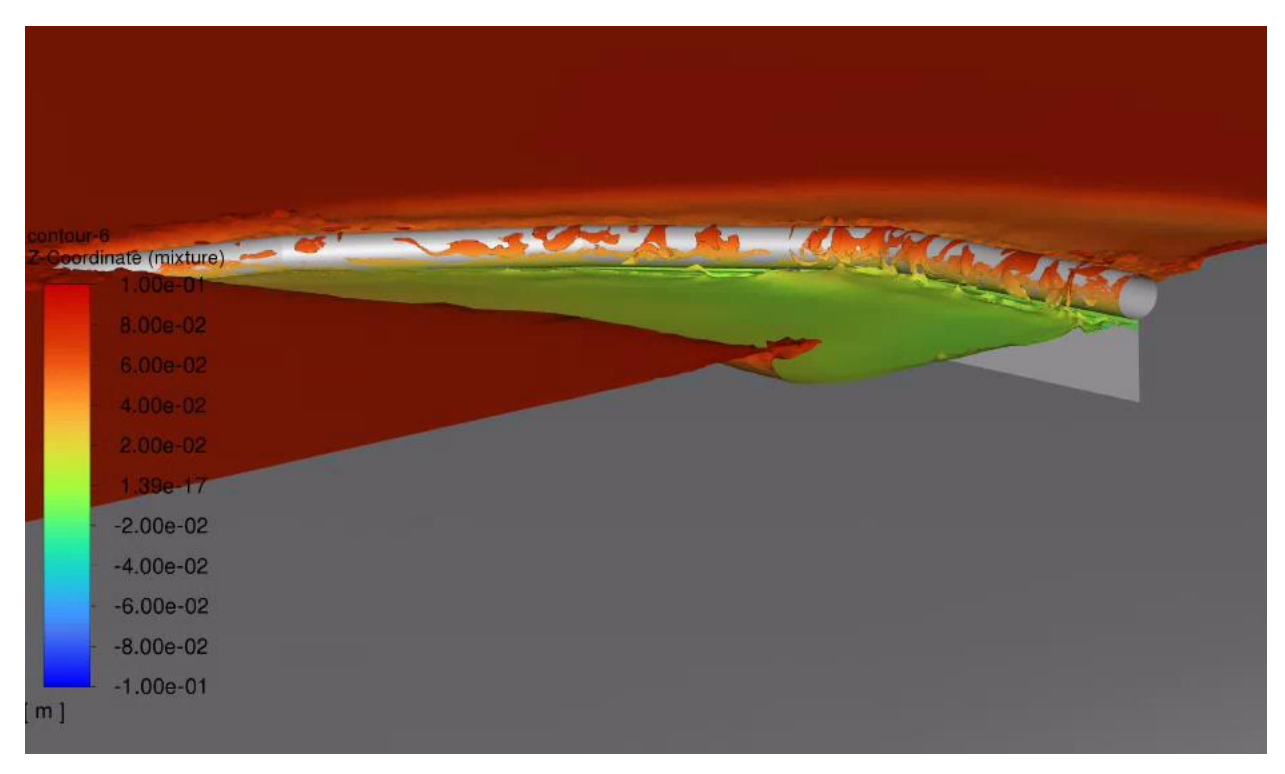


Fig. 52 Elastec Foam, 25%. Water surface colored by height at 60.865 s and 0.55 kts.

3.2.5.4. Abasco, 100 percent

The next boom that was analyzed was the Abasco boom at 100 percent scale. The CFD simulation again followed the experimental test, with an initial speed of 0.5 knots. There is an initial start-up period while the initial location of the oil is pressed up against the boom. The experimental results did not show entrainment until 1.0 knots. Thus, the numerical simulation will follow the procedure of the experiment, starting at a speed of 0.5 knots and increasing in speed by 0.1 knots every ten to twenty seconds.

The velocity was increased in a stepwise fashion until first loss was observed. This occurred at 1.1 knots and 120.92 seconds. This speed is slightly higher than the experiment. Fig. 53 and Fig. 54 show the velocity and phase, respectively, at two different planes in the simulation. The dispersion of within the tank is shown in Fig. 55, which clearly shows first loss.

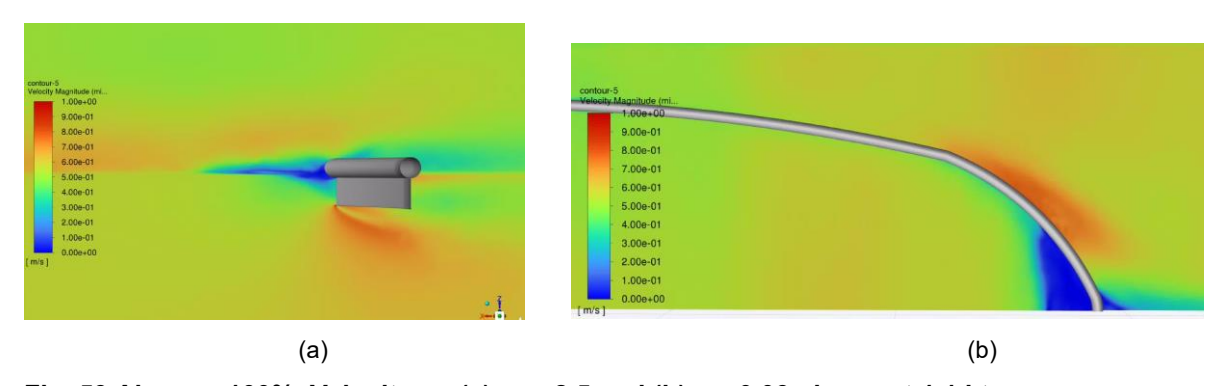


Fig. 53 Abasco, 100%. Velocity on (a) y = -2.5 and (b) z = 0.03 planes at 1.1 kts.

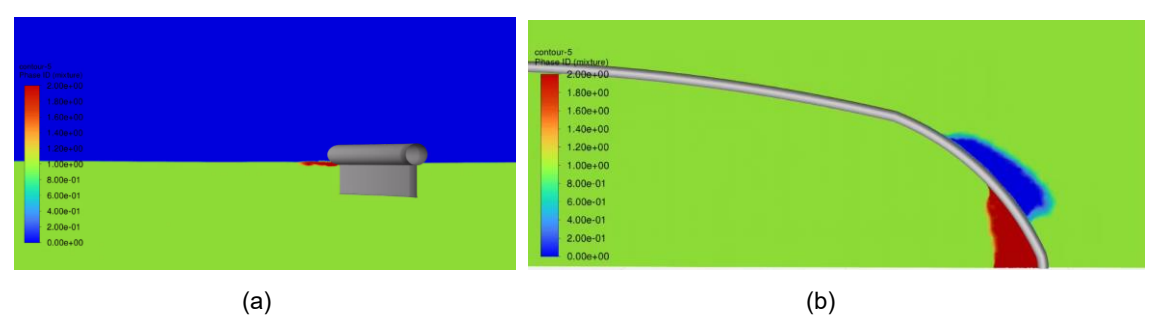


Fig. 54 Abasco, 100%. Phase on (a) y = -2.5 and (b) z = 0.03 planes at 1.1 kts.



Fig. 55 Abasco, 100%. Cells with oil at 120.92 s and 1.1 kts.

3.2.5.5. Elastec Airmax, 100 percent

The final full-scale boom simulated was the Elastec Airmax. The methodology for this analysis followed the same process as the previous. An initial speed of 0.5 knots was used, with a similar preload of oil to the other simulations. No entrainment was observed until 1.2 knots (172.98 seconds), which is a higher speed than the other simulations. The velocity on three different planes is depicted in Fig. 56 while the phase is shown on two planes in (a) (b)

Fig. 57. To highlight the interaction of the oil and water, the height of the water surface is in Fig. 58. The water surface is low just upstream of the boom as the oil has collected upstream of the boom. The oil sits on top of the water and as entrainment occurs it is pulling the water downward, showing the chaotic nature upstream of the boom. There is movement of the oil downwards due instability in the headwave, drawing drops of oil downward and under the boom (Baker et al., 2019). The volume of oil in the computational domain at 172.98 seconds, at a speed of 1.2 knots, is given in Fig. 59. This is first entrainment of the oil. It is surmised that the CFD

simulation is showing entrainment at a higher speed than the other booms due to the shape of the Elastec Airmax boom. The shape of the boom in the numerical model assumes a catenary shape, while the shape of the boom in the experimental shape is constantly fluctuating. It is likely that the shape of the boom and the connection between the individual sections of the boom contributed to an earlier entrainment in the physical test.

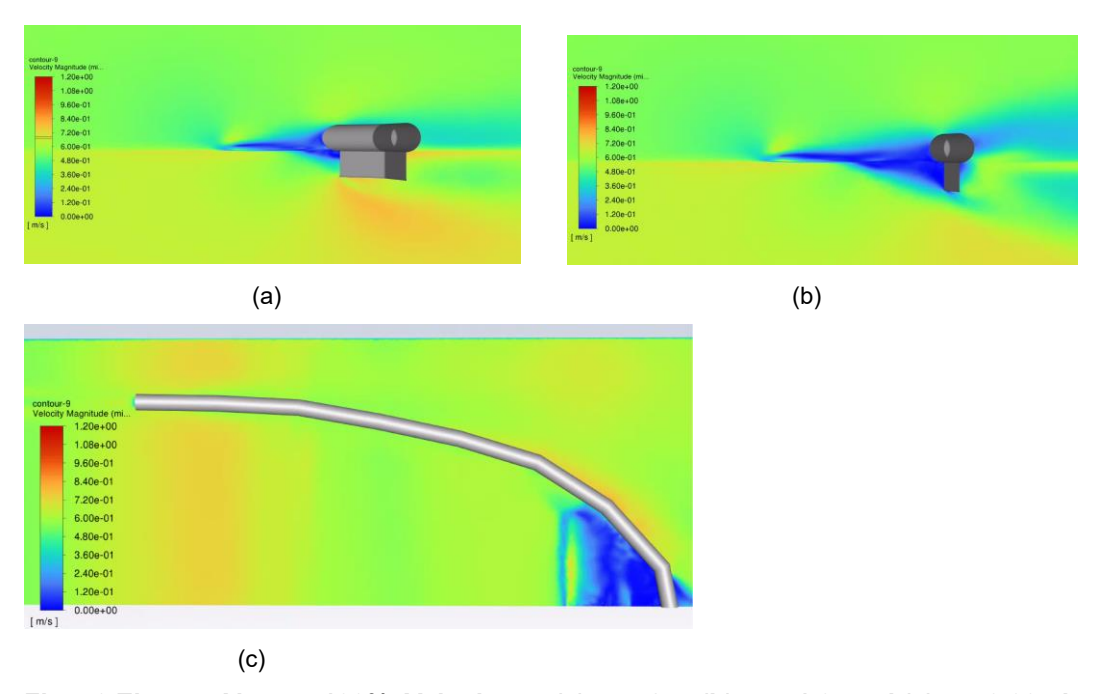


Fig. 56 Elastec Airmax, 100%. Velocity on (a) y = -2.5, (b) y = -1.0, and (c) z = 0.03 planes at 1.1 kts.

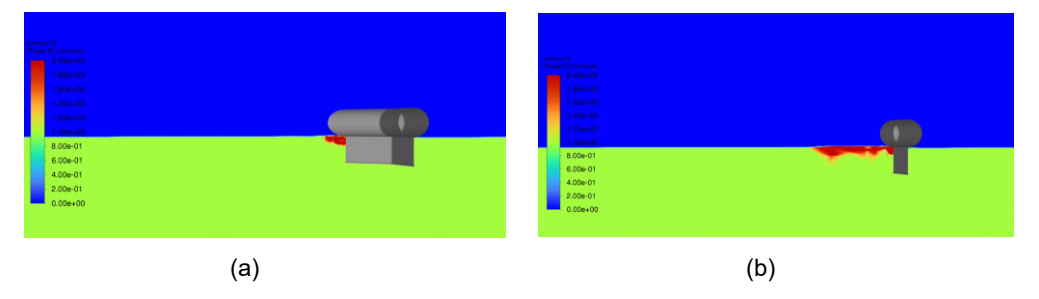


Fig. 57 Elastec Airmax, 100%. Phase on (a) y = -2.5 and (b) y = -1.0 planes at 1.1 kts.

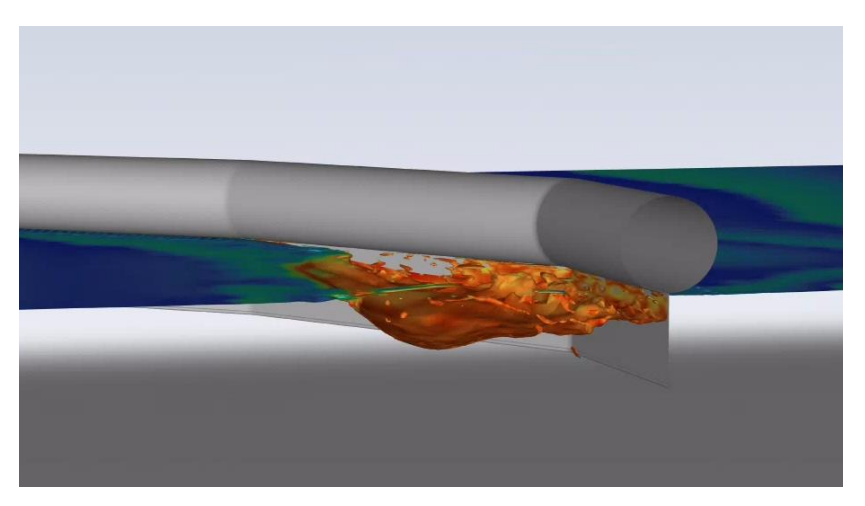


Fig. 58 Elastec Airmax, 100%. Water surface color by height at 1.1 kts.

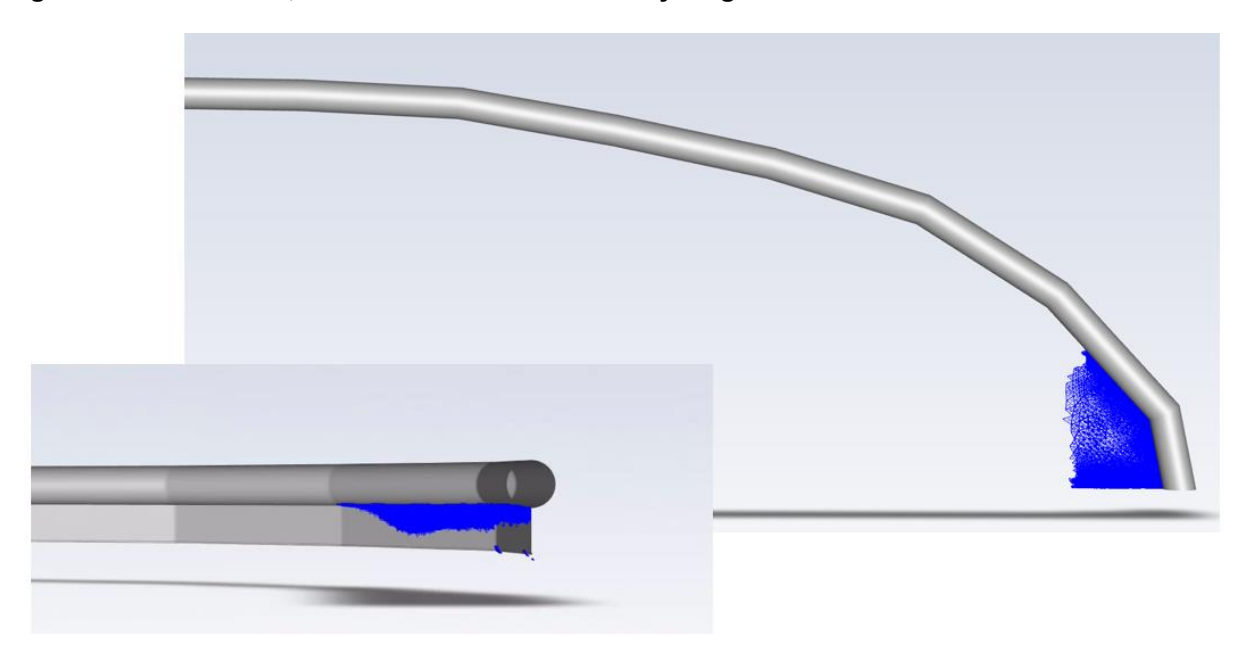


Fig. 59 Elastec Airmax, 100%. Cells with oil at 172.98 s and 1.2 kts.

As the results at 172.98 seconds only showed first loss, the simulation was continued. In the experiment it would be very easy to miss these few drops of oil going under the boom, giving a clear advantage to the numerical simulation in determining first loss. About 25 seconds (196.90 sec) later than first loss was initially observed more significant loss was seen, per Fig. 60. In an experiment the loss of the oil is approaching the amount where an observer would be able to notice first loss. The water surface at this time is similar to the prior time step discussed (see Fig. 61). The headwave is continuing to lose stability, resulting in additional oil being entrained and going under the boom.

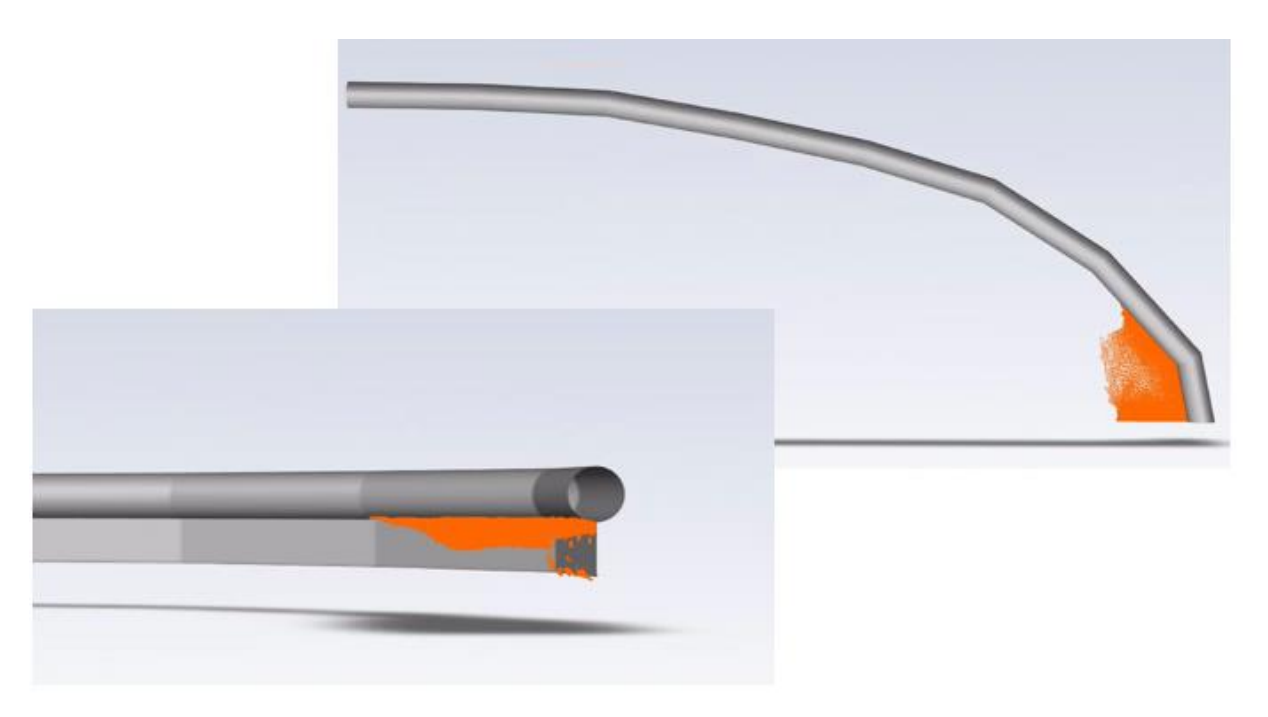


Fig. 60 Elastec Airmax, 100%. Cells with oil at 196.90 s and 1.2 kts.

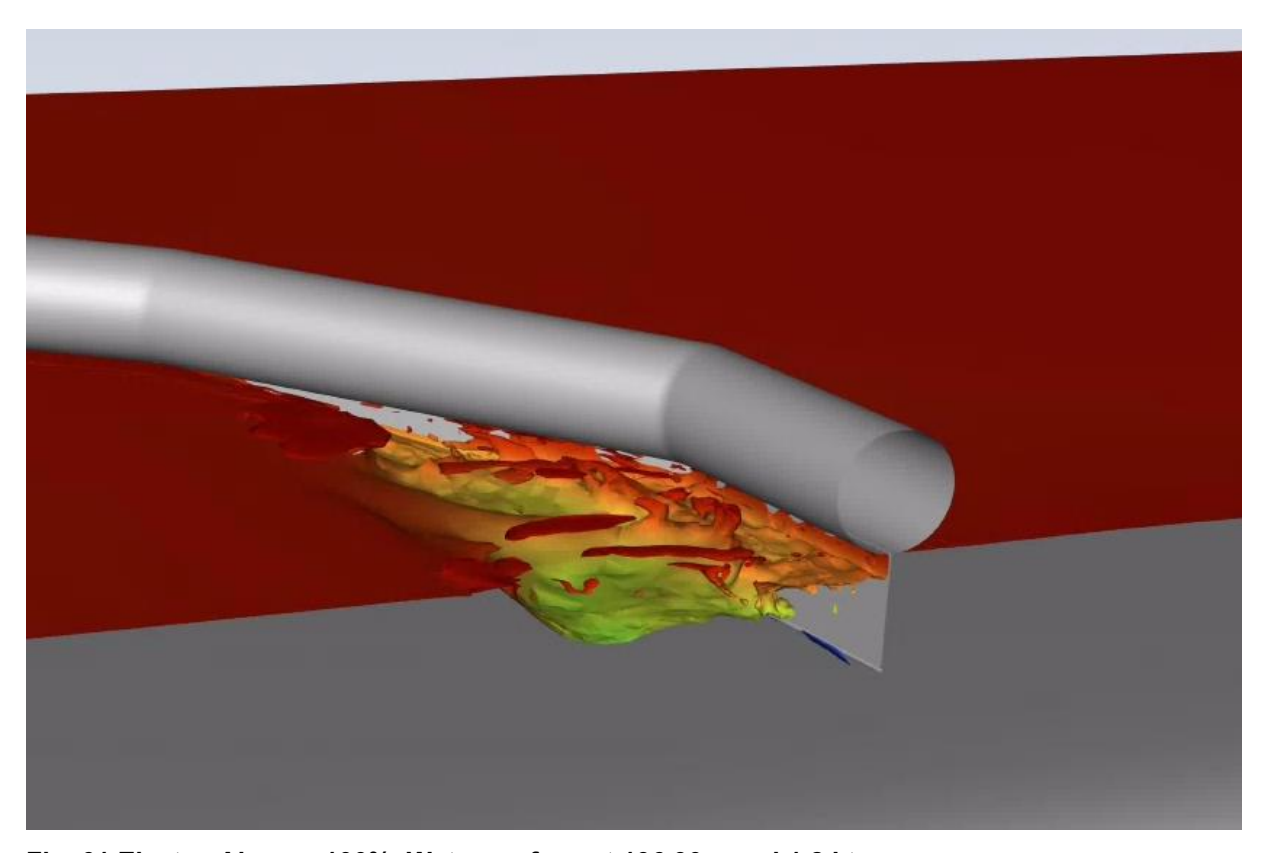


Fig. 61 Elastec Airmax, 100%. Water surface at 196.90 s and 1.2 kts.

One thing to note with these results is that consideration should be given to increasing the time between speed increases in the ASTM F2084 test standard. First loss is observed numerically,

but even 25 seconds later the loss of oil is just approaching what an observer might be able to identify in an experiment. The ASTM standard recommended an increase in velocity before this "observable" loss occurred. That would have resulted in a higher speed to be recorded for first loss. A suggestion that the time between speed increases to 20 or 30 seconds seems to have merit.

Table 12 shows a comparison of the CFD first and gross loss entrainments to the experimental test results.

Table 12 Physical and CFD entrainment comparison

Boom	Scale	Physical First Loss Spd (kts)	CFD First Loss Spd (kts)	Physical Gross Loss Spd (kts)	CFD Gross Loss Spd (kts)
Elastec Foam	100%	0.92	0.9-1.0	1.12	1.0
Elastec Foam	50%	0.78	0.725 ¹	0.91	0.725 ¹
Elastec Foam	25%	0.67	0.55 ¹	0.78	0.55 ¹
Abasco	100%	0.97	1.1	1.13	
Elastec Airmax	100%	0.88	1.2	1.08	

In the Elastec Foam 50% and 25 % models, oil escaped over the top of the boom before entrainment could occur.

4 Conclusions

4.1. Physical Testing Conclusions

The results shown here may have been influenced by the specific test procedure used and by the presence of the tank bottom. Since the largest scale booms were right at the recommended limit of skirt draft for the tank depth, the influence of the tank bottom could be expected to be greater for the large-scale tests, and smaller for the small-scale tests. It is possible that this variable influence may be responsible for some of the observed difference between the scaling theory and the test results.

For these tests, in general 20 seconds was used for the time interval between speed increases to allow for the oil in the boom to come to equilibrium. Keeping to a 10-second increment on speed changes leads to higher perceived entrainment speeds as the speed is increased before the oil is given a chance to entrain at the lower speed step. The preload testing was time consuming, and we did not find that it was of benefit. It added a huge number of tests to conduct and involved large quantities of oil that were difficult to keep within the boomed area and the results did not show the diminishing entrainment speed with increasing oil.

The camera angles are very important. Due to poor transmissivity through the water, it was difficult to see the entire boom apex – especially at the full-scale sizes. Keeping the camera close enough to be able to see clearly limits the area that can be viewed with a single camera. A PTZ camera does not really help as the zoom capability does not overcome the poor transmissivity of the water and panning does not allow for the entire apex to be seen at once. Multiple simultaneous views are needed to fully cover the boom apex (especially with large booms). In addition, the angle of the sun relative to the camera can greatly reduce visibility thus having multiple camera angles also provides alternatives so that not all cameras are blinded. An

upward looking view is good for watching the leading edge and head wave but hard to see oil going under the boom and can also be very impacted by the sun.

Although the theoretical speed scaling does not hold exactly based upon our test results, it does appear to give a good indication of entrainment speed with less than $\sim 30\%$ error. Using a cube root of the scale factor rather than a square root scale factor yielded slightly better results with a worst-case error of $\sim 25\%$ and an average of 11% vs an average of 21% for the square root case. And eliminating the anomalous Airmax boom test, the average error was only 7%. Larger boom scaling factors (1/4 size vs full size) magnifies any errors present so using half-scale models and extrapolating results to full size has less error.

There are several possible sources of error in the testing. First of all, the assessment of first loss (and gross loss) is very subjective and this can lead to variability in the results. Second, the boom systems were not scaled in every way. The boom materials were not scaled so smaller booms were stiffer in comparison to the full-scale booms. The oil properties were also not scaled. And third, it seemed to take sufficient speed through the water for the booms to assume the catenary shape and for the oil to compress to the point where entrainment would occur (oil thickness seems to be the key here). This speed may not really scale down to the smaller scales as expected. It might be worthwhile to study the turbulent flow behind the boom as a predictor of entrainment speed as it is the head wave build up that causes the oil to break loose and pass under the skirt.

4.2. CFD Modeling Conclusions

Computational fluid dynamics is used to predict the movement of oil that is being collected by an oil boom. This is a multiphase simulation, where all three fluids (i.e., air, water, and oil) are represented. A simulation of this type has not been published previously, to the authors' knowledge. Three different types of booms were simulated (Elastec Foam, Elastec Inflatable, and Abasco Inflatable) at full scale. For the Elastec Foam boom full scale simulation, oil loss is calculated to occur between 0.9 and 1.0 knots, which is consistent with the experimental results of 0.92 kts average. The Abasco boom in the simulation showed first loss at 1.1 knots; this is slightly higher than the experimental results (0.97 kts avg). The final full-scale boom, Elastec Airmax, numerically exhibited first loss at 1.2 knots compared to the experimental results of 0.88 kts average. This boom system had very anomalous results though so should not be trusted.

While the computational results for the full-scale booms were similar to the experimental results, the Elastec Foam boom at 50% and 25% scale were noticeably different. For each of these boom scales the oil failed over the boom, which was not seen in the experiment. Failure was observed for both smaller sized booms as the entrainment speed was approached. It is surmised that the abrupt increase of 0.05 knots was significant enough to create a disturbance or acceleration in the water that resulted in the oil over the boom. Additionally analyses, such as using finer increments to increase the inlet velocity as the entrainment speed is approached are suggested to determine if this is an artificial error that occurs at smaller scales. However, the need for conducting numerical analyses at smaller scales is questionable. When conducting experiments smaller scaled booms are sometimes required when the tank size is too small. This is not a concern for computational simulations, where the size of the tank is (in theory) infinite. Another reason to run smaller scale numerical simulations is a reduction in the number of grid

points used in the CFD analysis. This was not a benefit for the oil boom simulations as the smaller scale booms required at least as many grid points to accurately capture the oil-water interface along with the smaller grid spacing required near the boom. As the size of the boom decreased the cell spacing normal to the boom also decreased, resulting in almost the same number of grid points for all three Elastec Foam scales.

It should be noted that the models with these very large number of cells and the three fluids (air, water, and oil) take an extremely long time to simulate. The time step needs to be very small, and the time spent at each speed needs to be much longer than the ASTM standard of 10 seconds. This equated to a large number of simulation steps. Even using a computer with 32 processor cores, it took months to complete a single model. Coupled with changes to models to correct simulation errors and thus restarts of the simulation runs, as well as occasional computer and license issues to resolve, it took 2 years to complete the 5 simulations.

There are a few lessons learned from the investigation which could improve the execution times. After seeing the results, the total simulation time could be reduced by starting at a higher initial velocity. The full-scale simulations were conducted in a similar manner to the experiment, where the speed was ramped up slowly from a very low speed. Future runs could be conducted starting at a velocity that is substantial (e.g., 0.7 knots for full scale). If there are no experimental results upon which to base an estimate of first loss then a moderate speed can be used (e.g., 0.5 knots). Also, access to computing machines with larger number of cores could reduce the run time. There are additional costs associated with that beyond just the computer costs however, as the FLUENT license costs increase with the number of cores supported.

There are also changes that could be made to the modeling to improve execution speed. First, there is a small circular pocket at the bottom of the skirt that holds the attachment chain. Initially, there was a potential of the chain pocket having an influence on the movement of oil under the boom. However, since the entrainment is initiated from the formation of the head wave, the chain pocket does not influence the loss. As such, the number of grid points required to accurately simulate the flow around the chain pocket is not necessary. Secondly, the fine grid discretization normal to the boom is only needed near the apex of the boom. If the boom, as viewed from above, is divided into thirds then only the third of the boom near the apex requires small grid cell sizes. This does not alleviate the need for grid cell spacing that is adequate to capture the boundary layer along the boom, near the opening, but this could reduce the number of grid cells by at least twenty percent. It is recommended that a future grid study be conducted where the grid upstream of the apex is reduced in density. This could also include an overset grid, where a very fine grid is overlaid the grid near the apex, allowing for a smaller number of grid points overall. This would also allow the total number of grid cells to be more in proportion to the scale of the boom.

It should also be noted that this is the first CFD simulation that the authors are aware of that directly simulates all three fluids: air, water, and oil. The other simulations that are in the public literatures only model the water and air. The inclusion of the air may improve the accuracy of the simulations and could account for the prediction of the oil over the boom for the smaller scales.

There may be merit in recommending a change to the ASTM F2084. As mentioned previously from an experimental standpoint allowing the boom to come to an equilibrium at speed is suggested. This is further recommended by the numerical results where first loss at a speed would be very difficult for an observer to detect and a more noticeable loss was not seen at that speed for another 20 to 25 seconds. Allowing a longer time at one speed would prevent the premature increase in velocity of the boom.

5 Recommendations

The physical testing results indicate the ASTM committee F20 should review the standard F2084 and consider the following recommended revisions:

- When possible, within the constraints of the test facility, increase the time spent at each speed increment. For these tests, 20 or 30 seconds allowed for the oil in the boom to come to equilibrium. Increasing the speed at smaller time steps can lead to higher perceived entrainment speeds.
- Consider eliminating the preload testing. This is time consuming, and we did not find that it was of benefit. We recommend using a preload volume calculated to fill approximately 50% of the boom catenary length to a depth of 1 inch. A calculation or tables could be added to the standard. This applies to all scales.

The proposed change to the ASTM F2084 is also indicated in the CFD testing. As mentioned previously from an experimental standpoint allowing the boom to come to an equilibrium at speed is suggested. This is further recommended by the numerical results where first loss at a speed would be very difficult for an observer to detect and a more noticeable loss was not seen at that speed for another 20 to 25 seconds. Allowing a longer time at one speed would prevent the premature increase in velocity of the boom.

In addition to working with ASTM to update and improve the test standard there are two additional recommendations for future work, one for physical testing and one for CFD modelling.

1. In order to increase towing speed, the boom skirt needs to be larger (deeper draft) as seen in the testing. There are diminishing returns on this and it is not linear, but in general this is true. However, the larger the boom system, the more difficult it is for the towing vessel, requiring more and more power. Since most of the force of the water is concentrated on or near the apex (the water currents are more along the boom surface on the sides) if we could reduce the force in that region we could reduce the load on the towing vessel. We have had some success with using X-Tex fabric on an underwater boom project for the USCG in water speeds over 2 knots (designed for up to 8 knots). X-Tex fabrix is a semiporous material that allows water to flow through but not oil. We could segment the boom into 3 pieces and replace the middle section (apex and nearby) with a boom that has a skirt made of X-Tex fabric. This should reduce the load on the towing vessel and may increase the entrainment speed as well since the head wave should build up less since some of the water will pass through the fabric. We propose constructing a boom and testing this at Ohmsett. We could measure the towing force

- with load cells and assess any increase in entrainment speeds and compare to the same boom without the X-Tex fabric.
- 2. The CFD modeling we conducted produced good quality results; however, the computational time was excessive. There are several things that could be done to simplify the models which would reduce the computational time. We propose conducting a sensitivity study using the existing models and stripping away complexity bit by bit and the comparing the entrainment results to the high-fidelity model until we arrive at the optimum balance point between reduced complexity (faster run times) and acceptable quality results. This would be very useful to inform future boom system developers who would like to model performance before or without physical testing.

6 References

- Amini, A., Bollaert, E., Boillat, J.-L., & Schleiss, A. J. (2008). Dynamics of low-viscosity oils retained by rigid and flexible barriers. *Ocean Engineering*, *35*(14), 1479-1491. https://doi.org/https://doi.org/10.1016/j.oceaneng.2008.06.010
- Amini, A., & Schleiss, A. (2009). Numerical modeling of oil-water multiphase flow contained by an oil spill barrier. *Engineering Applications of Computational Fluid Mechanics*, 3(2).
- Baker, S., Babaei, H., Pilechi, V., & Potter, S. (2019). Research and Development of Oil Containment Boom Designs [Final Report](NRC-OCRE-2019-TR-032).
- Bjørvik, H. (2015). Simulation of Flow Around an Oil Boom [Masters, Norwegian University of Science and Technology].
- Gong, K., Tkalich, P., & Xu, H. (2014). The Numerical Investigation on Oil Slick Behavior behind the Oil Boom. *Journal of Environmental Protection*, *5*, 739-744. https://doi.org/10.4236/jep.2014.58075.
- Kwangu, K., Moonjin, L., & Jung-Yeul, J. (2013, 23-27 Sept. 2013). A numerical study on the wind effect on the oil containment by boom. 2013 OCEANS San Diego,
- Menter, F. (1994). Two-Equation Eddy-Viscosity Turbulence Models for Engineering Applications. *AIAA Journal*, 32(8).
- Menter, F. R. (2016, 26-28 September). Stress-Blended Eddy Simulation (SBES) A New Paradigm in Hybrid RANS-LES Modeling. Sixth HRLM Symposium, Strasbourg University, France.
- Standard Guide for Collecting Containment Boom Performance Data in Controlled Environments. (2018). [International Standard](F2084/F2084M 01).
- Wang, X. S., Ning, B., Yuan, R. M., & Zhang, X. X. (2012). Numerical Analysis of a New Type of Oil Boom with Diversion. *Applied Mechanics and Materials*, 214, 386-389. https://doi.org/10.4028/www.scientific.net/AMM.214.386
- Zhang, Z., An, C.-F., & Barron, R. M. (2002). Numerical Study on Kelvin-Helmholtz Instability and Oil Boom Failure Due to Droplet Entrainment. *International Journal of Transport Phenomena*, 4, 75-96.

Appendix A: Technical Summary

REPORT TITLE: Oil Spill Boom Computational Fluid Dynamics and Physical Modeling

CONTRACT NUMBER(S): 140E0121C0011

FISCAL YEARS(S) OF PROJECT FUNDING: FY2022 - 2024

CUMULATIVE PROJECT COST: \$382,500

COMPLETION DATE OF REPORT: 20 June 2024

BSEE COR(S): Kristi McKinney, Kevin Cabaniss

BSEE CO(S): Caroline Laikin-Credno

PROJECT MANAGER(S):Dr. Gregory Johnson

AFFILIATION OF PROJECT MANAGER: Serco, Inc.

ADDRESS: 1 Chelsea St., Ste 200, New London CT 06320

PRINCIPAL INVESTIGATOR(S): Dr. Gregory Johnson

KEY WORDS: physical testing, scale models, computational fluid dynamics, entrainment,

first loss, gross loss

Appendix B: Abbreviations and Acronyms

°C Degrees centigrade °F Degrees Fahrenheit

ASTM American Society for Testing and Materials

BSEE Bureau of Safety and Environmental Enforcement

CAD Computer-aided design

CFD Computational fluid dynamics

cm Centimeter(s)
CO Contracting Officer.

COR Contracting Officer's Representative

cP Centipoise

CPU Central processing unit
DNS Direct Numerical Simulation

ft Foot or feet

DOI Department of the Interior g/cm³ Grams per cubic centimeter kg/m³ Kilograms per cubic meter

kt(s) Knot(s)

LES Large Eddy Simulation

m Meter(s)

m/s Meter(s) per second

m²/s Square meters per second

m³ Cubic meter(s) mm Millimeter(s)

Ohmsett National Oil Spill Response and Renewable Energy Test Facility

OSPD Oil Spill Preparedness Division OSRO Oil Spill Response Organization

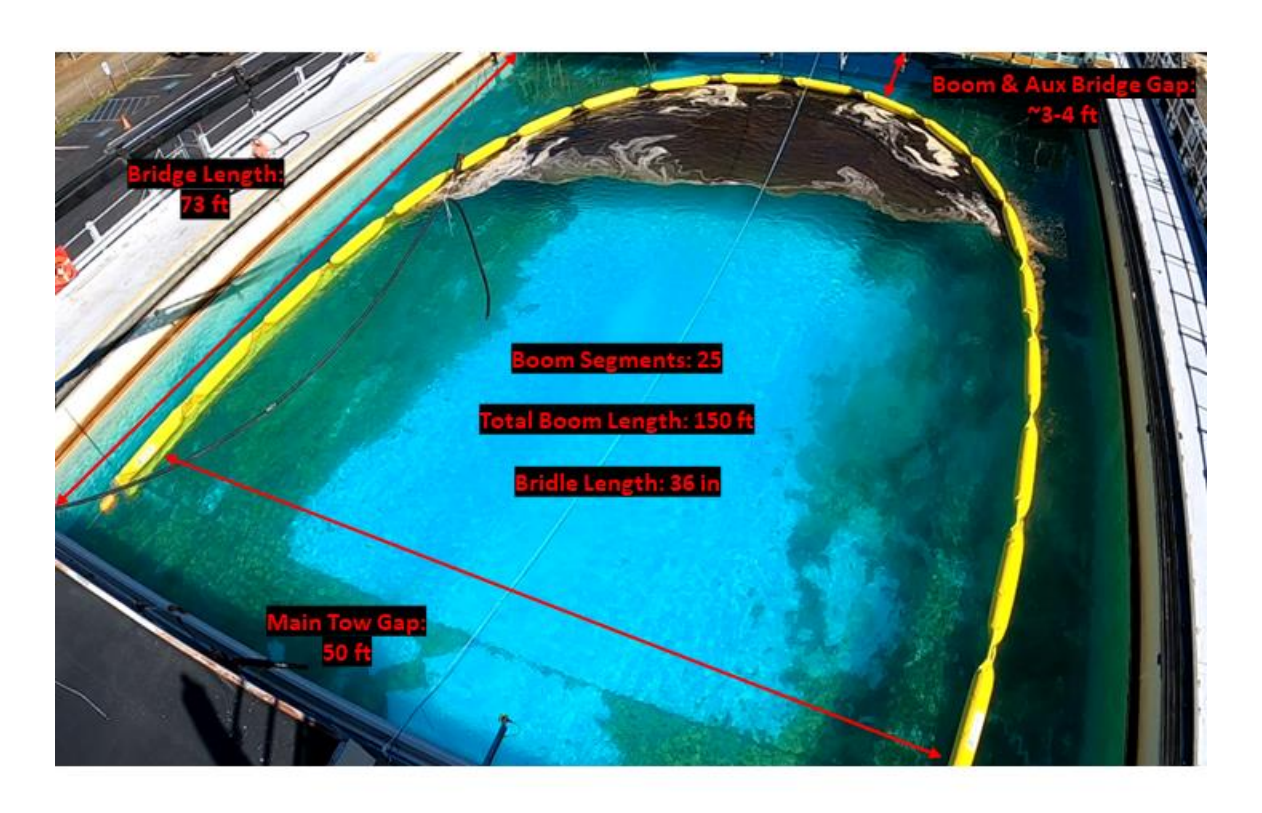
PTZ Pan-tilt-zoom

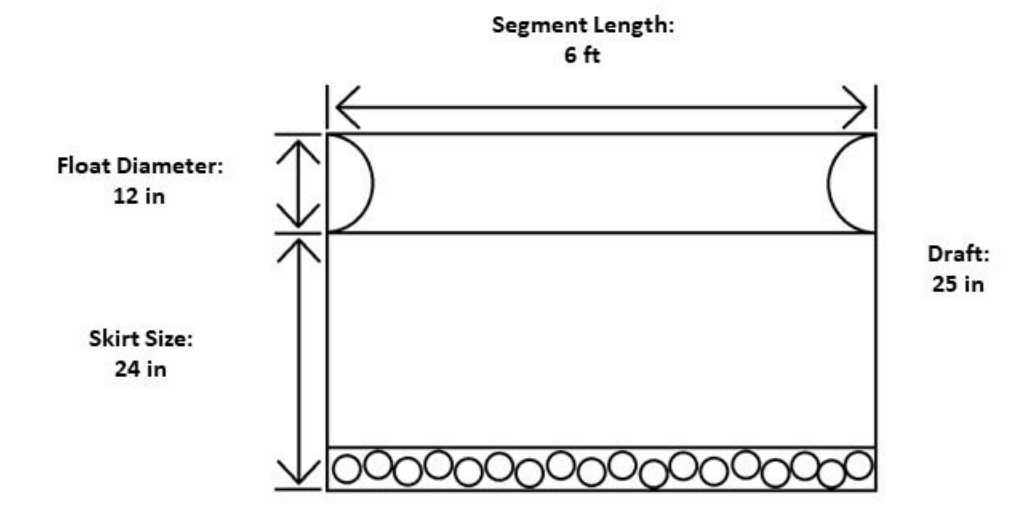
RANS Reynolds-Average Navier-Stokes SBES Stress-Blended Eddy Simulation

VOF Volume of Fluid

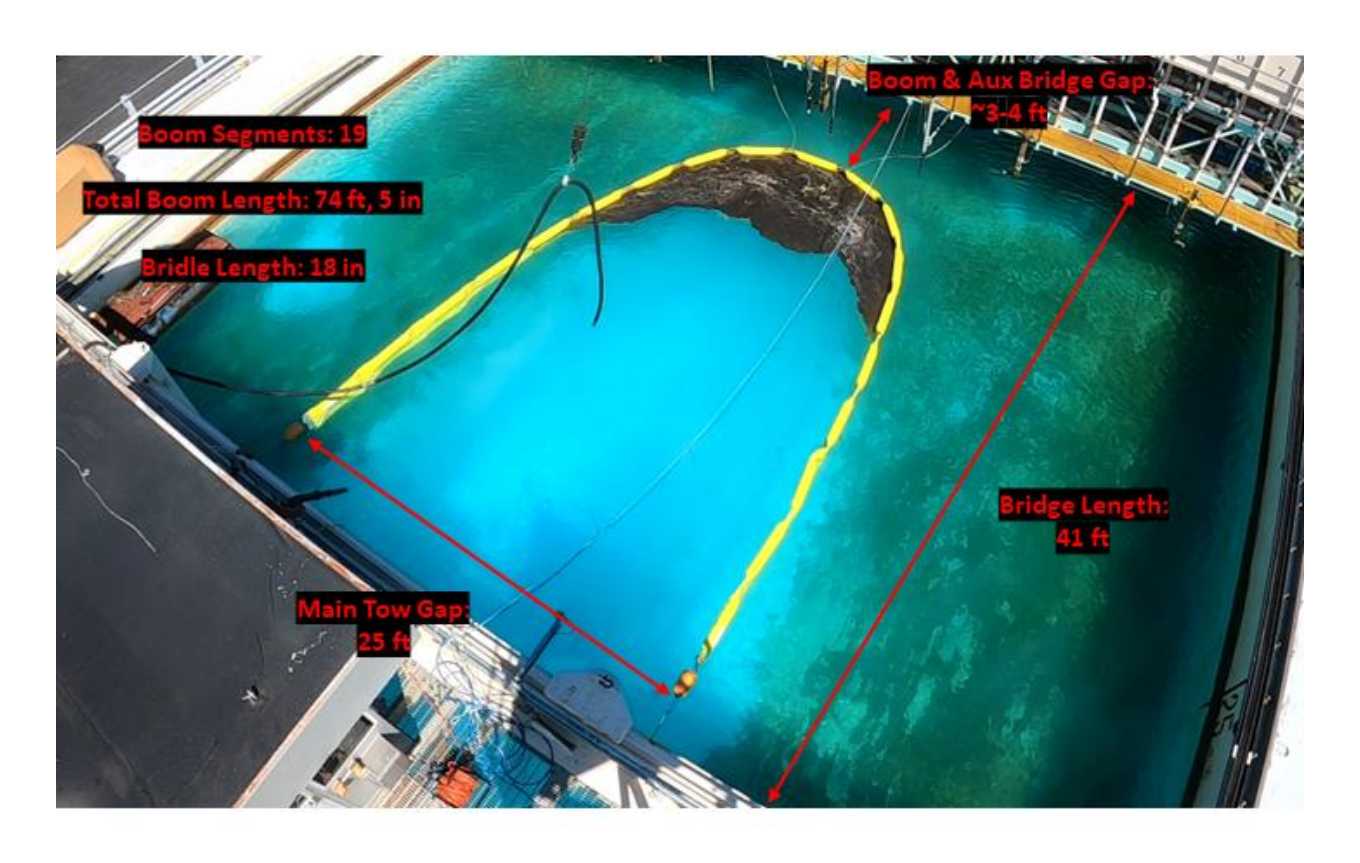
Appendix C: All Boom Systems

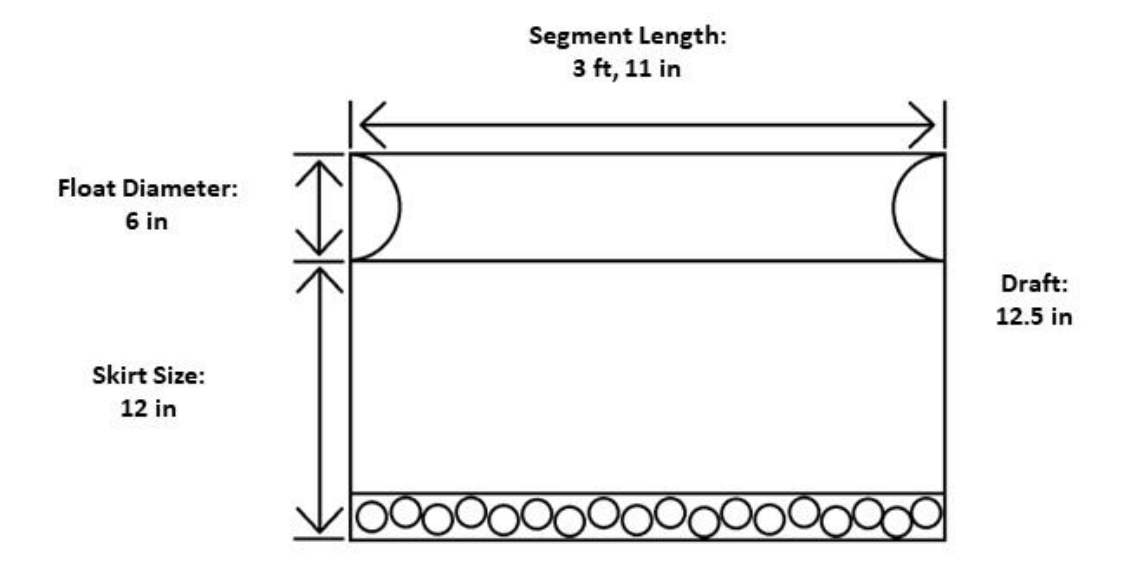
Elastec Foam - Full Scale



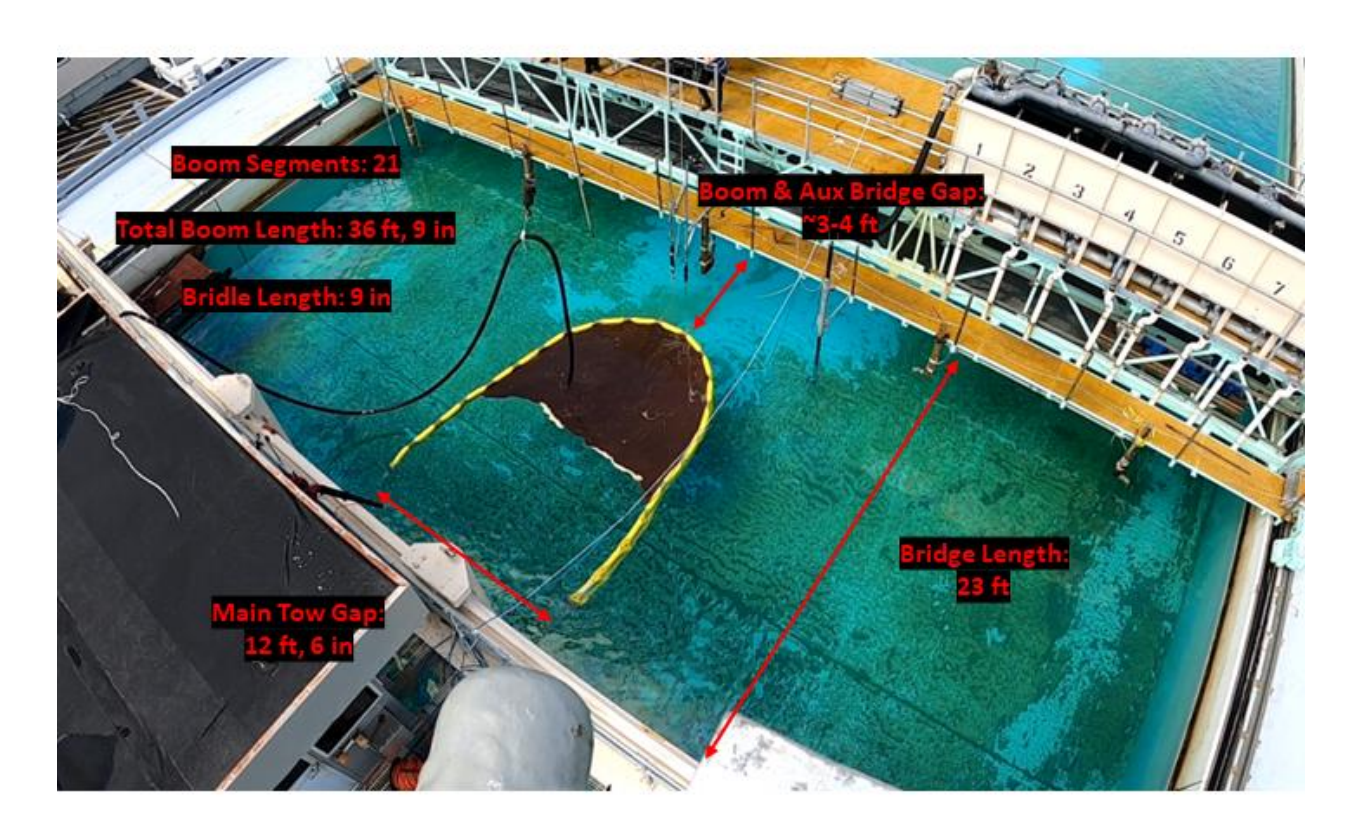


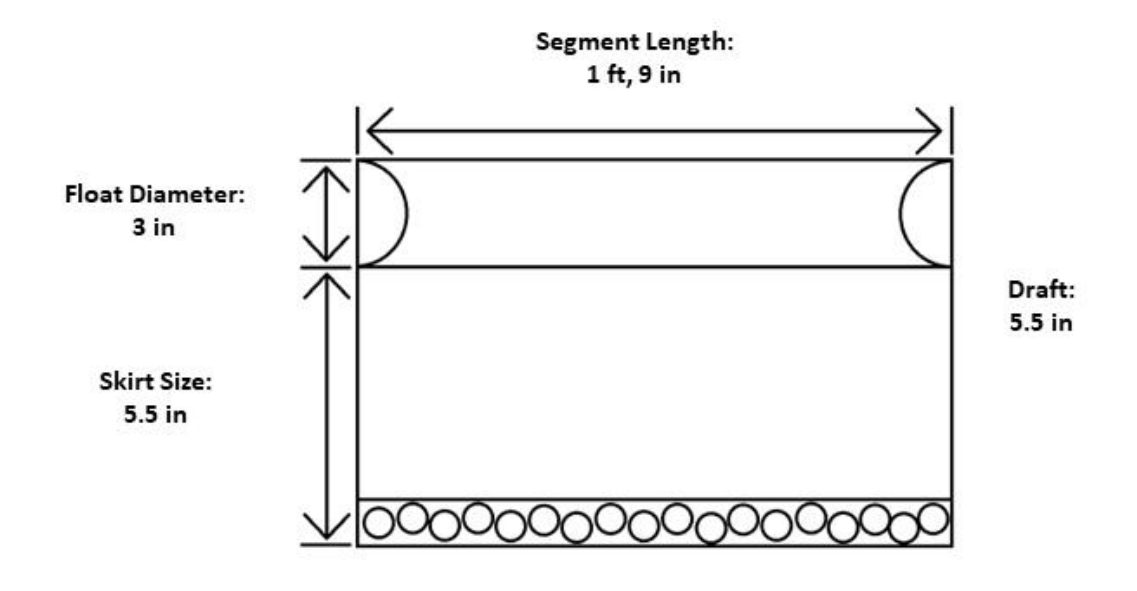
Elastec Foam - Half Scale



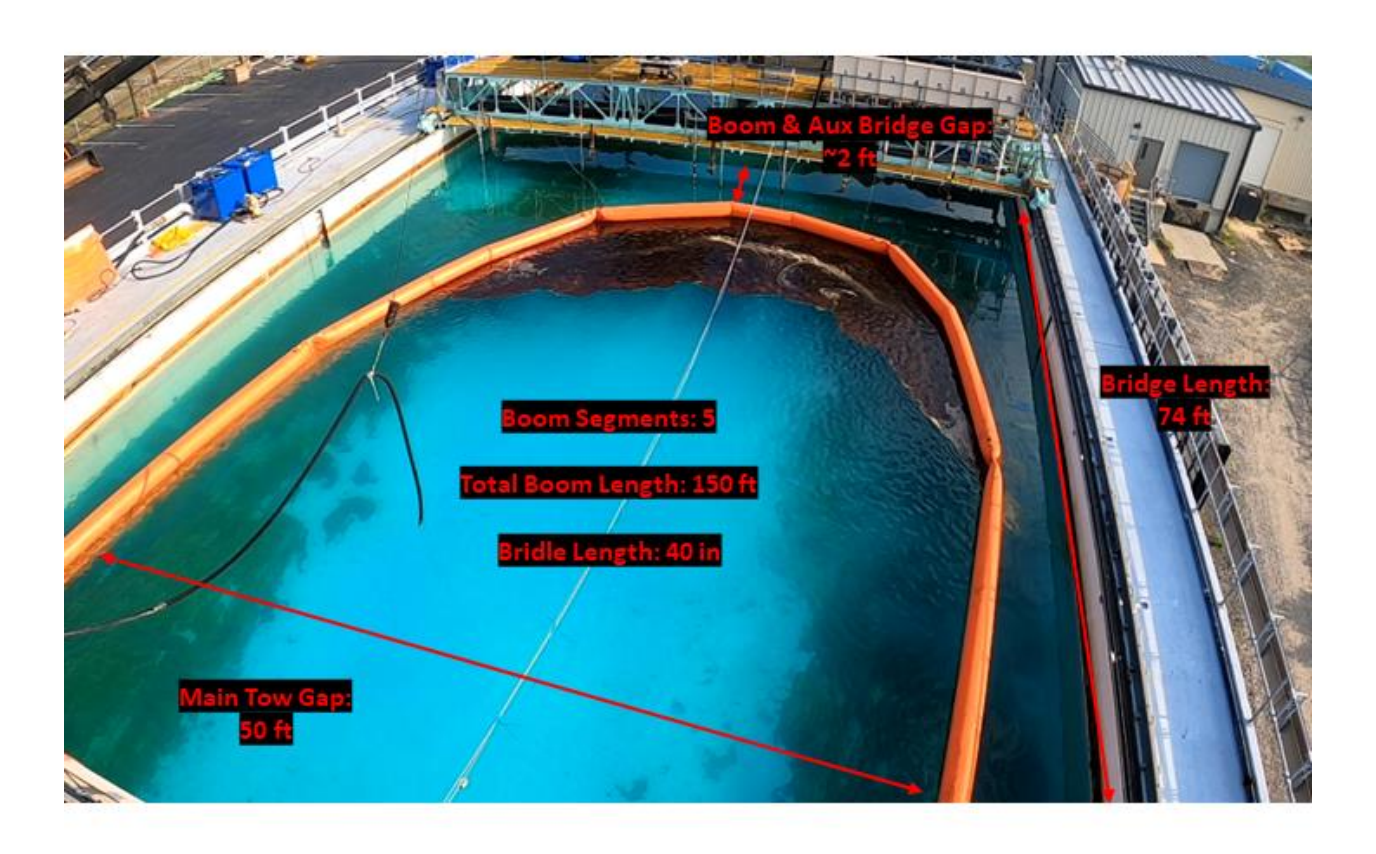


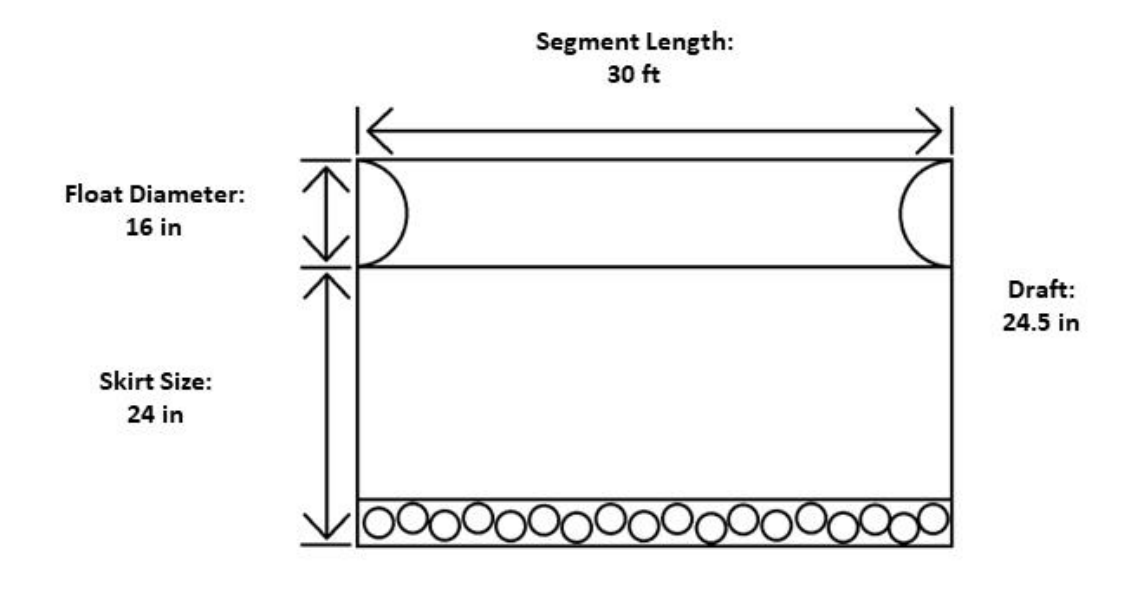
Elastec Foam – Quarter Scale



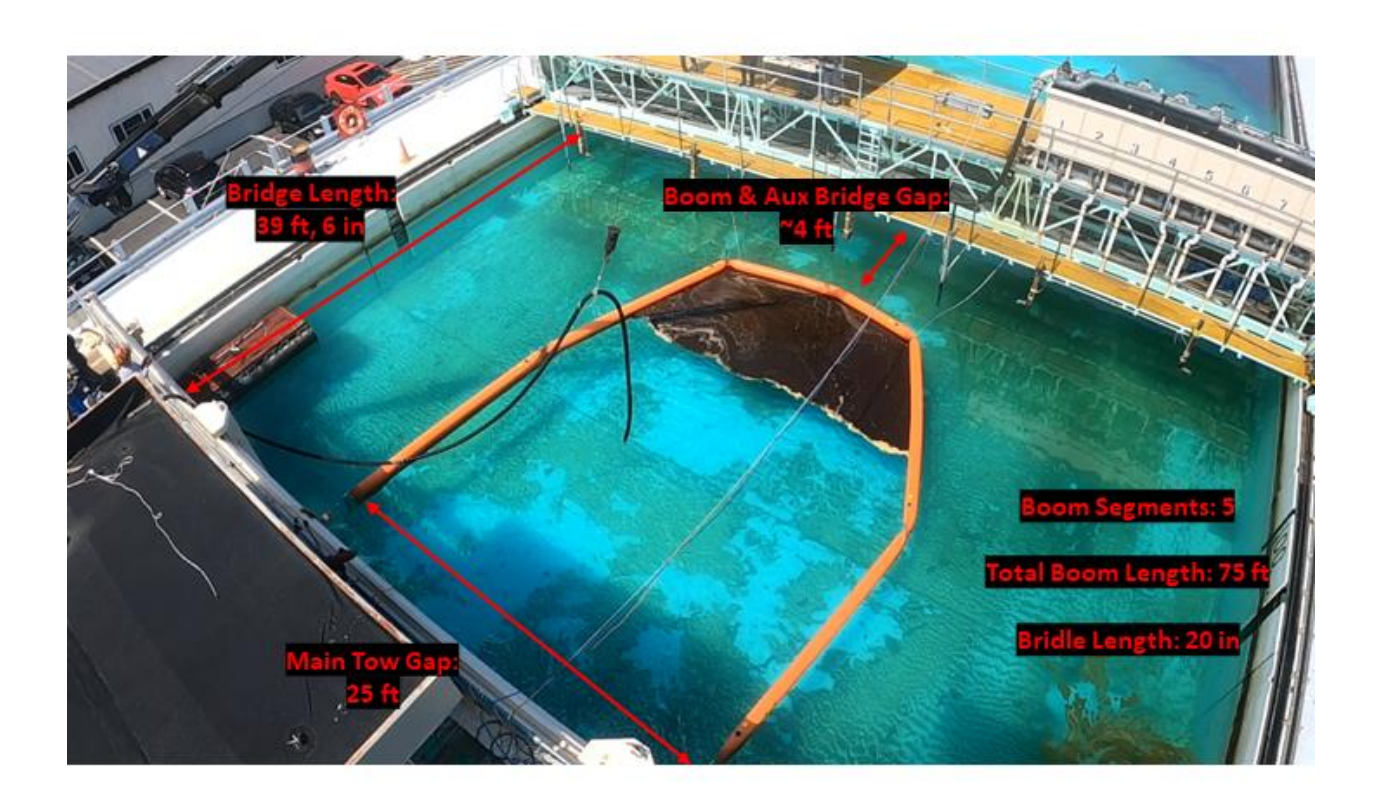


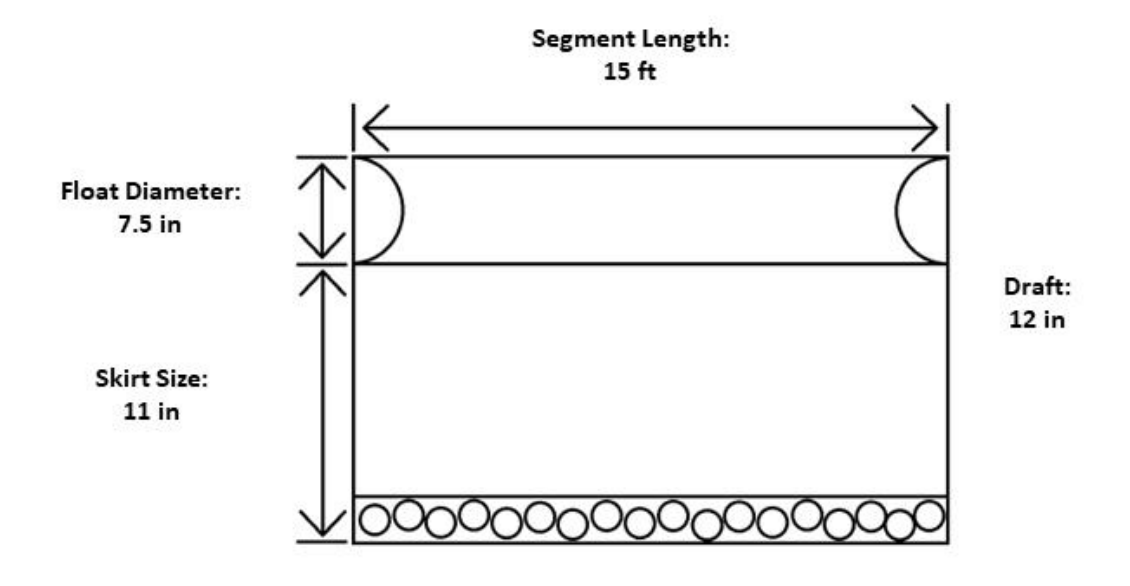
Abasco - Full Scale



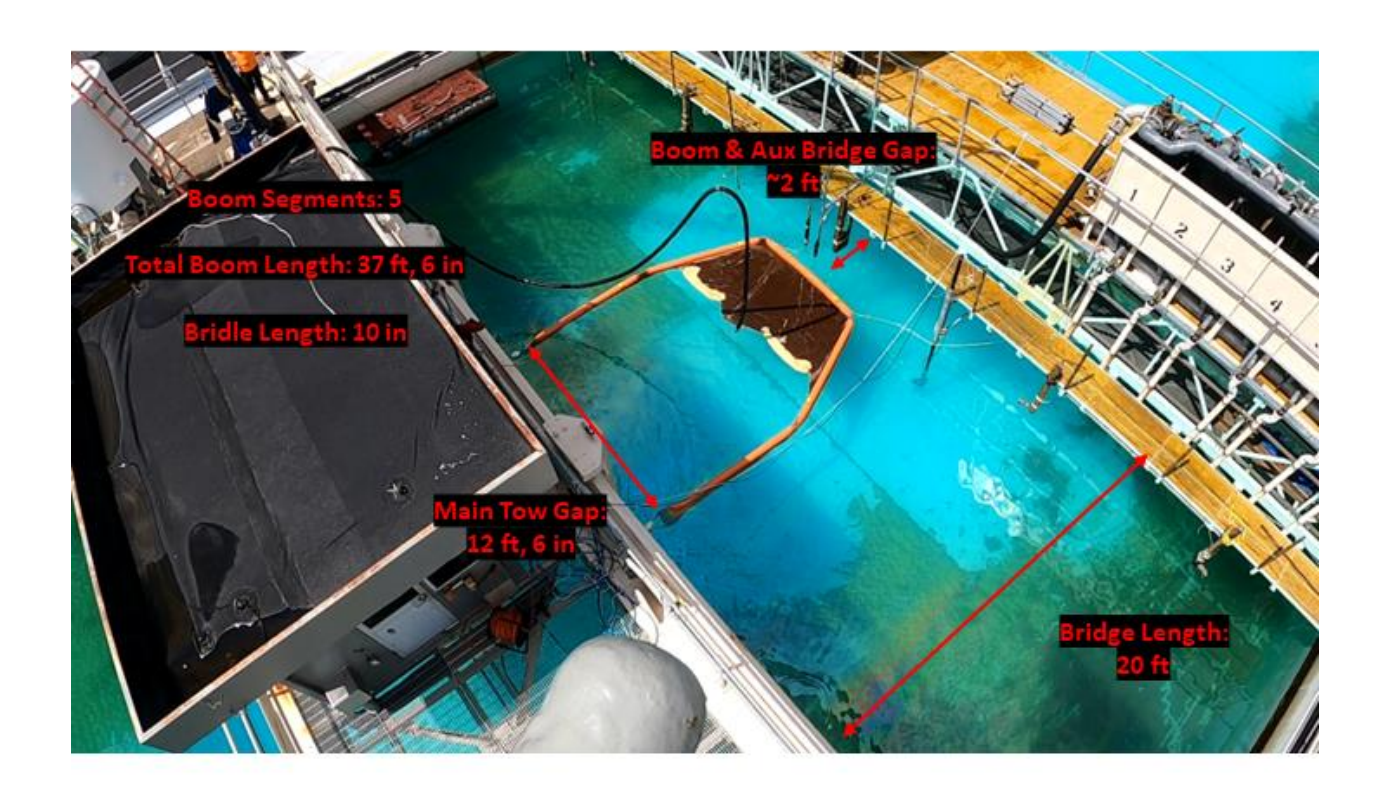


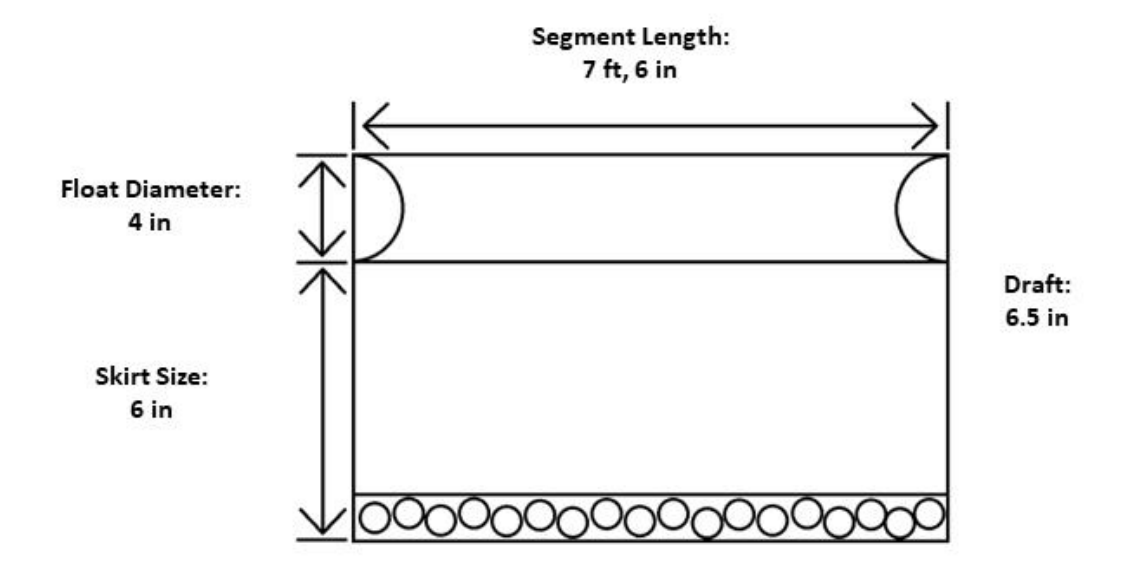
Abasco - Half Scale



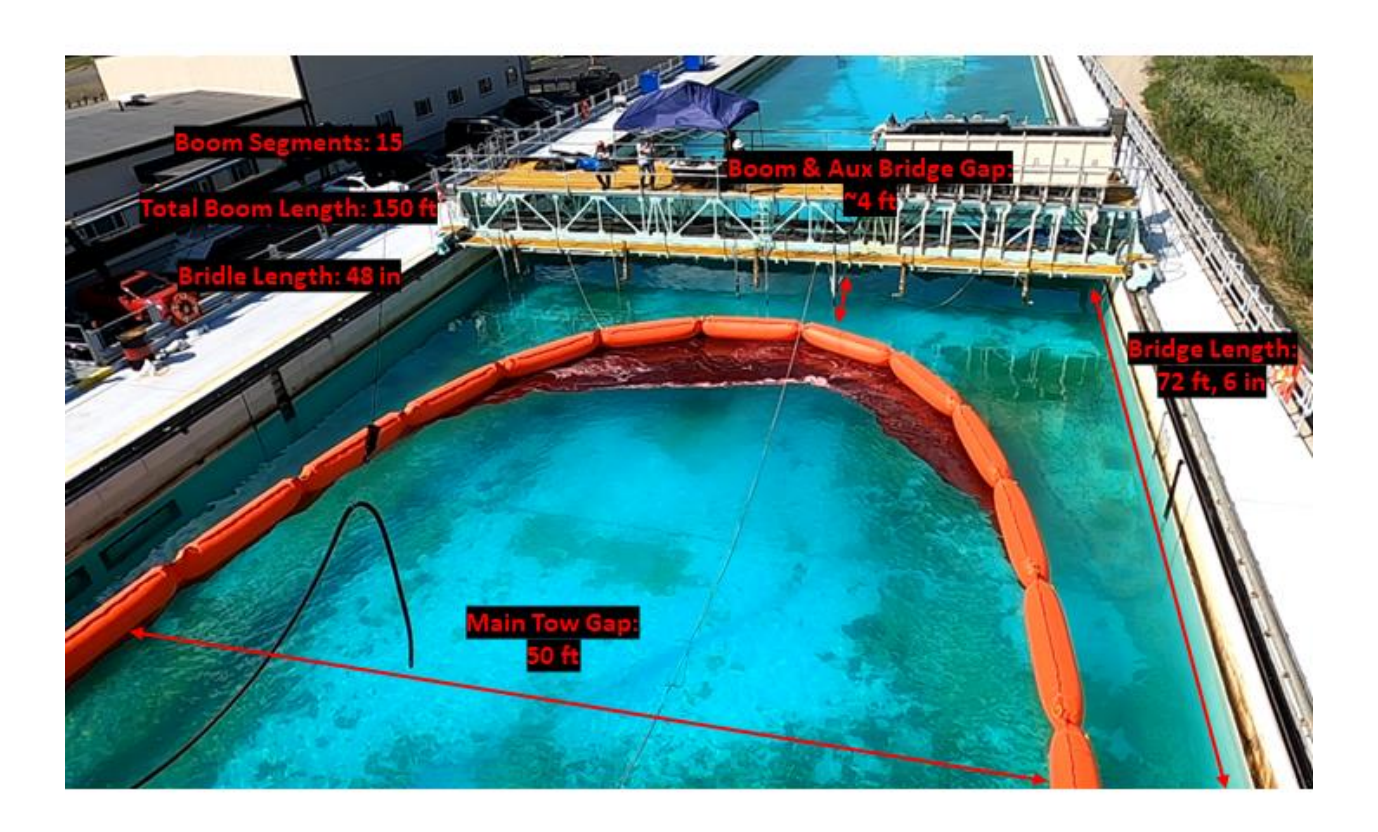


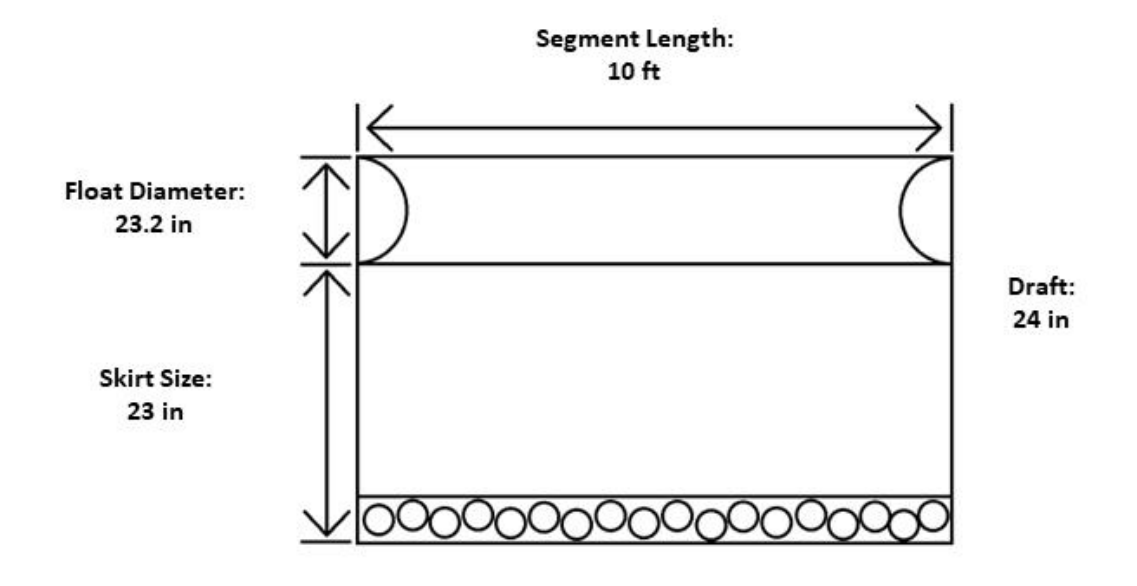
Abasco – Quarter Scale



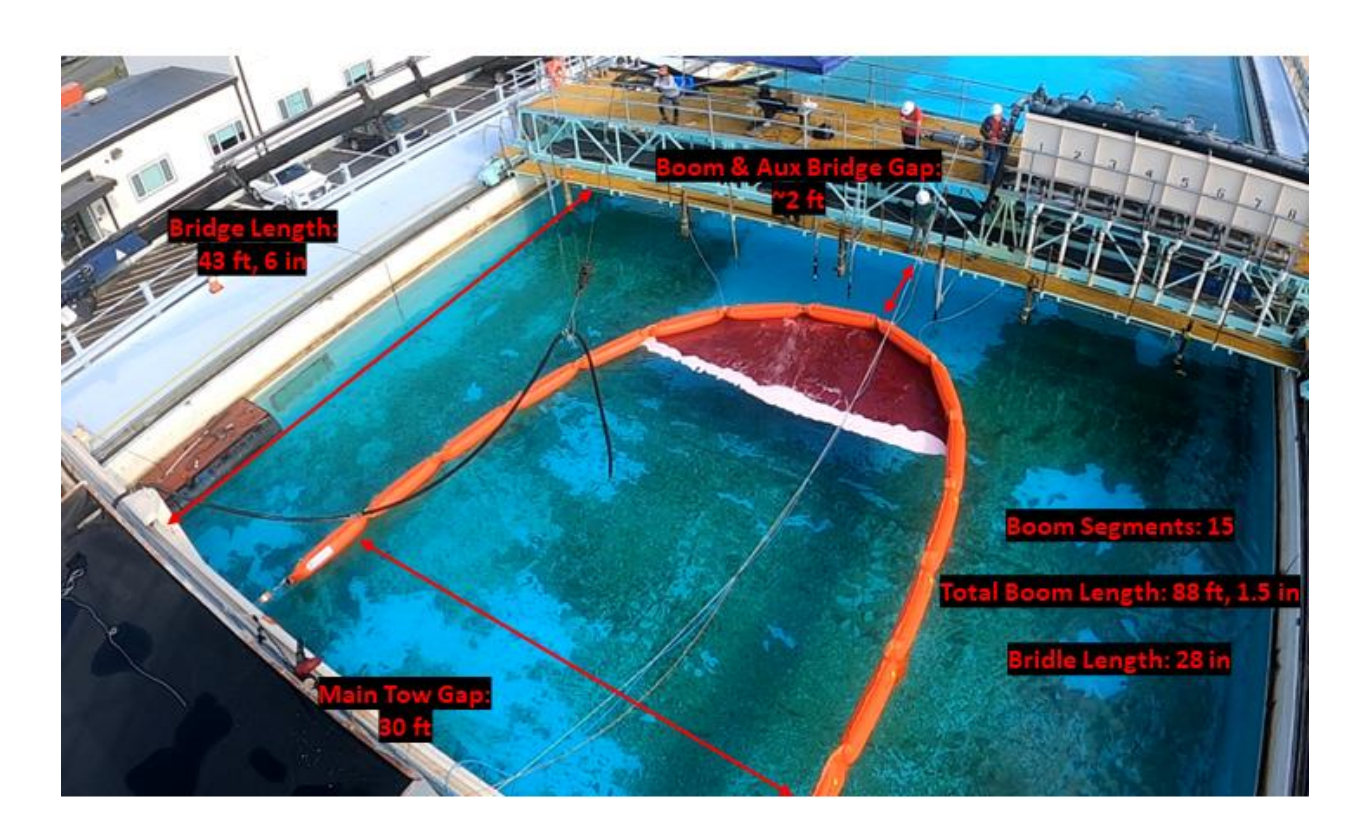


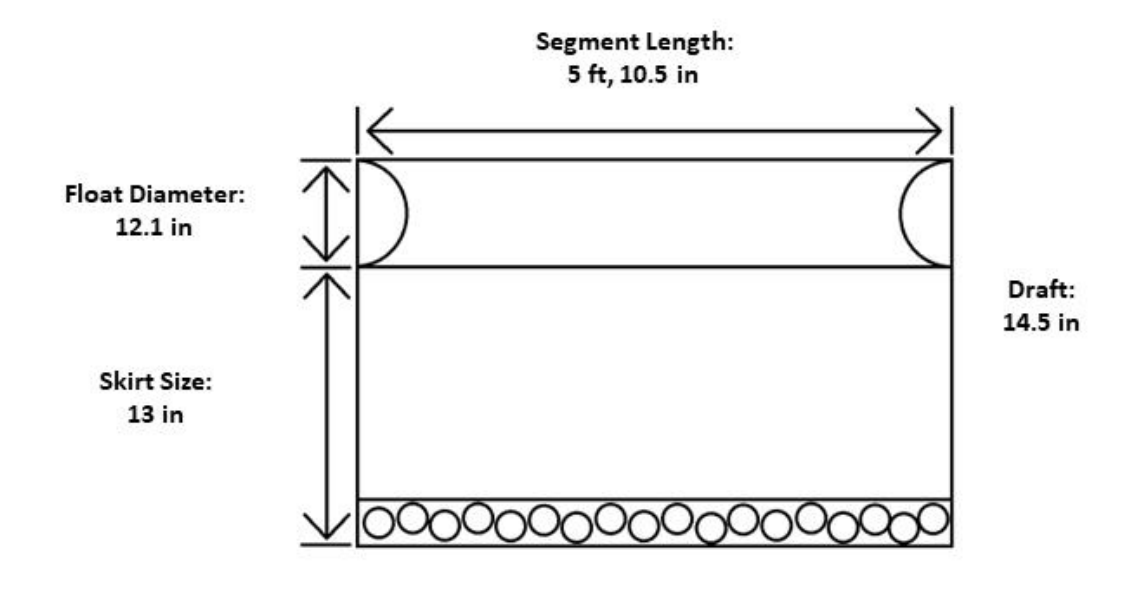
Airmax - Full Scale



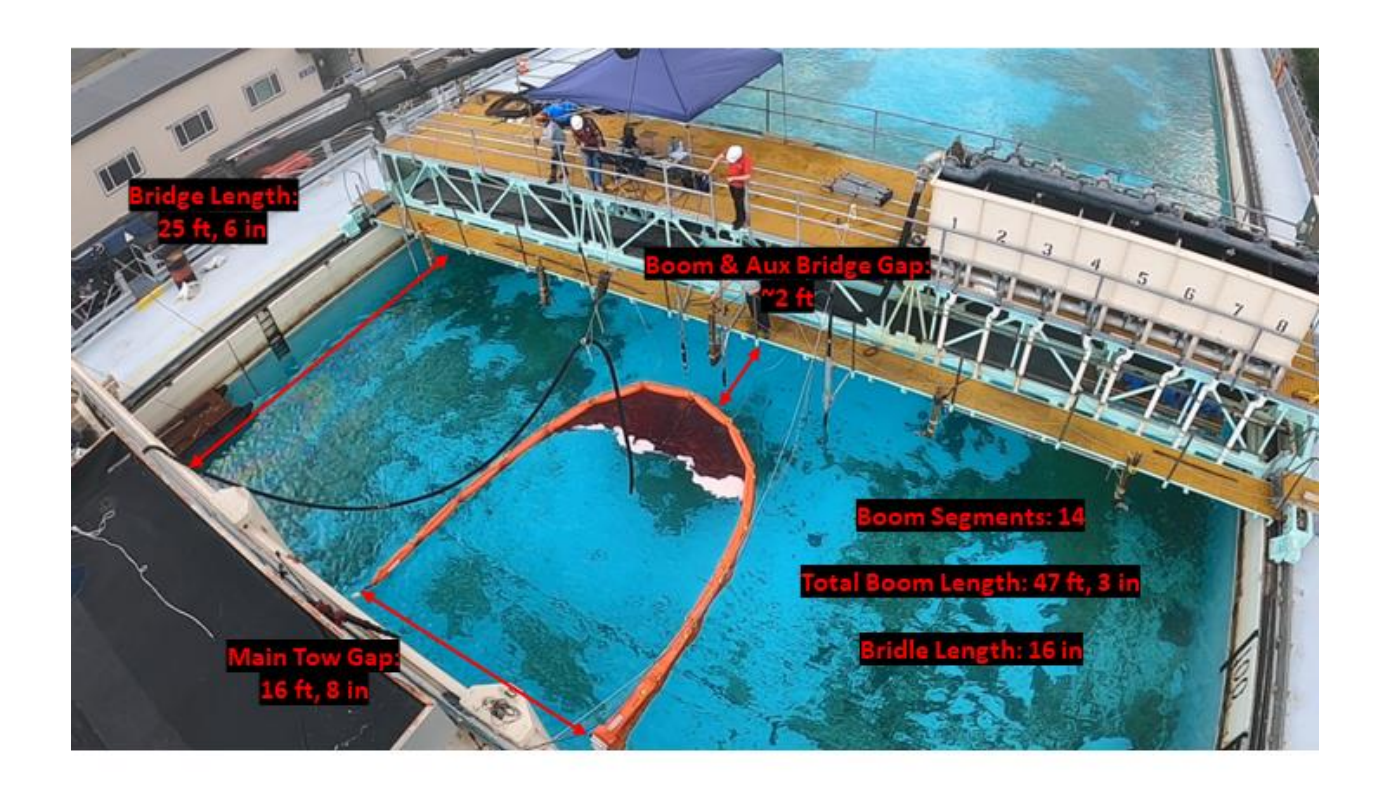


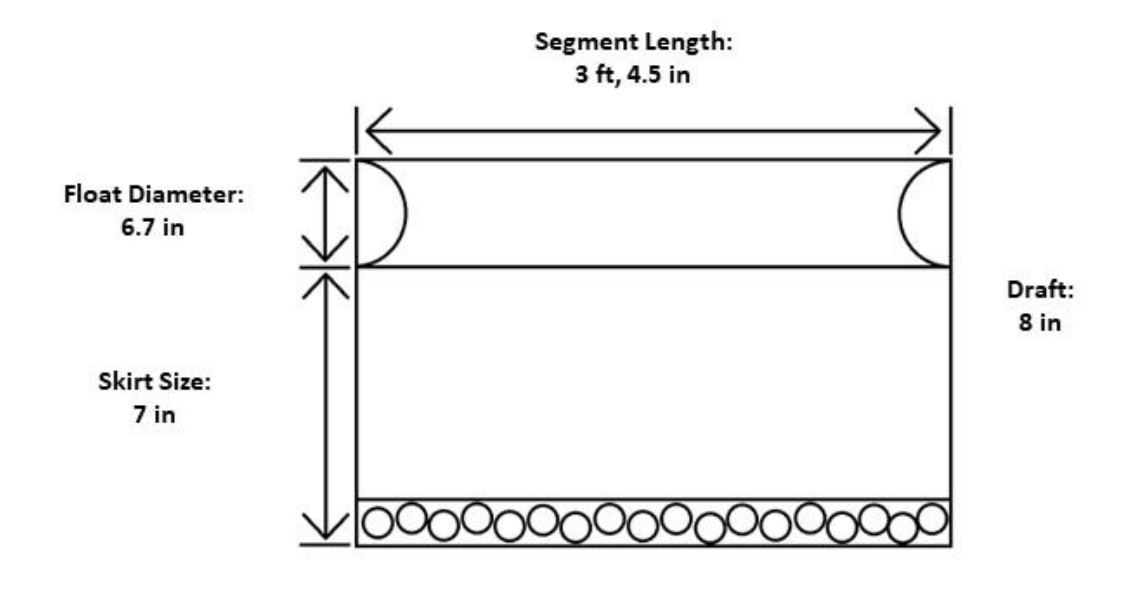
Airmax – 60% Scale



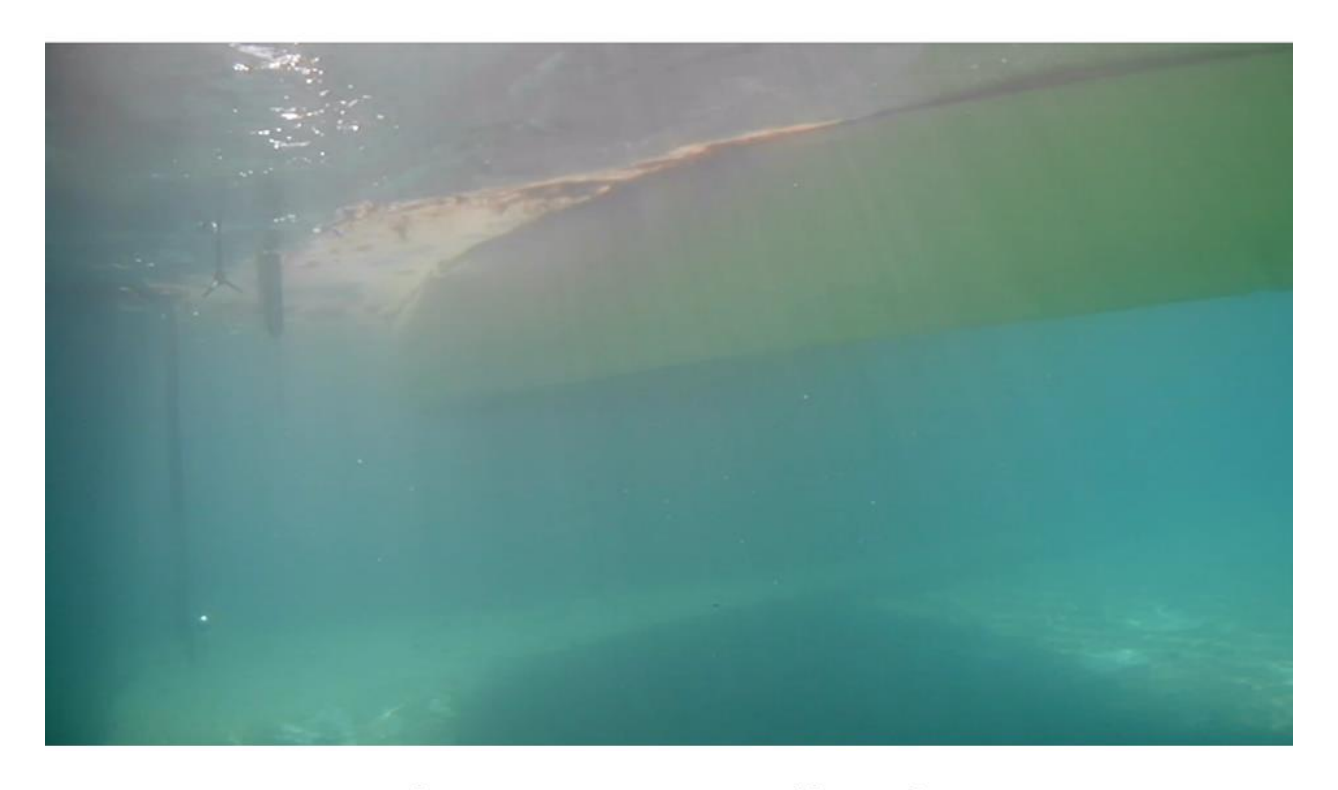


Airmax - 33% Scale





Appendix D: Underwater Pictures of Boom Systems
Elastec Foam – Full Scale



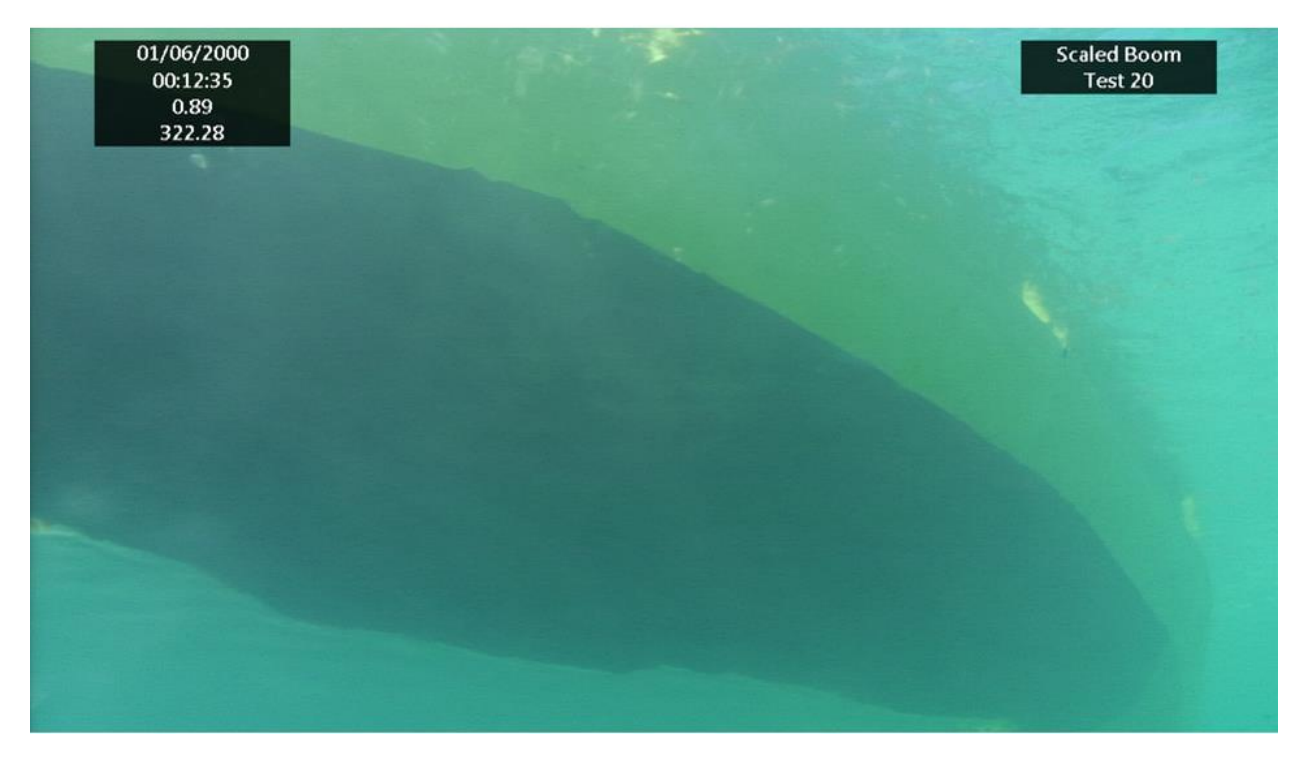
Elastec Foam - Full Scale



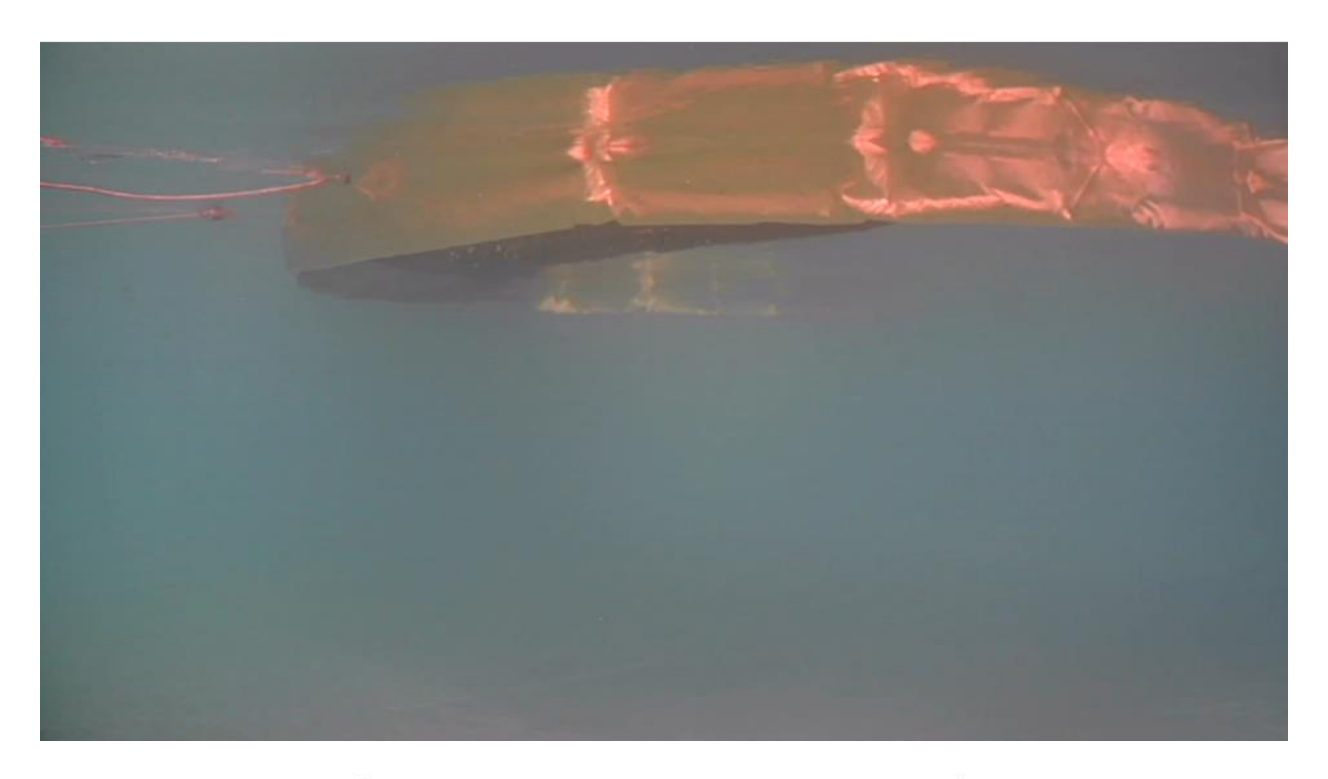
Elastec Foam - Half Scale



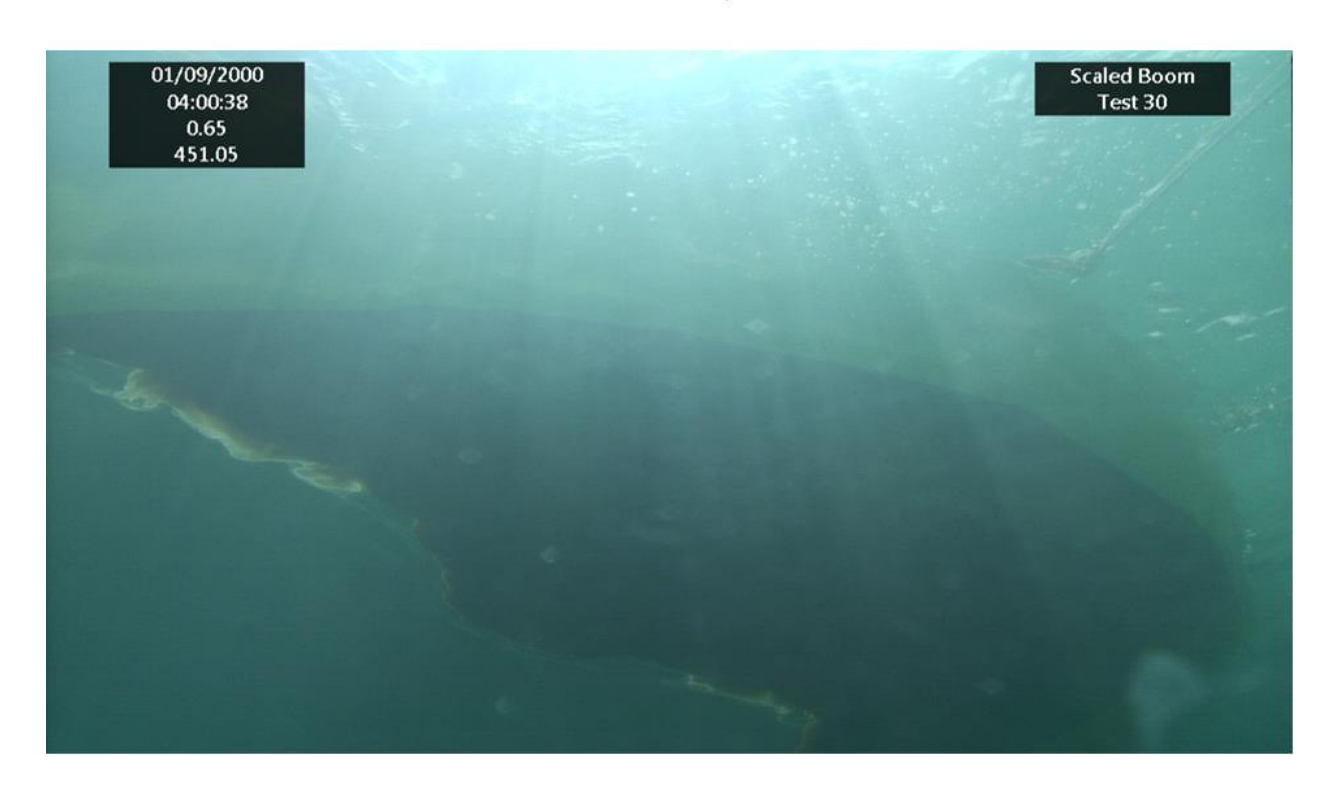
Elastec Foam – Half Scale



Elastec Foam – Quarter Scale



Elastec Foam – Quarter Scale



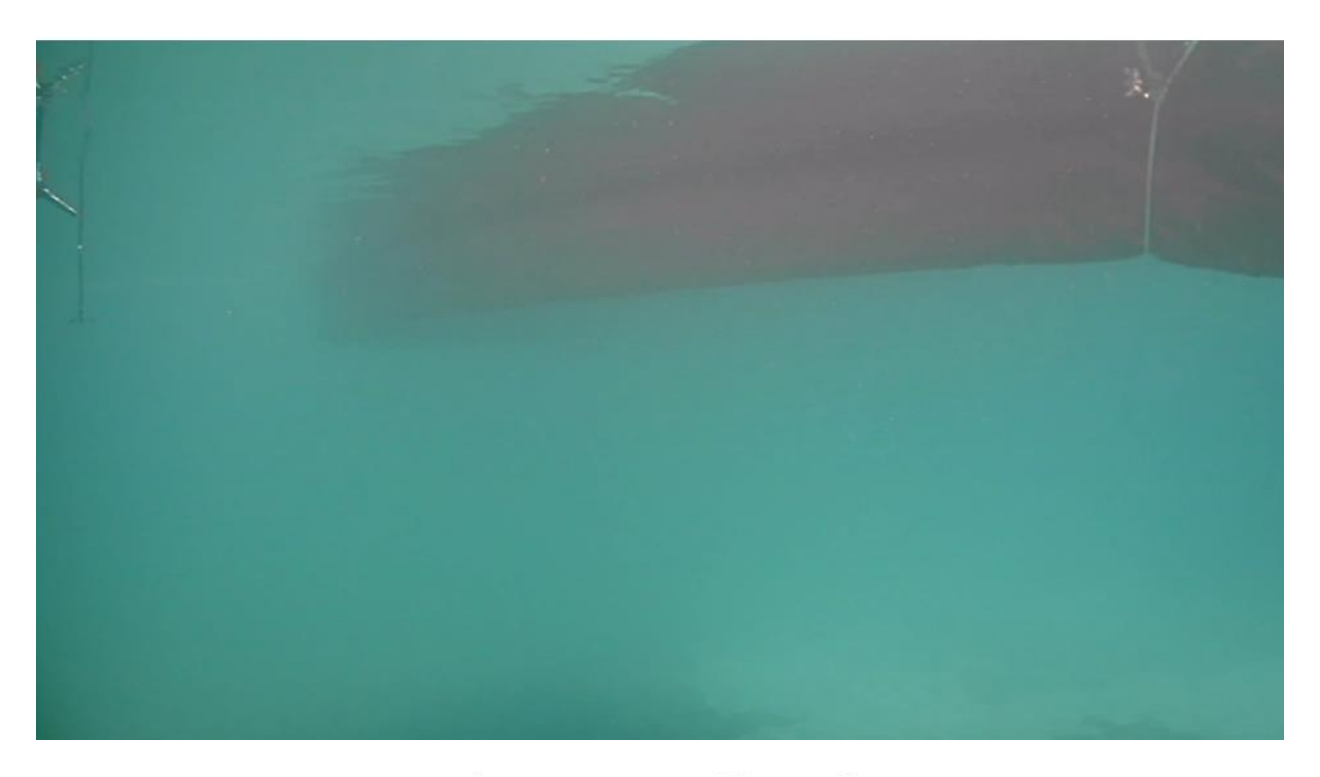
Abasco – Full Scale



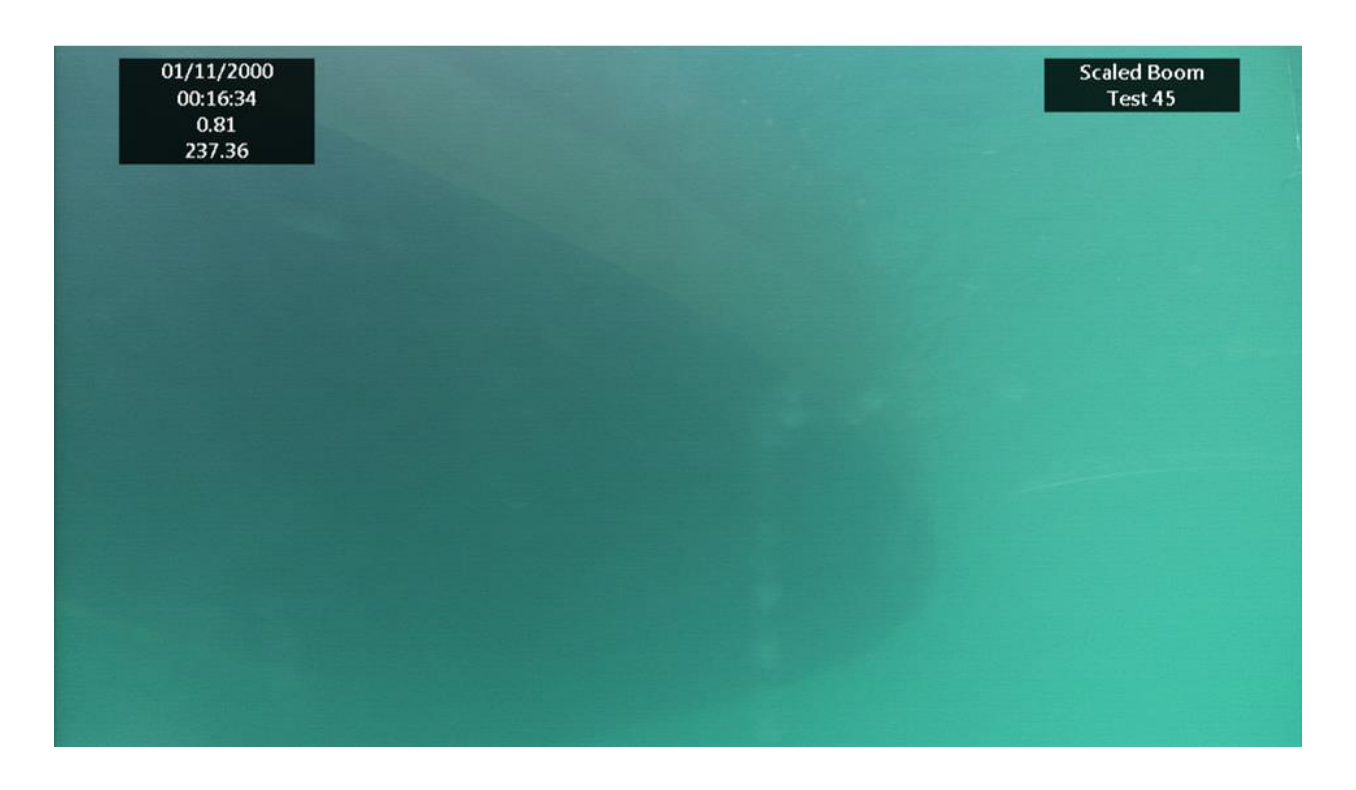
Abasco – Full Scale



Abasco – Half Scale



Abasco – Half Scale



Abasco – Quarter Scale



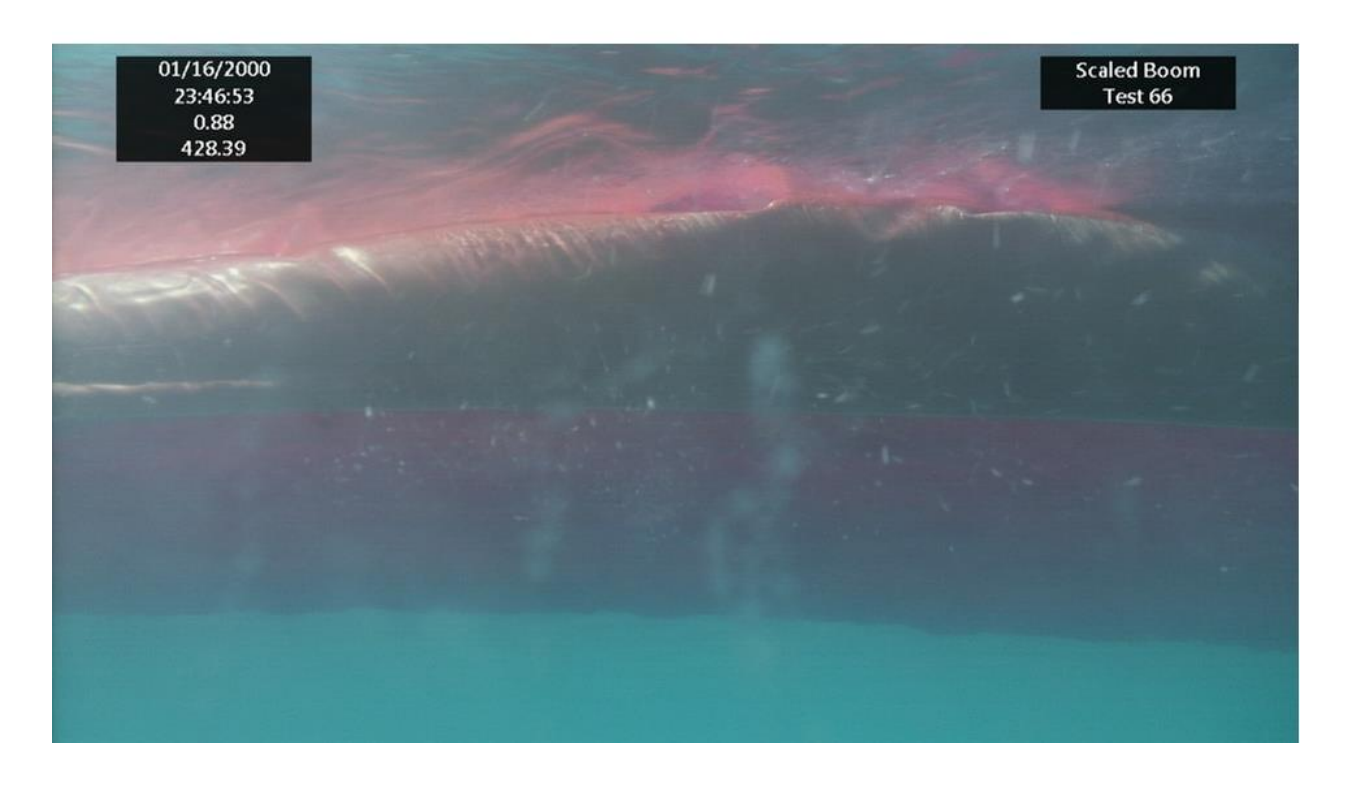
Abasco – Quarter Scale



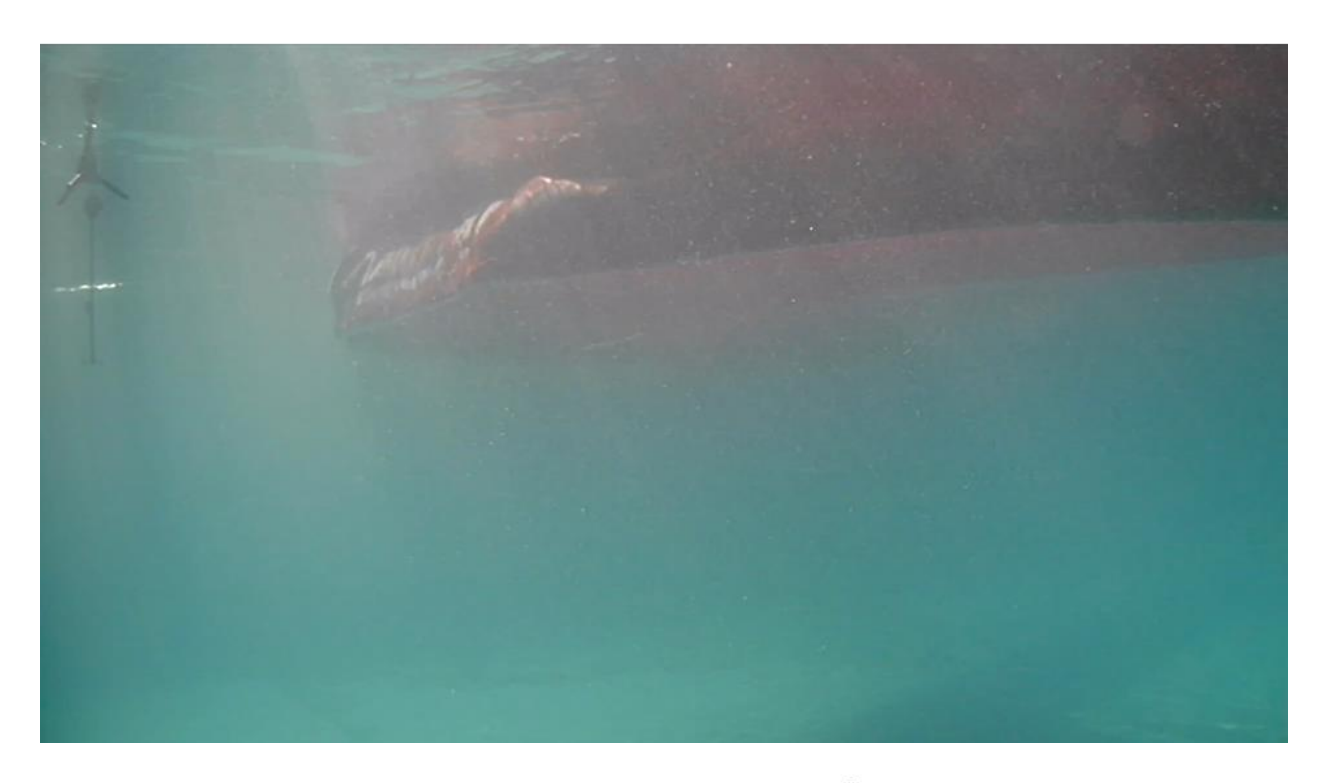
Airmax – Full Scale



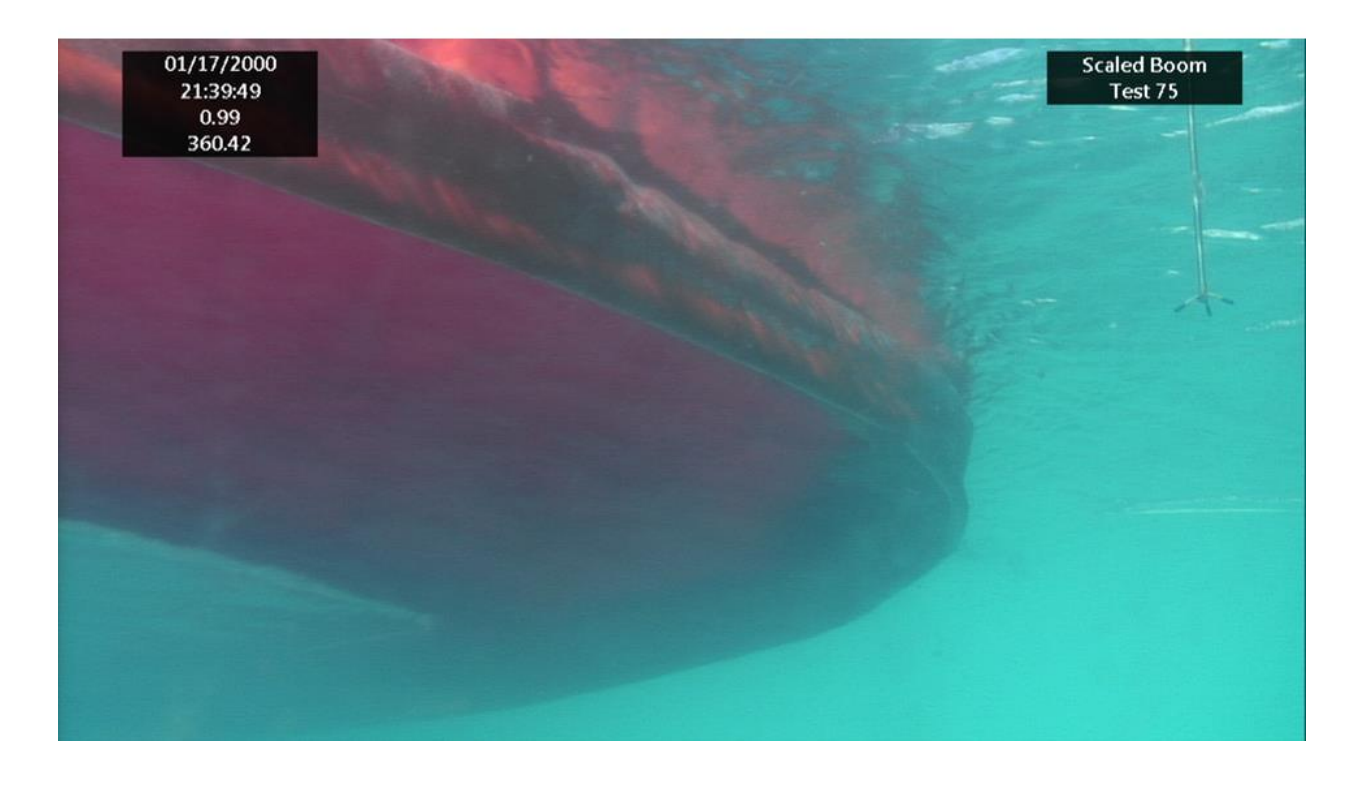
Airmax – Full Scale



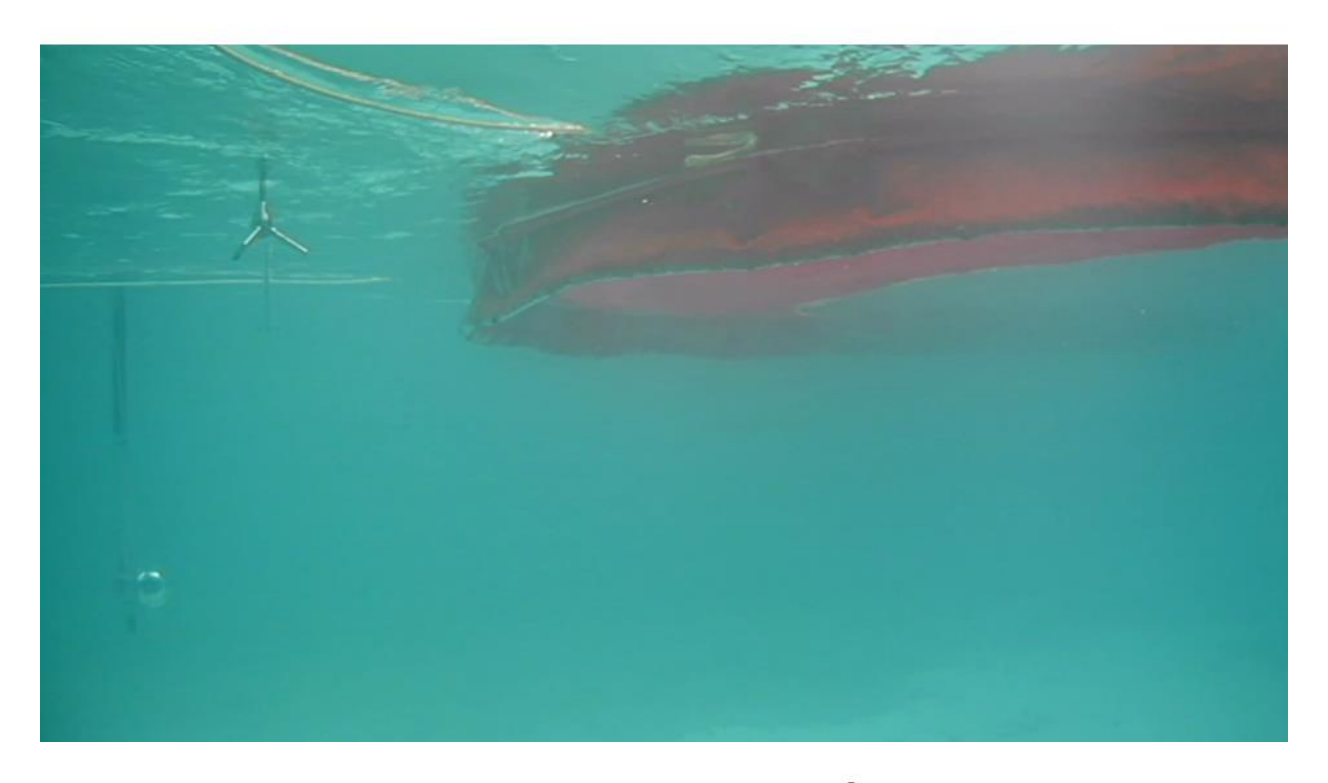
Airmax - 60% Scale



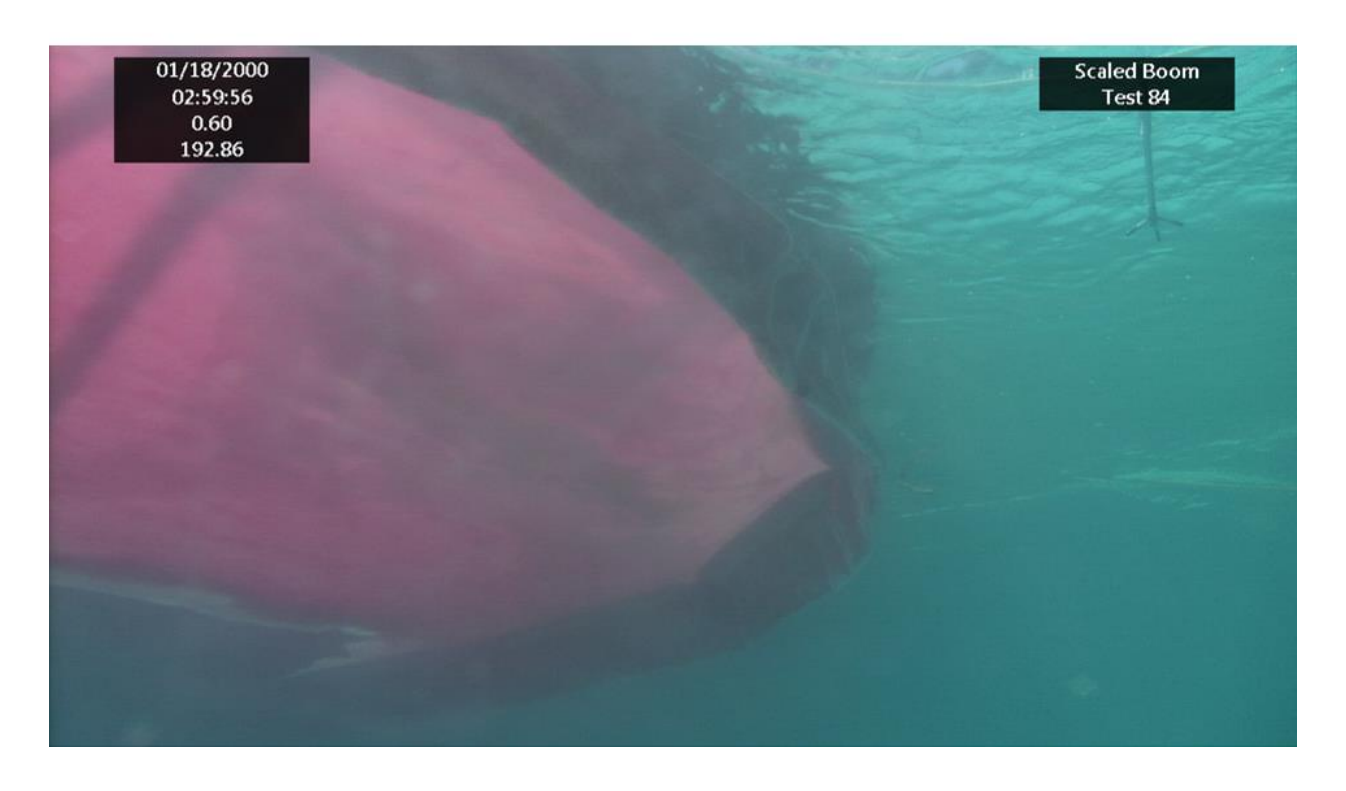
Airmax - 60% Scale



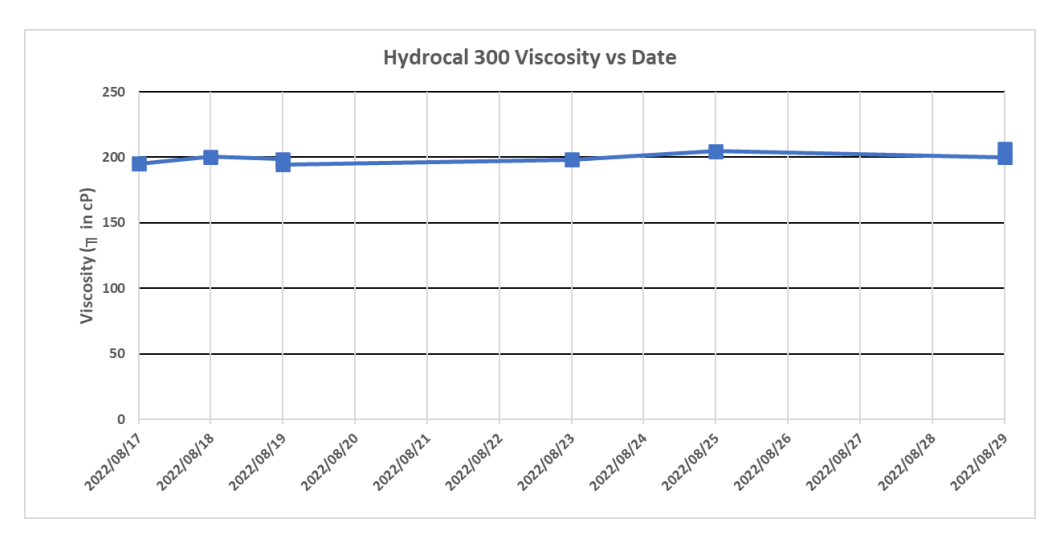
Airmax – 33% Scale

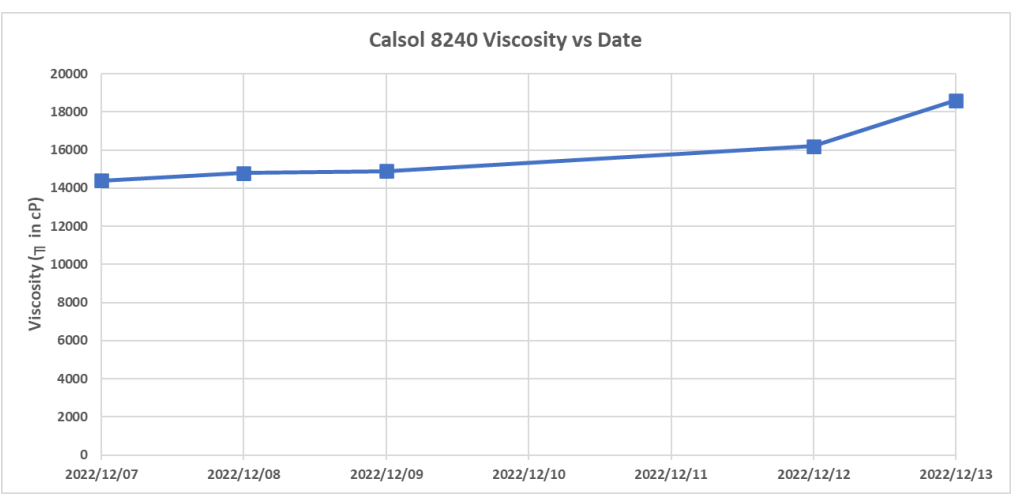


Airmax - 33% Scale



Appendix E. Viscosity Data





Fluid Sample	Date	Viscosity (in cP)
Hydrocal 300	2022/08/17	195.2
Hydrocal 300	2022/08/18	200.4
Hydrocal 300	2022/08/19	198.7
Hydrocal 300	2022/08/19	194.7
Hydrocal 300	2022/08/23	198.2
Hydrocal 300	2022/08/25	204.7
Hydrocal 300	2022/08/29	200.2
Hydrocal 300	2022/08/29	206.6
Calsol 8240	2022/12/07	14400
Calsol 8240	2022/12/08	14800
Calsol 8240	2022/12/09	14900
Calsol 8240	2022/12/12	16200
Calsol 8240	2022/12/13	18600

Appendix F. Entrainment Pictures



Figure 62 Elastec Foam 100% scale – first loss entrainment.



Figure 63 Elastec Foam 100% scale – gross loss entrainment.



Figure 64 Elastec Foam 50% scale – first loss entrainment.



Figure 65 Elastec Foam 50% scale – gross loss entrainment.

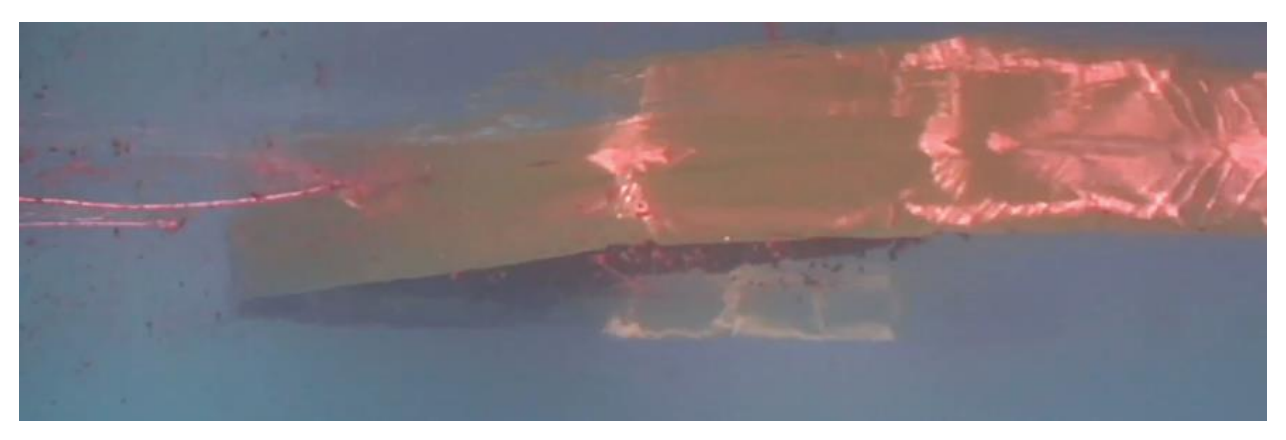


Figure 66 Elastec Foam 25% scale – first loss entrainment.



Figure 67 Elastec Foam 25% scale – gross loss entrainment.



Figure 68 Abasco 100% scale – first loss entrainment.

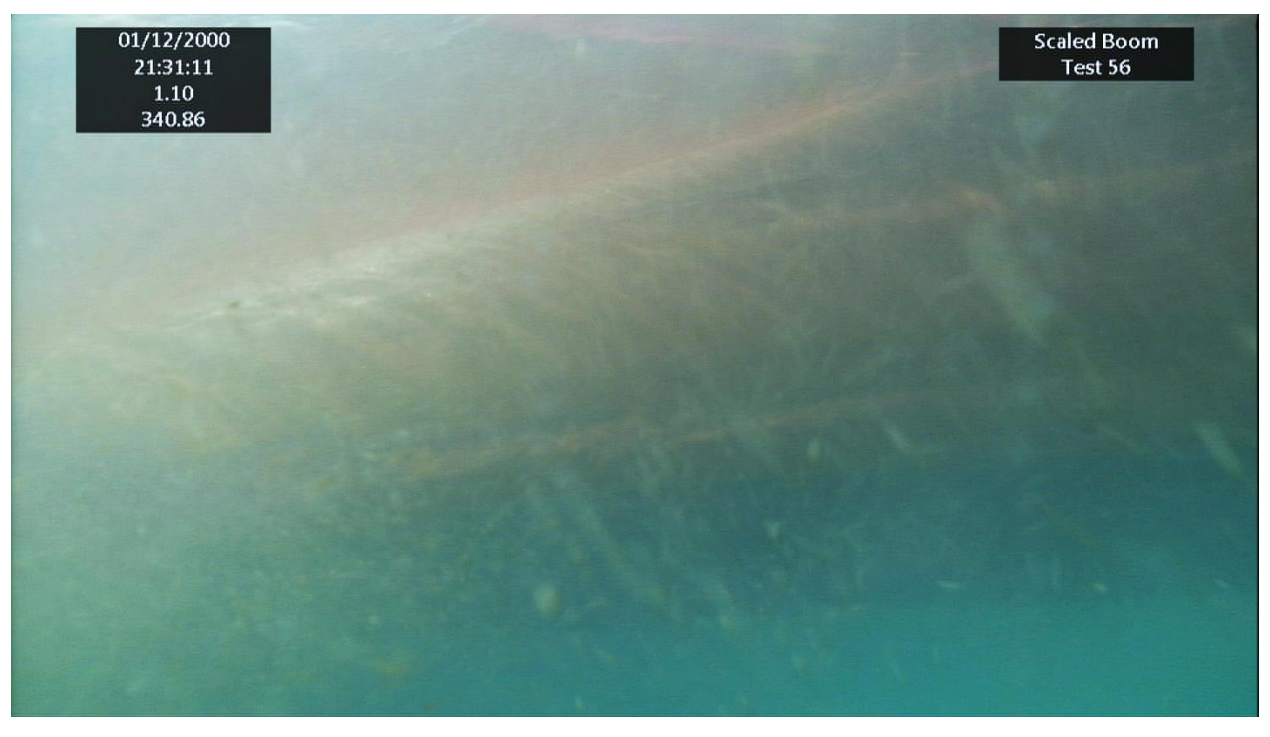


Figure 69 Abasco 100% scale – gross loss entrainment.



Figure 70 Abasco 50% scale – first loss entrainment.



Figure 71 Abasco 50% scale – gross loss entrainment.



Figure 72 Abasco 25% scale – first loss entrainment.



Figure 73 Abasco 25% scale – gross loss entrainment.



Figure 74 Elastec Airmax 100% scale – first loss entrainment.



Figure 75 Elastec Airmax 100% scale – gross loss entrainment.



Figure 76 Elastec Airmax 66% scale – first loss entrainment.



Figure 77 Elastec Airmax 66% scale – gross loss entrainment.

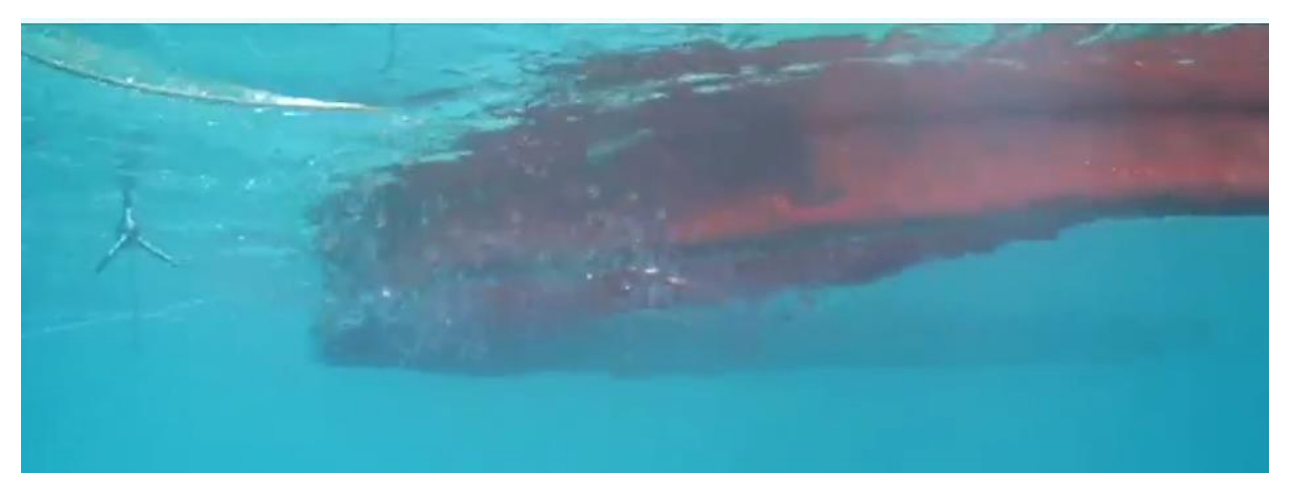


Figure 78 Elastec Airmax 33% scale – first loss entrainment.

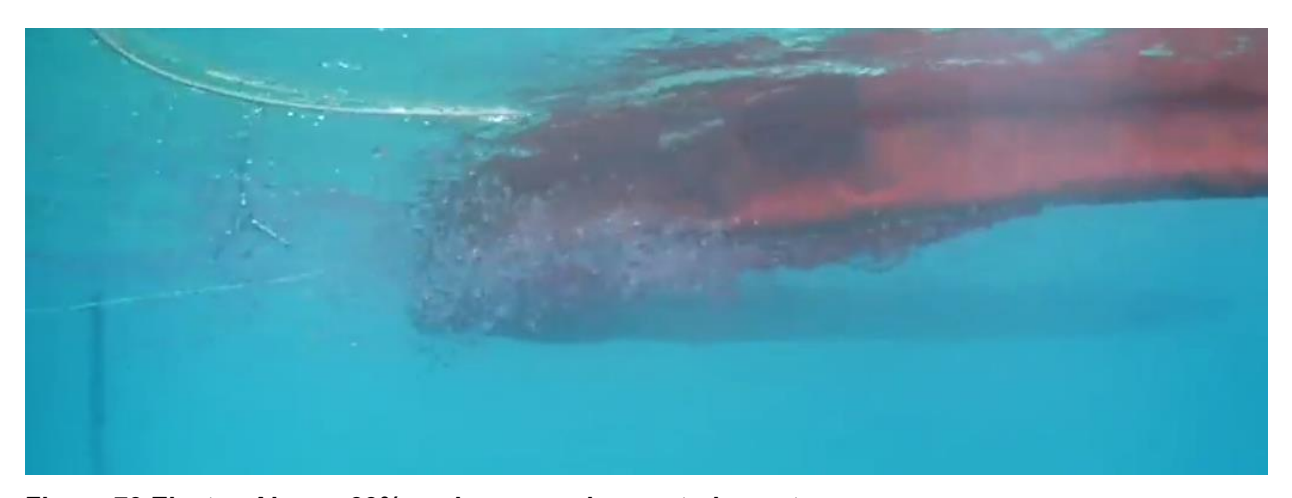
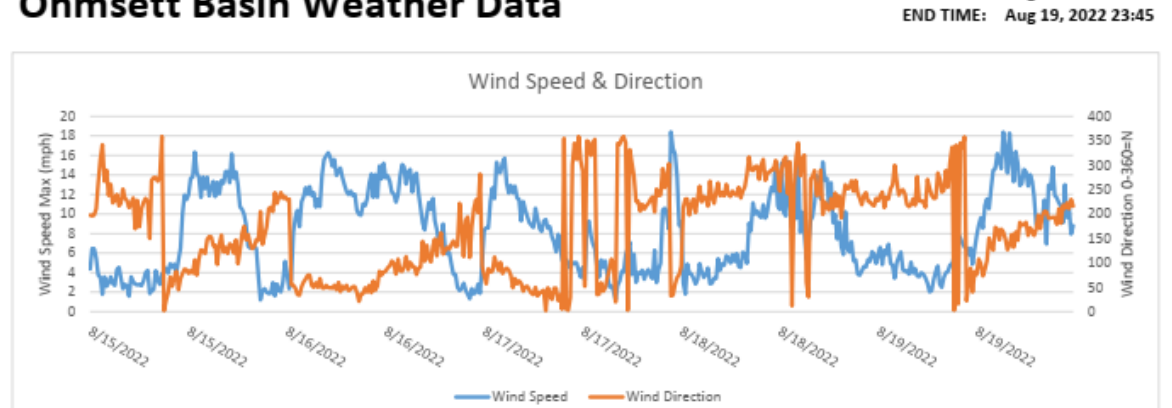


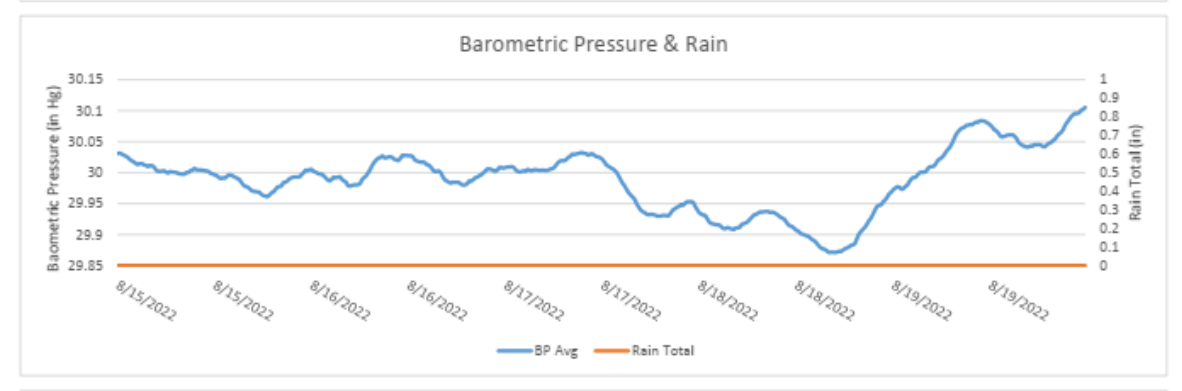
Figure 79 Elastec Airmax 33% scale – gross loss entrainment.

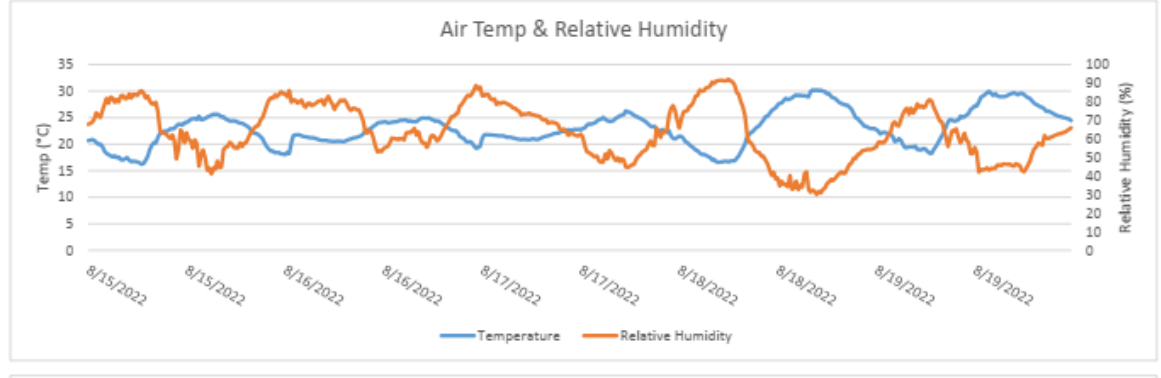
Appendix G. Weather

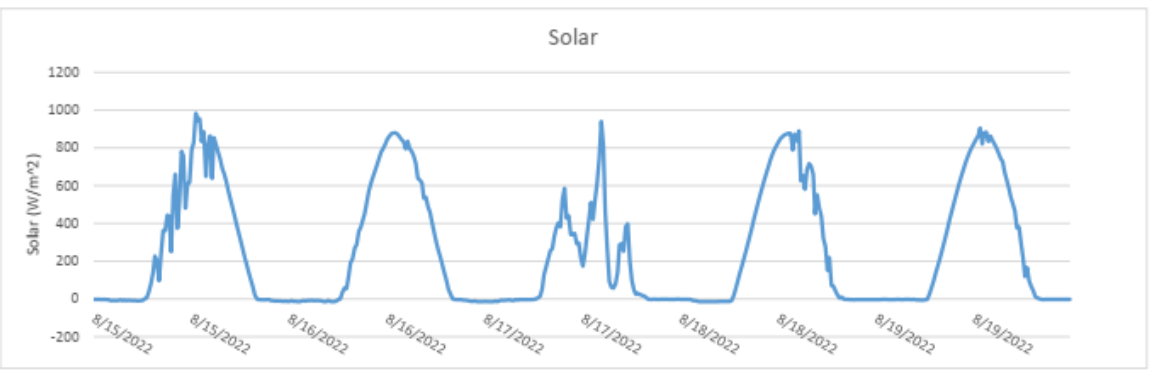
Ohmsett Basin Weather Data



START TIME: Aug 15, 2022 00:00



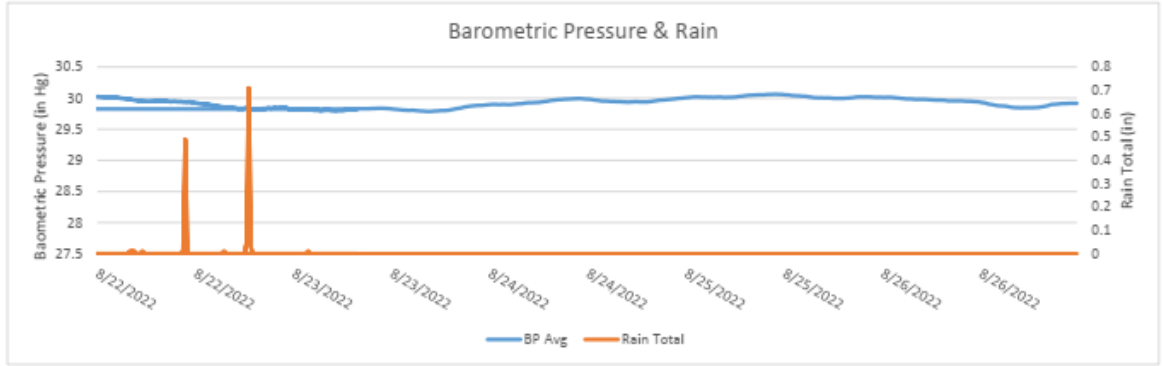


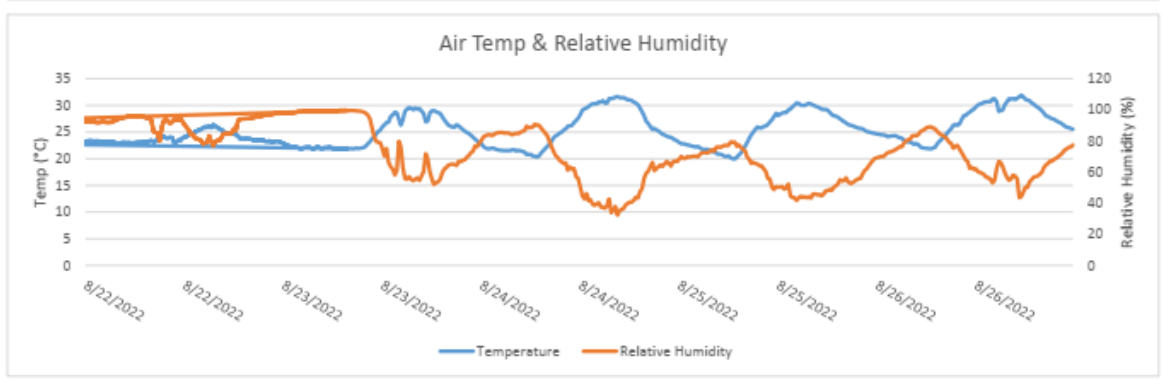


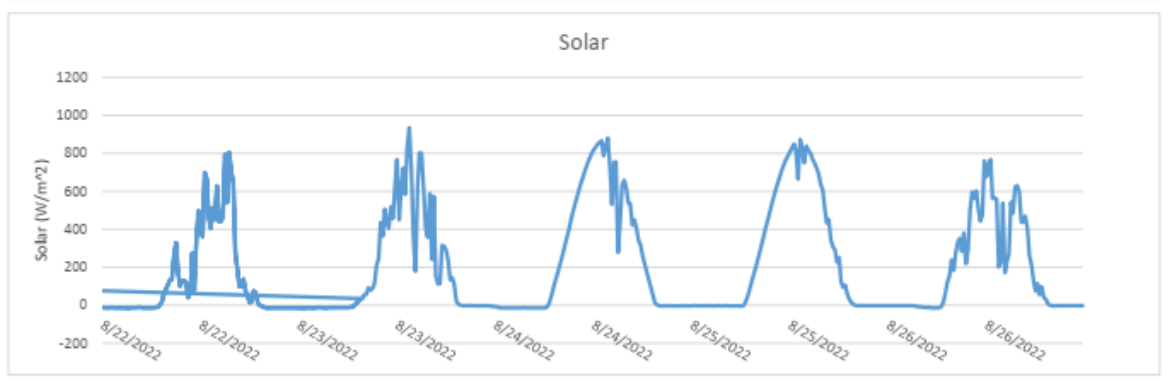
Ohmsett Basin Weather Data

START TIME: Aug 22, 2022 00:00 END TIME: Aug 26, 2022 23:45





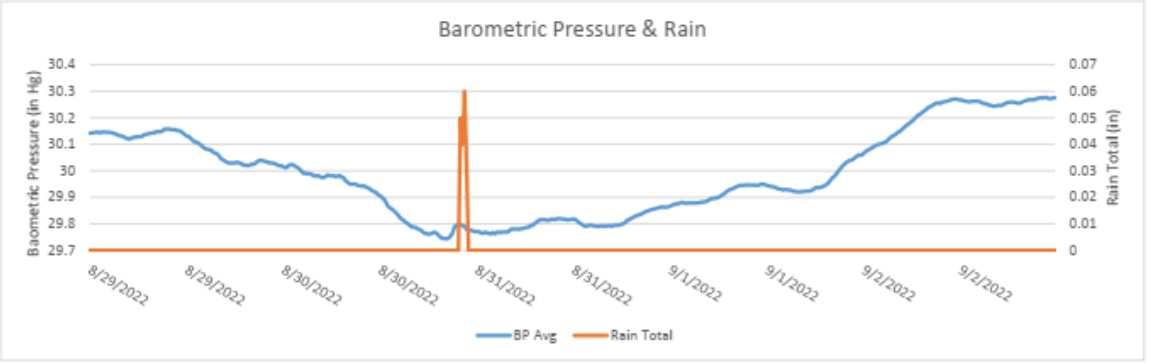


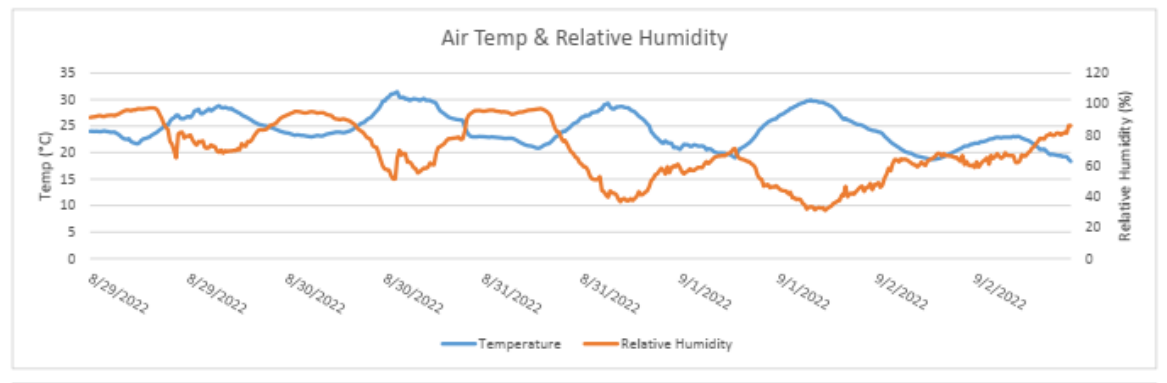


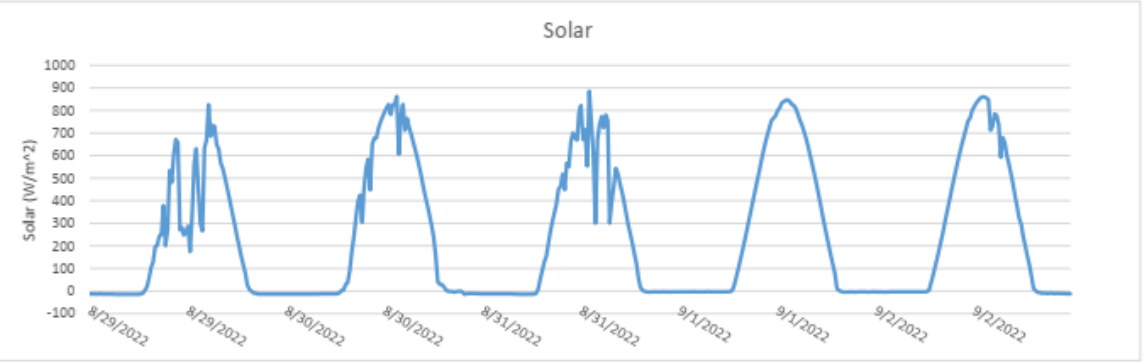
Ohmsett Basin Weather Data

START TIME: Aug 29, 2022 00:00 END TIME: Sep 02, 2022 23:45





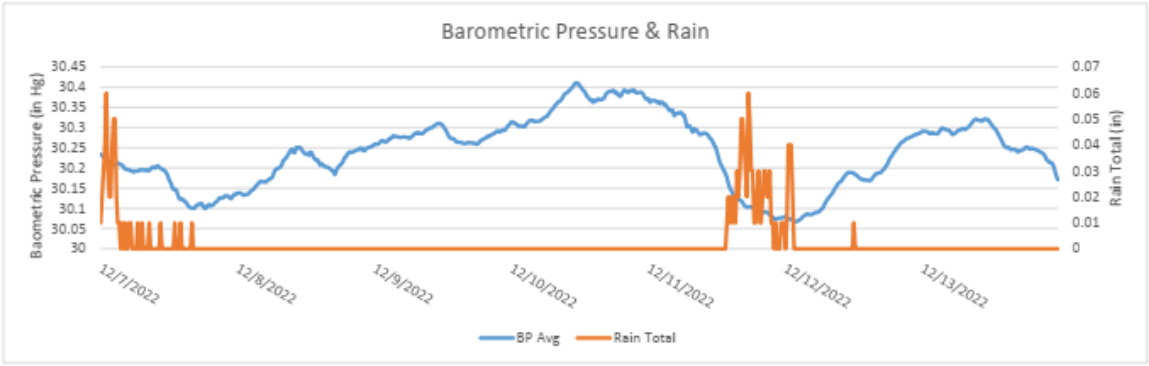


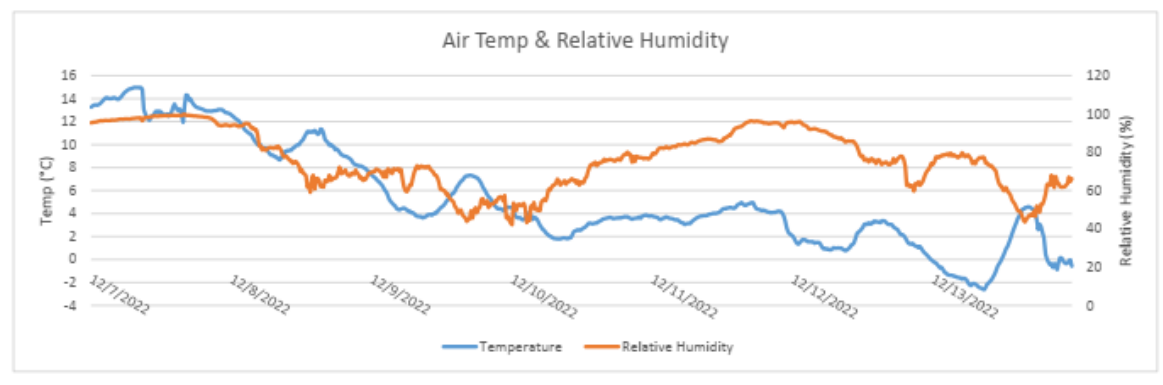


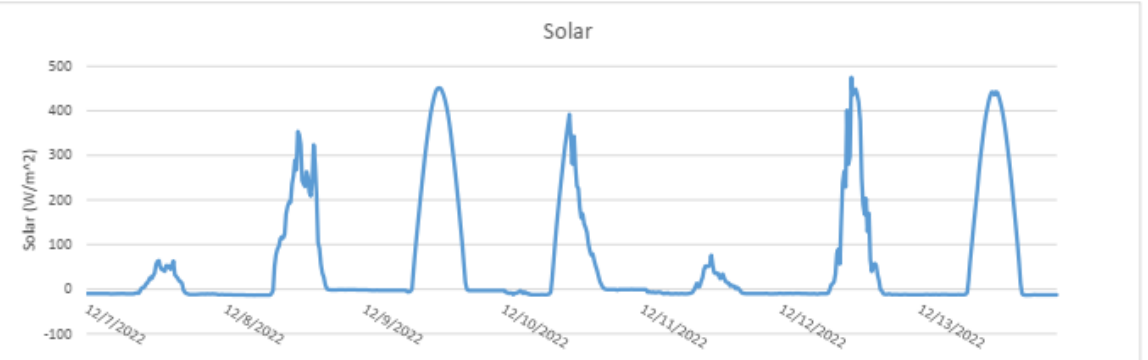
Ohmsett Basin Weather Data

START TIME: Dec 07, 2022 00:00 END TIME: Dec 13, 2022 23:45











Department of the Interior (DOI)

The Department of the Interior protects and manages the Nation's natural resources and cultural heritage; provides scientific and other information about those resources; and honors the Nation's trust responsibilities or special commitments to American Indians, Alaska Natives, and affiliated island communities.



Bureau of Safety and Environmental Enforcement (BSEE)

The mission of the Bureau of Safety and Environmental Enforcement works to promote safety, protect the environment, and conserve resources offshore through vigorous regulatory oversight and enforcement.

BSEE Oil Spill Preparedness Program

BSEE administers a robust Oil Spill Preparedness Program through its Oil Spill Preparedness Division (OSPD) to ensure owners and operators of offshore facilities are ready to mitigate and respond to substantial threats of actual oil spills that may result from their activities. The Program draws its mandate and purpose from the Federal Water Pollution Control Act of October 18, 1972, as amended, and the Oil Pollution Act of 1990 (October 18, 1991). It is framed by the regulations in 30 CFR Part 254 – Oil Spill Response Requirements for Facilities Located Seaward of the Coastline, and 40 CFR Part 300 – National Oil and Hazardous Substances Pollution Contingency Plan. Acknowledging these authorities and their associated responsibilities, BSEE established the program with three primary and interdependent roles:

- Preparedness Verification,
- Oil Spill Response Research, and
- Management of Ohmsett the National Oil Spill Response Research and Renewable Energy Test Facility.

The research conducted for this Program aims to improve oil spill response and preparedness by advancing the state of the science and the technologies needed for these emergencies. The research supports the Bureau's needs while ensuring the highest level of scientific integrity by adhering to BSEE's peer review protocols. The proposal, selection, research, review, collaboration, production, and dissemination of OSPD's technical reports and studies follows the appropriate requirements and guidance such as the Federal Acquisition Regulation and the Department of Interior's policies on scientific and scholarly conduct.